

**EFFECT OF PROGRESSIVE RECYCLING ON CELLULOSE FIBER
SURFACE PROPERTIES**

A Thesis
Presented to
The Academic Faculty

by

Adam A. Brancato

In Partial Fulfillment
of the Requirements for the Degree
Doctor of Philosophy in the
School of Chemical and Biomolecular Engineering

Georgia Institute of Technology
December 2008

EFFECT OF PROGRESSIVE RECYCLING ON CELLULOSE FIBER SURFACE PROPERTIES

Approved by:

Dr. Sujit Banerjee, Advisor
School of Chemical and Biomolecular
Engineering/IPST
Georgia Institute of Technology

Dr. Peter Ludovice
School of Chemical and Biomolecular
Engineering
Georgia Institute of Technology

Dr. Yulin Deng
School of Chemical and Biomolecular
Engineering/IPST
Georgia Institute of Technology

Dr. Frances Walsh
Kimberly-Clark

Dr. Timothy Patterson
School of Mechanical Engineering/IPST
Georgia Institute of Technology

Date Approved: July 11, 2008

“I have had my results for a long time: but I do not yet
know how I am to arrive at them.”

Karl Friedrich Gauss

ACKNOWLEDGEMENTS

This work would not have been possible without the support of many people. First, I would like to thank my advisor, Sujit Banerjee. He aided me in setting up experimental plans without restricting the goals of my work, allowing me to grow as a scientist. I would also like to thank all the members of my research group who have come and gone throughout my time here, especially Ron Sabo, for my initial AFM training, Fran Walsh, for her collaboration on refining experiments, and Tuan Le, who assisted me in the lab on many occasions. Without their help this project would not have progressed to the extent that it has.

I have also been the beneficiary of excellent technical support and advice while working on this project. The engineering staff at Asylum Research was always willing and able to help me with any problems I had with the AFM, from the extraordinarily hard problems to the glaringly obvious oversights. I would also like to thank Dr. Bottomley for reviewing my research plan and helping me to design a series of AFM experiments capable of generating the data I needed, and Brett Brotherson for helping me with the day to day problems and surprises that cropped up in the lab.

In addition to the support I received while working on my thesis, I also have had the benefit of many friends on the Georgia Tech campus to keep me on an even keel. I will always remember the members of the Graduate Student Government, who made my Tuesday mornings eventful and always helped to keep campus events and my work in perspective with the rest of my life. The list of people who I have come

to consider close friends is long, but I should mention Greg Smith and Josh Teitelbaum for being excellent apartment-mates during my time here and Lee Goetz and Rich Bowers-Dean, who have always been willing to take time out of their busy schedules to hang out when I needed to relax. I also want to thank my parents and my sister, because even though I don't see them as often as I would like to, they are a constant source of unconditional support.

Finally, I would like thank the members of my thesis committee for their time and effort on my behalf and the member companies of IPST and the IPST foundation for the monetary support that has made this work possible.

TABLE OF CONTENTS

	Page
ACKNOWLEDGEMENTS	iv
LIST OF TABLES	x
LIST OF FIGURES	xi
LIST OF EQUATIONS	xiv
SUMMARY	xv
 <u>CHAPTER</u>	
I INTRODUCTION	1
II LITERATURE REVIEW	3
2.1 Components of Paper	3
2.1.1 Wood Structure	4
2.1.2 Cellulose	6
2.1.3 Hemicelluloses	9
2.1.4 Lignin	10
2.1.5 Extractives	12
2.2 Bonding	12
2.3 Papermaking	13
2.3.1 Kraft Pulping	13
2.3.2 Thermomechanical Pulping	14
2.3.3 Bleaching	14
2.3.4 Refining	16
2.3.5 Papermaking Additives	17

2.3.6	Recycling	19
2.4	Hornification	22
2.4.1	Effects of Hornification	22
2.4.2	Causes of Hornification	26
2.4.2.1	Irreversible Hydrogen Bonding	27
2.4.2.2	Formation of Covalent Bonds	29
2.4.2.3	Fiber Crystallinity	29
2.4.2.4	Hemicellulose Loss	30
2.4.2.5	Surface Inactivation	30
2.4.2.6	Cellulose Chain Cleavage	31
2.4.3	Rate of Hornification	32
2.5	Methods of Analysis	33
2.5.1	Water Retention Value	33
2.5.2	Freeness	34
2.5.3	Coarseness	34
2.5.4	Fiber Length and Pulp Fines Content	35
2.5.5	Tritium Tracer Analysis	35
2.5.6	Atomic Force Microscopy	40
2.5.6.1	Imaging	41
2.5.6.2	Force Measurements	42
2.5.6.3	AFM Analysis of Cellulose and Paper	46
III	THESIS OBJECTIVES	51
IV	MATERIALS AND METHODOLOGY	53
4.1	Materials	53
4.1.1	Bleached Kraft Softwood	53

4.1.2	Bleached Kraft Hardwood	53
4.1.3	Thermomechanical Pulp	53
4.1.4	Mill Samples	54
4.2	Sample Preparation	54
4.2.1	Handsheet Preparation	54
4.2.2	Refining Method	54
4.2.3	Recycling Method	55
4.2.4	Drying Methods	56
4.3	Experimental Procedures	56
4.3.1	Water Retention Value	56
4.3.2	Freeness	57
4.3.3	Coarseness, Fiber Length, Fines Content	58
4.3.4	Tensile Strength	60
4.3.5	Tritium Tracer Analysis	60
4.3.6	Atomic Force Microscopy	62
4.3.6.1	Sample Preparation	62
4.3.6.2	Humidity Control	62
4.3.6.3	Force Curves	63
4.3.6.4	Imaging	67
4.3.6.5	Probe Contamination and Damage	67
V	RESULTS AND ANALYSIS	69
5.1	Unrefined Recycling	69
5.1.1	Bleached Kraft Softwood	69
5.1.1.1	Sheet Surface Adhesion By Test Location	73
5.1.1.2	Humidity	73

5.1.2	Bleached Kraft Hardwood	75
5.1.2.1	Accelerated Drying	77
5.1.2.2	Inhibition of Hornification	79
5.1.3	Thermomechanical Pulp	82
5.1.4	Handsheet Recycling Summary	83
5.2	Single Fiber Wetting and Drying	87
5.3	Refining	89
5.4	AFM Imaging of Fiber	93
5.4.1	25 μm^2 Images	94
5.4.2	0.25 μm^2 Images	96
5.4.3	2500 nm^2 Images	98
5.5	Mill Sample Analysis	100
5.6	Summary	103
VI	CONCLUSIONS AND RECOMMENDATIONS	106
6.1	Recommendations for Future Work	107
APPENDIX A: ADDITIONAL FIBER AFM IMAGES		109
REFERENCES		122

LIST OF TABLES

	Page
Table 1: Chemical components of hardwood and softwood	4
Table 2: Surface charge of species commonly present in recycled pulp	21
Table 3: Degree of hornification observed in literature	24
Table 4: Tritium tracer analysis of refined pulp	36
Table 5: Bleached softwood kraft recycling	70
Table 6: Surface adhesion by test location	73
Table 7: Humidity control results	74
Table 8: Bleached hardwood kraft recycling	76
Table 9: Accelerated drying of hardwood pulp	78
Table 10: Inhibition of hornification	79
Table 11: TMP recycling	82
Table 12: Refining experiment data	89
Table 13: RMS roughness results for 25 μm^2 images	96
Table 14: RMS roughness results for 0.25 μm^2 images	98
Table 15: RMS roughness results for 2500 nm^2 images	100
Table 16: Surface adhesion analysis of mill newsprint samples	101

LIST OF FIGURES

	Page
Figure 1: Diagrams of softwood (top) and hardwood (bottom)	5
Figure 2: Cellulose polymer diagram	7
Figure 3: Assembly of a cellulose fiber	8
Figure 4: Polymer chain organization within a microfibril	9
Figure 5: Hemicellulose structure	10
Figure 6: Possible lignin structure	11
Figure 7: Strength development during refining	17
Figure 8: Schematic of undried and dried fibers	22
Figure 9: Fiber size (top) and fiber collapse (bottom) due to rewetting	23
Figure 10: Effect of recycling on bleached kraft sheet properties	24
Figure 11: Comparison of TMP and kraft pulps upon recycling	25
Figure 12: Fiber swelling model	28
Figure 13: Chain scission due to aging at elevated humidity	32
Figure 14: K_{pw} results compared to historical FSP data	37
Figure 15: Light microscopy images of refined fiber at 358 mL CSF (left) and 261 mL CSF (right)	37
Figure 16: Effect of refining on FSP, WRV, K_{pw} , and fines content	38
Figure 17: SEM images of refined fiber at 358 mL CSF (left) and 261 mL CSF (right)	39
Figure 18: Schematic of typical AFM	40
Figure 19: Image distortion during topographic mapping	42

Figure 20: Typical force curve	43
Figure 21: Tip-surface interaction forces as a function of separation	44
Figure 22: Surface adhesion vs. humidity using a silicon nitride tip and lithium fluoride crystal	45
Figure 23: Structure of straw cell walls (left) and enlarged image of deposited lignin (right)	47
Figure 24: AFM image of bleached kraft fiber, arrows highlight visible wrinkling (inset bar = 500 nm)	48
Figure 25: AFM image of unbleached kraft fiber (inset bar = 250 nm)	48
Figure 26: AFM image of cellulose fiber with oriented structure (inset bar = 200 nm)	49
Figure 27: Height traces of unaged sheet (left), aged without mold (center), and aged with mold (right)	50
Figure 28: Valley beater	55
Figure 29: Schematic of CSF tester	57
Figure 30: FQA fluid flow diagram (left) and optical image representation (right)	59
Figure 31: Closed fluid cell	63
Figure 32: AC 240 TS cantilever SEM image	64
Figure 33: Sample AFM force curves	65
Figure 34: Hi'RES-W cantilever SEM image	67
Figure 35: Degree of hornification and tensile strength loss as a function of recycling for bleached softwood kraft pulp	70
Figure 36: Effect of refining on breaking length	71
Figure 37: Surface adhesion as a function of relative humidity	75
Figure 38: Degree of hornification for bleached hardwood kraft pulp	76

Figure 39: Accelerated drying WRV and surface adhesion measurements	78
Figure 40: Effect of sucrose on recycling hardwood pulp	81
Figure 41: Degree of hornification for TMP	83
Figure 42: Surface adhesion data for recycled handsheets	84
Figure 43: Degree of hornification data for recycled handsheets	85
Figure 44: Effect of recycling on the surface adhesion of single fibers	88
Figure 45: Effect of refining on degree of hornification	90
Figure 46: Refining and recycling surface adhesion measurements	92
Figure 47: 2D and 3D rendering of 25 μm^2 unrecycled kraft fiber	95
Figure 48: 2D and 3D rendering of 0.25 μm^2 unrecycled kraft fiber	97
Figure 49: 2D and 3D rendering of 2500 nm^2 unrecycled kraft fiber	99
Figure 50: Mill newsprint histogram	102
Figure 51: Illustration of surface laminating effect from virgin fiber (left) to recycled fiber (right)	104

LIST OF EQUATIONS

	Page
Equation 1: Water retention value	56
Equation 2: Degree of hornification	57
Equation 3: Temperature corrected freeness	58
Equation 4: Fully corrected freeness	58
Equation 5: Coarseness	59
Equation 6: Length-weighted fiber length	60
Equation 7: Partition coefficient	61
Equation 8: dpm in bound water	61
Equation 9: dpm in free water	61
Equation 10: The Sader equation	64

SUMMARY

Cellulose fibers undergo a series of irreversible changes when exposed to cycles of wetting and drying. This process is known as "hornification." Although the effects of hornification have been observed in many studies, the exact mechanism behind hornification is still debated, and several hypotheses have been advanced. This work presents the results of an AFM study on hornified fiber surfaces to further quantify these changes and determine the causes of hornification.

Several different studies were carried out. Upon using a hydrophilic AFM probe to analyze the fiber surface, the fibers appeared to become more hydrophilic when hornified, an effect that was not observed in the bulk scale analyses of the fiber. It was later determined that the fiber surface became smoother on the nanometer scale after cycles of wetting and drying, increasing the contact area between fiber and probe.

Further studies determined that there are two separate effects of hornification, the loss of water retention capability of the pulp and the smoothing of the fiber surface. Through the use of refining and heat treatment, it was proven that the changes to WRV and surface roughness are not directly linked, and that it was possible to greatly affect WRV while making little to no changes to the surface roughness on the nanometer scale. Changes in WRV are known to be driven mainly by loss of pore volume within the fiber, while these changes to surface roughness occurred on a much smaller scale. It is proposed that the free microfibrils of the fiber surface draw together during cycles of wetting and drying, forming intrafiber hydrogen bonds, laminating, and presenting a more uniform fiber surface to the AFM probe.

A small study using AFM to analyze samples of paper provided by a recycle paper mill is also presented. While the AFM was able to detect changes in the paper sample prepared in the lab, the data from mill samples varied greatly. It was determined that, due to the variability of the pulp and chemicals in the mill samples, the AFM was too sensitive to analyze the mill paper.

CHAPTER I

INTRODUCTION

Over the past decades, recycling has become an increasingly more important part of the pulp and paper industry. Environmental concerns have fueled a desire to reduce landfill usage and to decrease the harvest of trees for the production of new paper. In the United States in 1993, more paper was recycled than was sent to landfills for the first time [36]. Since then, the amount of paper recycled annually has continued to grow. The EPA estimates that, with current technology, the production of recycled paper uses 50% less water and reduces air pollution by 74%, compared to the production of new, virgin paper [22]. Each metric tonne of paper used in recycling also reduced landfill usage by three cubic meters [88].

Recycling paper presents several technical challenges for the pulp and paper industry, including the de-inking and cleaning of pulp, especially of paper from post-consumer sources. Depending on the original purpose of the furnish supplied to the recycle mill, the feed-stock can contain a myriad of chemicals, including fillers such as titanium oxide or clay, polymers to enhance the wet or dry strength of the paper, sizing agents to make the paper water-resistant, and a variety of inks and dyes used for printing. There is little uniformity in any given lot of paper to be recycled, and any of these additives can be carried through the recycling process to affect the properties of the new paper being manufactured. Most important, even with careful management and quality control, the cellulose fibers themselves undergo irreversible degradation when exposed to cycles of wetting and drying, as well as aging. These

changes are collectively referred to as “hornification,” and while the exact mechanisms are still debated, the effects are seen in recycling mills worldwide.

This thesis represents an addition to the base of knowledge about the process of hornification, and an evaluation of the current hypotheses of the mechanisms of hornification in light of this new research. A more thorough understanding of the nature of the changes a fiber undergoes during the hornification may one day help the pulp and paper industry manufacture stronger and better paper from recycled fiber. Chapter II reviews the current literature on hornification, including a brief summary of the nature of paper fibers, pulping, and recycling, and the fundamental background of the methods of analysis used in this thesis. Chapter III summarizes the specific objectives of this research, while Chapter IV presents the materials and experimental procedures used in this work. Chapter V presents the results in detail, and Chapter VI summarizes the conclusions of this research and presents a plan for future work.

CHAPTER II

LITERATURE REVIEW

Chapter I introduced the rationale for recycling and introduced the concept of hornification as a reason for the decrease in quality of recycled paper products. This literature review first summarizes the nature of cellulose fibers used for papermaking and the techniques used to manufacture these fibers from wood and recycle waste paper. It then presents the most prevalent hypotheses of the mechanisms that cause hornification, followed by a summary of the techniques used in this research to study the hornification process.

Paper manufactured from wood is composed primarily of cellulose fibers, but also can contain hemicelluloses, lignin, and extractives that were present in the initial wood. In addition, there are several common additives used in the paper industry to enhance the properties of the manufactured paper. The type of wood used to make pulp, the pulping method, and the additives used all affect the final properties of a paper sheet.

2.1 Components of Paper

The fiber for paper comes mainly from plant matter, specifically the cell walls of wood. These cell walls consist mostly of cellulose, hemicelluloses, and lignin, and also contain a small amount of extractives [10, 16, 54, 81]. Generally, 40% to 50% of the cell wall is cellulose, while 15% to 35% is lignin and 20% to 30% is hemicelluloses [20, 81]. The ratio of these components varies depending on the

species of wood, although general trends are apparent when comparing hardwoods and softwoods, as shown in Table 1 [10].

Table 1: Chemical components of hardwood and softwood

Component	Softwood	Hardwood
Cellulose	~42%	~45%
Hemicellulose	~27%	~30%
Lignin	~28%	~20%
Extractives	~3%	~5%

In general, softwoods have slightly less cellulose and more lignin than hardwoods, due to the more simplistic structure of softwoods [10, 81]. The difference in wood structure affects not only the exact ratio of these components, but also their chemical composition and properties.

2.1.1 Wood Structure

Fibers from different species of trees have different characteristics, but a primary classification is to separate pulps that come from hardwood (angiosperm) and softwood (gymnosperm) trees. Figure 1 shows a crossection of the two types of wood [81].

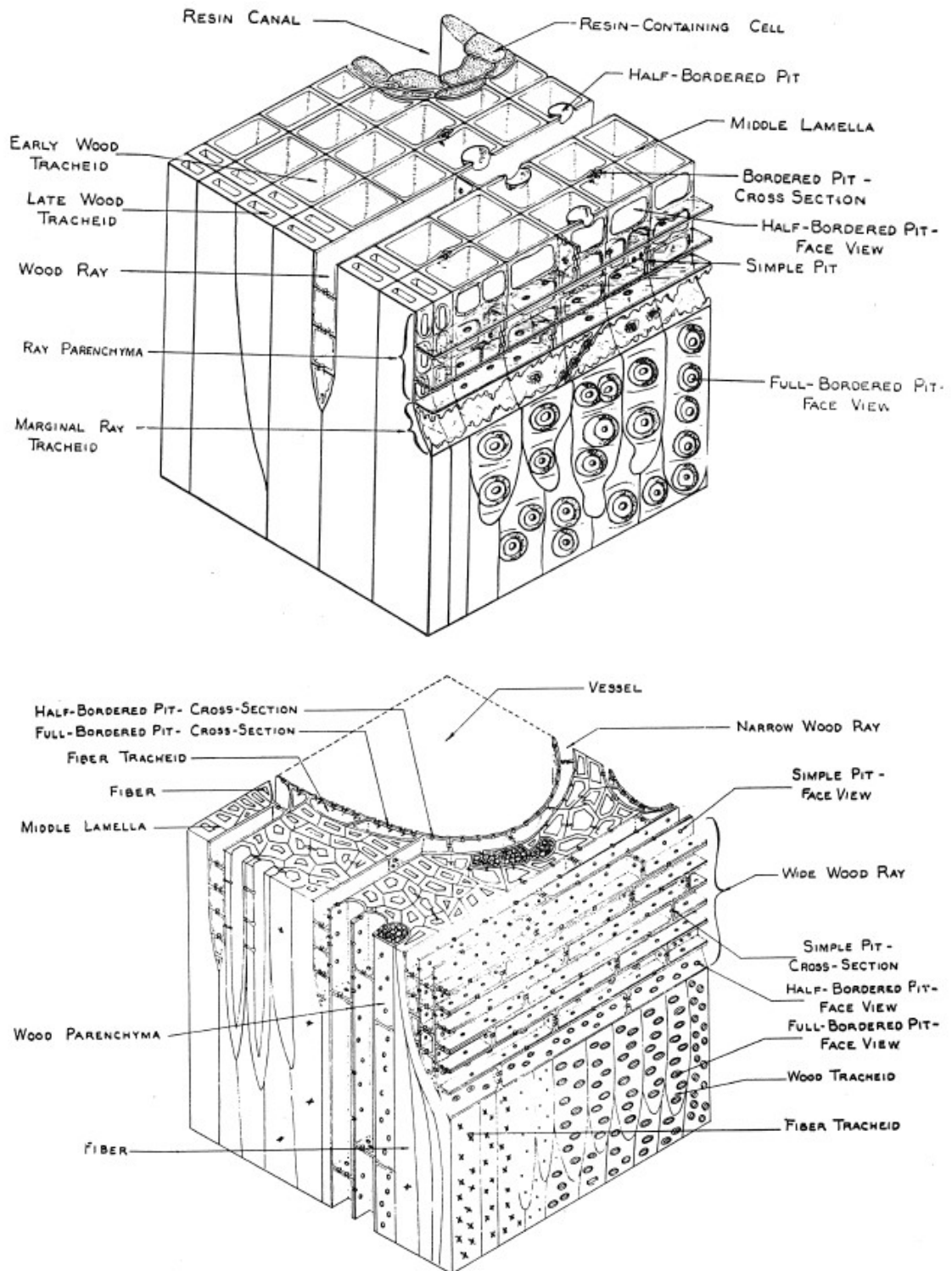


Figure 1: Diagrams of softwood (top) and hardwood (bottom)

From these diagrams, the more complex structure of the hardwood is evident.

Softwood consists mainly of longitudinal fiber tracheid cells (>90%) that give the

wood an open structure that allows for the flow of water through the tree, ray cells (5-10%), and resin cells (<1%) [10, 81]. Hardwood also possesses fiber tracheids (36-70%), but contains a large percentage of vessel elements (20-55%) and ray cells (6-20%), forming a more closed internal structure [10, 81]. Cellulose fibers come mainly from the tracheid cells. In softwood, the long tracheids yield long fibers, often 2.5 mm to 7 mm long, with larger pores and large internal voids [10, 81]. The hardwood tracheids produce fibers that are shorter (less than 1.5 mm long) and denser than softwood fibers, with smaller pores and internal voids [10, 81]. Because of this difference in fiber structure, sheets of hardwood paper are smooth but the shorter fiber leads to a lower tensile strength, and sheets of softwood paper are stronger while possessing a rough surface.

2.1.2 Cellulose

Cellulose, the primary component of wood, is a polymer chain formed of cellobiose (a linkage of two glucose molecules) base units [16]. The cellobiose units form a long, flat polymer chain that exposes a number of hydroxyl groups, bonding sites that allow the polymer chain to form a large amount of hydrogen bonds, as shown in Figure 2 [81].

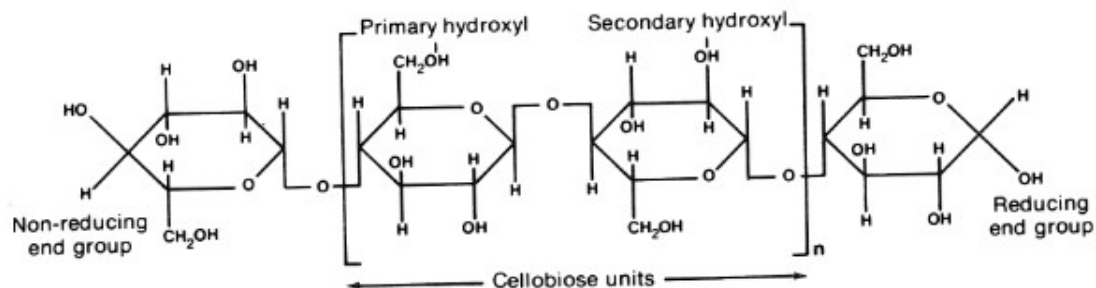


Figure 2: Cellulose polymer diagram

In wood pulps, these chains are typically from 300 to 1700 units long [42].

In nature, the cellulose chains are oriented in a parallel structure, creating “microfibrils” within the cell wall [12]. From these basic structures, an entire fiber is assembled, as shown in Figure 3 [81].

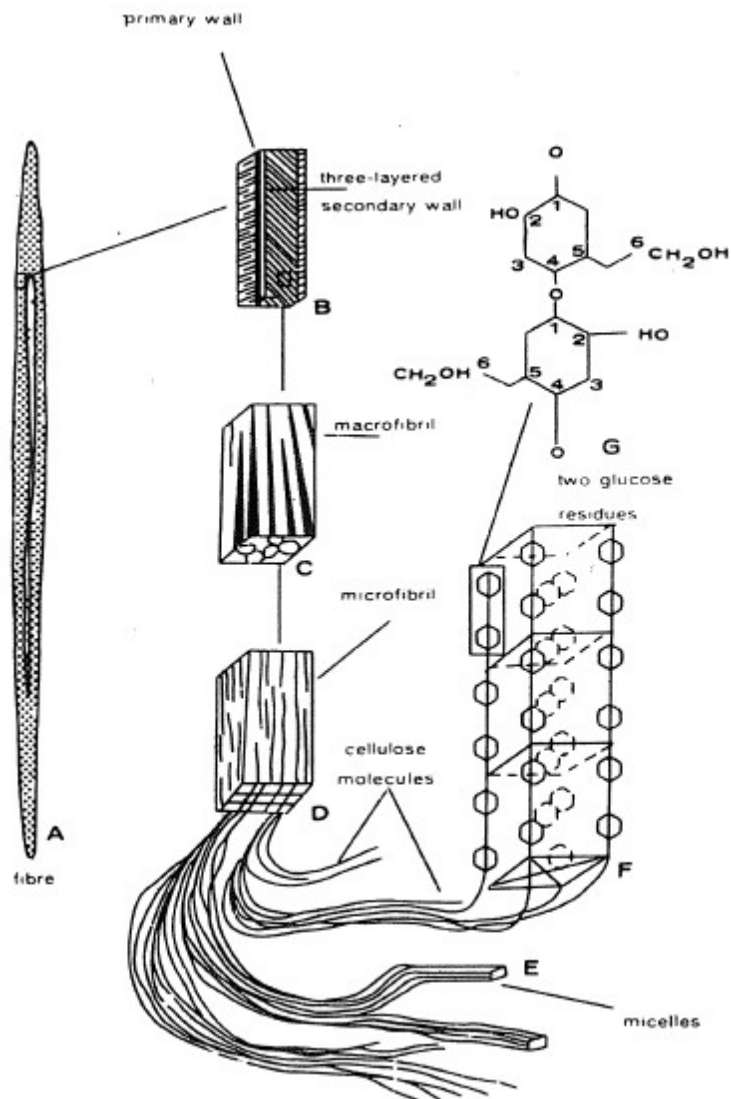


Figure 3: Assembly of a cellulose fiber

As seen in this illustration, the cellulose polymer chains that make up the fiber can be quite long, and perfect orientation of these polymers into an entirely ordered, crystalline structure is not possible.

Fibers possess both crystalline and amorphous regions, as shown in Figure 4 [81], which contribute differently to the properties of the resulting fiber [12, 14, 24, 51, 81].

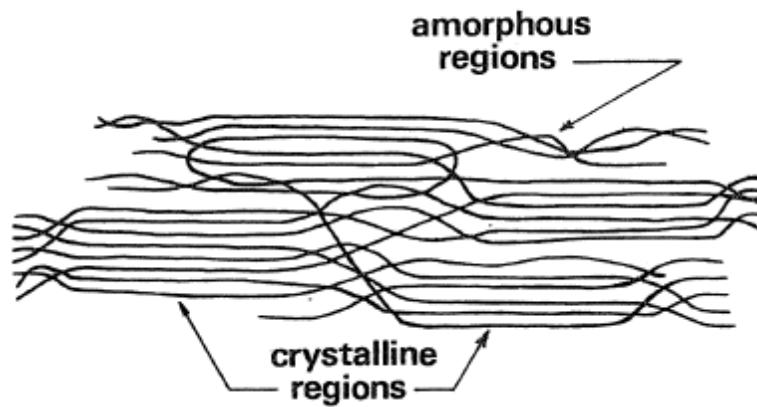


Figure 4: Polymer chain organization within a microfibril

The crystalline regions occur when the polymers' regularity allows for the formation of a neat, ordered structure joined by hydrogen bonds, while amorphous regions occur when defects or substitutions (often involving hemicelluloses) in the polymer chains prevent crystal formation [81]. This microfibril formation of cellulose is referred to as native cellulose or cellulose I, and is further categorized as cellulose I_α and I_β , which differ in terms of hydrogen bonding [51, 103]. Cellulose I_α has a one-chain triclinic structure, while cellulose I_β has a two-chain monoclinic structure. In addition to native cellulose there is also regenerated cellulose, or cellulose II. Cellulose II can be manufactured from native cellulose by breaking down the interpolymer bonds that form the microfibrils, such as by dissolving fiber and reconstituting the cellulose polymer. This reconstituted cellulose forms non-parallel polymer bonds and does not produce a microfibril structure [51].

2.1.3 Hemicelluloses

Hemicelluloses are amorphous polymers consisting of 5- and 6- carbon sugars and uronic acids that are roughly 100 to 200 units long [10, 15]. These sugars

(glucose, mannose, and galactose [the hexoses], and xylose and arabinose [the pentoses]) and acids form a myriad of different polymeric structures, some of which associate closely with cellulose and others with lignin within the wood structure [81]. Figure 5 is a model of a hemicellulose base unit with both 5- and 6- carbon sugars [17].

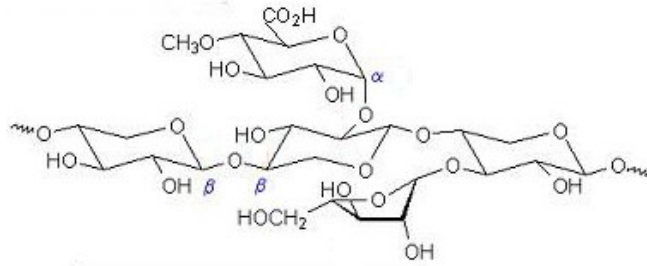


Figure 5: Hemicellulose structure

Hemicelluloses are the most water soluble of the main components of wood [15]. Because of their short chain length and prevalence of hydrogen bonds, they swell greatly and absorb a good quantity of water when wet [15]. However, hemicelluloses are also the most easily degraded compound present in wood. Any pulping process degrades or dissolves at least some of the hemicelluloses present in wood. During high yield pulping, only a small fraction of hemicelluloses may be removed, but in low yield pulping the majority of hemicelluloses are often lost [10, 16, 81].

2.1.4 Lignin

Lignin is a hydrophobic amorphous polymer consisting of phenylpropane monomers [16]. Lignin polymers are extremely complex three dimensional structures, as shown in Figure 6 [109].

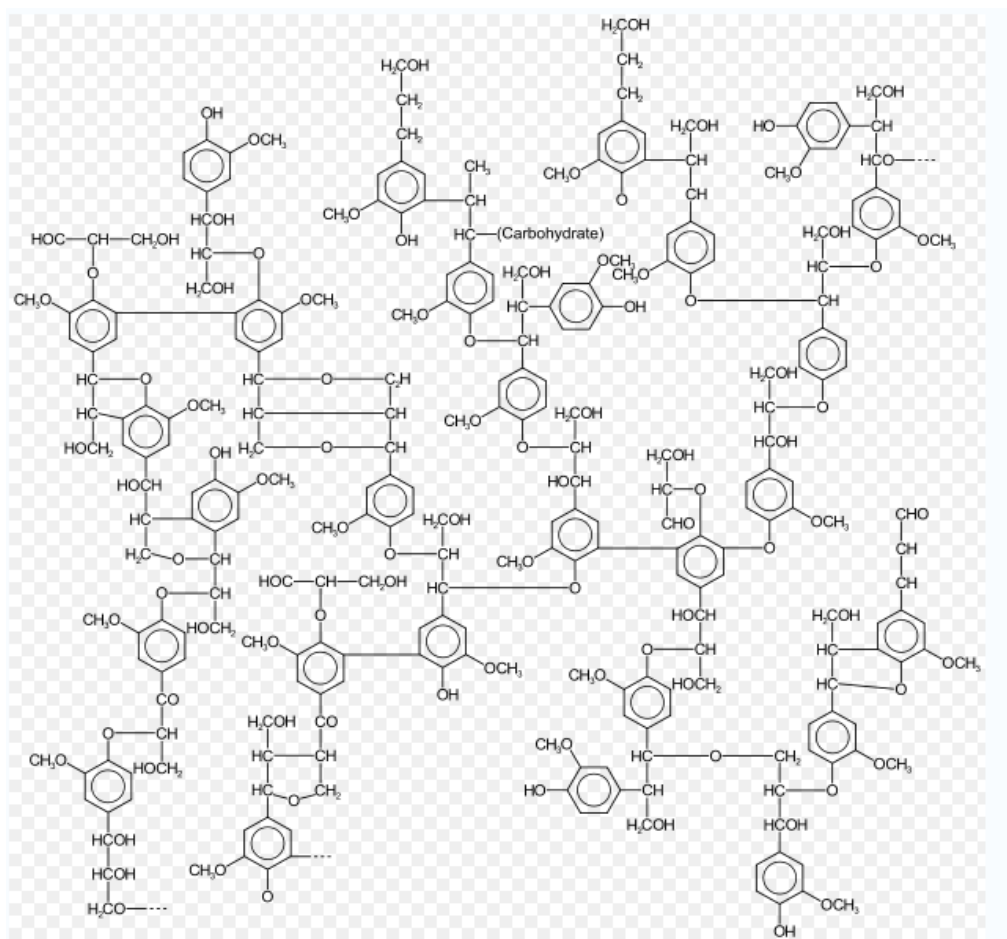


Figure 6: Possible lignin structure

Lignin polymers have a high atomic mass, but the degree of polymerization is often hard to determine because of the irregularity of the polymer structure [50]. A lignin polymer often consists of random, connected substructures constructed from the monomer units. This randomness prevents the lignin polymers from forming crystalline structures, rendering the polymer mass completely amorphous. In wood, lignin fills the cell wall, binding the cellulose fibers and hemicelluloses together [10]. The majority of lignin coats the fiber surfaces, but some lignin exists within the fibers.

2.1.5 Extractives

Wood also contains extractives in small amounts [10, 16]. These extractives, such as resins, fatty acids, turpentine, and alcohols, are mostly soluble in water or neutral organic solvents. They are liberated from the wood during the pulping process, and are often separated out and collected as byproducts.

2.2 Bonding

The strength of the bond between cellulose fibers helps determine the strength of the resulting sheet of paper. Fibers join together by forming hydrogen bonds, and the strength of the sheet can be correlated to the number of interfiber bonds formed [13, 19]. Although there are a large number of hydroxyl groups in cellulose chains [16], the majority of these are taken up by internal bonding and are unavailable to form interfiber bonds [13]. In order to achieve a strong sheet, the fibers must have a large number of free hydroxyl groups and also be able to bring them into contact [13]. The amorphous areas of the cellulose chain are hydrophilic and swell when wet, allowing for a flexible structure, while the crystalline areas remain rigid and do not allow water penetration [14]. In order to form strong interfiber bonds, the fibers must have amorphous regions, allowing for fiber entanglement to bring hydroxyl groups together and allow hydrogen bonding as the pulp dries [13]. Studies have shown that a larger average fiber pore size is linked to swellability and increased sheet strength [27]. Water penetration into the internal areas of the fiber greatly enhances the efficacy of the fiber consolidation process during paper formation, directly contributing to the number of hydrogen bonds formed [41, 55].

Hemicelluloses play an important role in bonding. Because they possess a large number of hydrogen bonds, hemicellulose chains distributed on the surface of the fiber can provide valuable linkages between two cellulose fibers [13, 15]. The presence of hemicellulose aids in fiber swelling by drawing more water into the fibers [9, 15]. However, unlike cellulose, hemicelluloses are water soluble and prone to being washed out of the fiber [81]. Lignin, conversely, inhibits the formation of good interfiber bonds. Lignin present on the fiber surface will block hydrogen bond formation, reducing the number of available bonding sites and lowering the strength of the resulting sheet [10, 81].

2.3 Papermaking

Cellulose fibers must be released from the wood structure in order to manufacture paper. There are a variety of pulping methods, including chemical methods that have a low yield but are considered to produce better paper to mechanical methods that have a high yield but produce lower quality paper with lower strength properties [10, 81].

2.3.1 Kraft Pulping

Chemical pulping methods use chemical treatments to free the cellulose from the cell wall of the wood. Because hemicellulose chains are more water-soluble than cellulose, the bulk of the hemicelluloses dissolve and are removed from the fiber structure during chemical pulping [81]. The majority of the lignin present in wood is dissolved and de-polymerized, allowing for the easy separation of the cellulose fibers [10, 16]. The most common method of chemical pulping is kraft pulping, which was

patented in 1870 and has since come to account for more than 80% of the world's chemical pulp while sulfite pulping, the other major method of chemical pulping, is employed less frequently. [43, 80]. Kraft pulping uses sodium hydroxide and sodium sulfide to delignify the wood and free the cellulose chains [43]. In most kraft pulps, the lignin content of the wood is reduced by at least 50%, which results in the loss of at least 50% of the hemicelluloses and 10% to 15% of the cellulose, resulting in a total yield of less than 50% of pulp from the wood [43]. The removal of the lignin, a hydrophobic compound, allows for excellent bonding between the hydrophilic cellulose fibers, giving paper sheets of chemically processed pulps a much higher strength than equivalent sheets of mechanical pulp.

2.3.2 Thermomechanical Pulping

Mechanical pulping uses grinding or other mechanical action to release the cellulose fibers. Thermomechanical pulp (TMP) is made by heating the wood chips with pressurized steam before grinding [80]. The grinding action separates the fibers without removing the bulk of the lignin or hemicelluloses, resulting in a very high yield (up to 97%) [80]. Mechanical pulps form paper with high opacity and good printability, but it has lower strength than an equivalent sheet of kraft pulp, and it discolors upon exposure to light due to the presence of lignin and lignin derivatives [81]. For these reasons, it is commonly used to make newsprint and other papers of low quality.

2.3.3 Bleaching

Bleaching further increases the brightness of pulp through the use of chemicals. In chemical pulps, bleaching removes additional lignin, which is dark,

resulting in a brighter sheet [10, 81]. The removal of more lignin further increases the ability to ability of the cellulose fibers to bond, which can lead to increased sheet strength, but the chemicals can damage the fibers resulting in a strength loss [10]. The chemical usage must be balanced to allow sufficient brightening without severe loss of fiber integrity. The lignin can be removed using a variety of chemicals, including chlorine compounds (such as chlorine dioxide), ozone, oxygen, alkaline hydrogen peroxide or enzymes such as xylanase, all of which degrade the lignin polymer [10, 90]. The lignin is broken down into smaller, water soluble units that can be washed out of the pulp. These small pieces, although no longer bound to the pulp, can still be further oxidized by bleaching chemicals. Therefore, bleaching processes are carried out in several stages, with washing and extraction processes between each stage to remove the partially degraded lignin fragments, in order to efficiently use the bleaching chemicals [10, 81]. Multi-stage bleaching processes can use several different bleaching methods between extraction phases in an effort to design an efficient bleaching sequence that achieves maximum pulp brightness with a minimal chemical load.

Bleaching mechanical pulps is often referred to as “brightening” because the lignin is not removed, but rather chemically altered so that it does not absorb light [10]. Brightening is accomplished through the use of either reducing or oxidizing agents to break double bonds in the lignin polymer that give it a darkened color [10]. Alkaline hydrogen peroxide (at a lower dosage than is used in chemical bleaching processes) is a common oxidizing agent used in brightening, while sodium dithionite is a common reducing agent [10]. While these two compounds can both be used to

brighten pulp, the methods required to use them effectively differ. The hydrogen peroxide decomposition reaction is catalyzed by transition metals such as manganese, iron, and copper, so removal of these metals from the pulp prior to brightening allows for more effective use of hydrogen peroxide. Similarly, sodium dithionite reacts with oxygen, so brightening processes that use it are most effective in a low oxygen environment. Excessive degradation of the brightening chemicals, due to either metals or oxygen, results in increased chemical consumption during the brightening process. Unlike bleaching, brightening processes are prone to reversion. Because the lignin is chemically altered without being removed, exposure to light and air can cause the chromophores to reform [10, 81]. This process is responsible for the pronounced aging effects seen in brightened mechanical pulps, such as the yellowing of newsprint.

2.3.4 Refining

Pulps are commonly refined to increase their ability to form interfiber bonds and strengthen the resulting sheet of paper. The refining process uses mechanical action to deform and shear cellulose fibers, increasing the ability of the fibers to bond and the strength of the resulting sheet [7, 21, 29, 32, 67]. The mechanical action of the refining process breaks the bonds holding cellulose fibers together, creating new fibrils and microfibrils as potential bonding sites [32]. The effect of the refining process depends on several factors, including the composition and swellability of the pulp and fiber as well as the conditions (such as pulp pH and consistency) under which the refining occurs [7, 32]. Refined fibers demonstrate an increased ability to retain water and form sheets of increased tensile and burst strength, but they sacrifice

drainage and tear strength and the fibers may be cut and irreversibly damaged by the refining process [29]. Likewise, there is an upper limit to the increase in paper properties gained by refining. Because refining uses mechanical action to break the bonds holding the fibers together, over-refining can destroy the fiber structure entirely [32]. Figure 7 shows a typical pattern of strength development due to pulp refining [81].

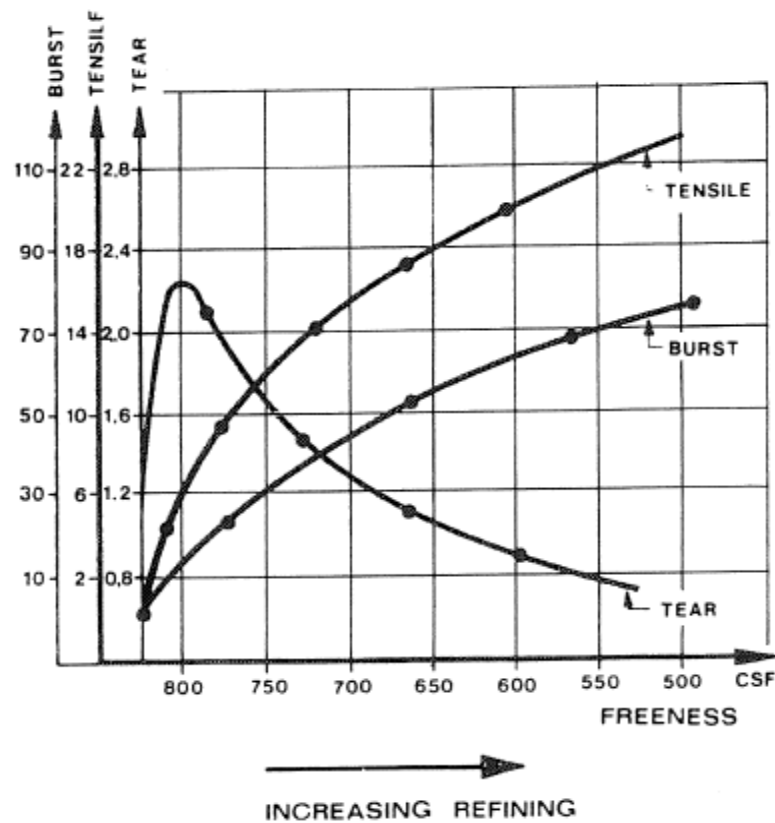


Figure 7: Strength development during refining

2.3.5 Papermaking Additives

The addition of fillers and other additives greatly affects the properties of a paper sheet. Mineral fillers, such as clay, talc, and titanium dioxide, are added to the pulp before the paper sheet is formed to enhance the optical properties of a sheet,

increasing brightness and opacity, and fill in the gaps between fibers, creating a smoother, denser sheet [81]. These mineral particles are small (between 0.5 and 20 μm in diameter for clay), and retention aids, charged polymers such as cationic polyacrylamide (cPAM), are used to link the particles and fiber. The retention aids form flocs of fibers and filler particles, and care must be taken to prevent overflocculation of the pulp that would result in poor sheet formation. The formation of flocs in the pulp also affects the drainage rate.

Sizing agents such as rosin (a type of resin) are used to control the penetration of liquid into the paper sheet [10, 81]. When mixed into the pulp, sizing agents can coat the fibers, reducing their ability to absorb water and swell, making the sheet more impermeable to water although the paper maintains a porous structure. Coats of sizing agents can also be applied to the paper surface, sealing the pores and creating paper that is impenetrable to water and water vapor, in necessary.

Strength additives are used to alter the tensile characteristics of a paper sheet. A variety of dry strength and wet strength additives can be used depending on the desired function of the paper. Dry strength additives (starches and gums) increase the burst and tensile strength of the sheet [10, 81]. Wet strength additives (water-soluble resins that reinforce interfiber bonds) increase the strength of the dry sheet, maintain their effectiveness when the paper is wet [81]. Wet strength paper maintains a minimum of 15% of its dry strength when wet. Wet strength additives are common for products like paper towels, which need to maintain their structure when wet.

The use of additives to control the properties of paper is a matter of balancing the desired sheet properties. Retention aids to increase the amount of fillers within

the sheet can adversely affect the sheet formation. Fillers enhance the optical properties and smoothness of a sheet, making it better for printing, but can adversely affect the strength properties of the resulting paper [81]. Starch not only enhances dry strength, but may also be used as a sizing agent when applied as a coating on dried paper [81]. Any chemical that is added to the paper sheet has an effect on the sheet properties and complicates the task of recycling that paper.

2.3.6 Recycling

The manufacture of paper from recycled fibers has become increasingly important in an environmentally-conscious world [3, 6]. Recovering waste fiber reduces landfill usage and provides a source of pulp for papermaking, providing proper treatment of the waste paper [6]. Recycled paper is sorted into categories, such as Old News Paper (ONP), Old Magazine (OMG), Mixed Office Waste (MOW), and Old Corrugated Containers (OCC) [3].

Newsprint and magazine paper are often TMP or a mixture of TMP and kraft pulp with the addition of fillers and, in the case of magazine paper, clay coating. Consisting mainly of mechanical fibers, these papers are prone to yellowing with age. The ink used for printing is usually a hydrophobic ink carried by a mineral oil base [10, 81]. Office paper, on the other hand, may be made entirely of kraft pulp, and covered with a variety of different inks. Printers and photocopiers use a variety of methods to print on office paper. Personal printers such as inkjets often use water-based inks to print [108]. Photocopiers and laser printers, however, melt the toner to bond it to the paper surface [110]. Corrugated paperboard, used for shipping containers and similar products, consists of softwood kraft pulp that has often not

been brightened or bleached for liner and recycle pulp for medium [81]. It often contains sizing and strength additives to improve its durability, and it may or may not have printing on its surfaces, although it does contain adhesives that hold the layers of facing and corrugation together.

As the amount of paper recycled grows, many paper products are more likely to contain at least some recycled fiber. In some products, such as tissue, aesthetics are just as important as the performance properties, while in others, such as corrugated board, the various strength requirements of the product are paramount. In order to meet the necessary specifications, careful control of the recycling process is required.

The largest problems faced by mills using recovered fiber is the lack of homogeneity in the furnish, accompanied by the need to extensively clean and treat the recovered fiber. Furnish supplied to a recycle mill can contain dirt, plastics, and metals, as well as stickies, inks, and dyes on the fiber [3]. These contaminants pose a danger to mill equipment and will adversely affect the quality of the final product.

In a typical recycling setup for newsprint, incoming waste paper (such as ONP and OMG) is repulped with water and mechanical action to liberate the fibers from the paper. The fiber length, age, and ratio of chemical to mechanical pulp in recycled furnish is never constant, and the lack of regularity in this furnish can lead to overpulped or incompletely pulped fiber, causing excessive mechanical damage to the fiber or not fully liberating the fibers from their paper structure, respectively [2, 25]. Pulping is followed by screens and cleaners to remove contaminants such as metal, plastic, and stickies. After the fiber has been cleaned and screened, flotation and

washing processes remove the ink, leaving cellulose fiber suitable for use in newsprint manufacture [3, 6]. However, this fiber is not analogous to the virgin fiber from a chemical or mechanical pulping process. This fiber has already been processed into paper at least once before, and exposed to a myriad of chemicals during the initial papermaking process and throughout its useful lifetime.

Fibers undergo a series of changes during the recycling process. The surface chemistry of recycled fibers is affected by the chemicals the pulp contains [47, 71]. De-inking chemicals, residual polymer such as retention aids in the furnish and the flotation surfactants used during de-inking, and filler can all change the surface charge of the fiber [47]. The charges of common materials present in recycled pulp is given in Table 2 [71].

Table 2: Surface charge of species commonly present in recycled pulp

Species	charge (C/g)
CaCO ₃	-3.2
Clay	-5.6
Coating	-9.1
Carbon Black	-3.3
TMP (Pine)	-11.7
CCS (Eucalyptus)	-15.8
Kraft (Pine)	-0.42
Soda AQ (Eucalyptus)	-2.4

The surface charge of the chemical additives differed greatly from those of the pulps that were analyzed. In the case of kraft fiber, which had an extremely low surface charge, the presence of inks and filler would cause a drastic increase in the observed charge of a pulp sample. The increase in the observed surface charge of recycled pulps is due to the presence of chemicals, and not to a change in the fiber itself [71]. In addition to these chemical changes, the mechanical action of repulping can damage

and shorten the fibers leading to decreased fiber strength and lower sheet tensile strength [3, 6]. Finally, the rewetting and drying of cellulose fiber causes hornification.

2.4 Hornification

Hornification is the term used to describe the irreversible changes that a fiber undergoes as it is dried and rewet. While the effects of hornification on the pulp and the resulting sheet have been well documented, the exact causes of hornification are still being determined.

2.4.1 Effects of Hornification

Hornification causes both a loss of water retention in pulp and a decrease in the tensile strength of the resulting sheet. At the most basic level, hornification is the permanent loss of swellability in cellulose fibers, leading to a loss of fiber flexibility [8, 11, 61, 73]. As has been previously mentioned, fiber flexibility and swellability are the main contributors to the strength of interfiber bonding [13, 14, 19, 27]. Fibers that have been dried more closely resemble their dried state after rewetting than they do their never-dried state. The fiber wall collapses upon the initial drying and can never fully reinflate, as shown in Figure 8 [8].

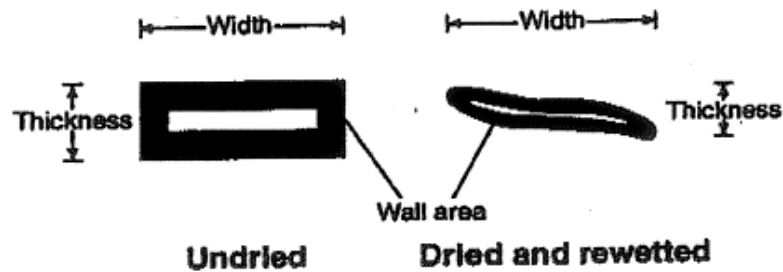


Figure 8: Schematic of undried and dried fibers

With each cycle of drying and rewetting, the fiber continues to collapse as shown in Figure 9, although the effect is the most dramatic during the initial drying step [8].

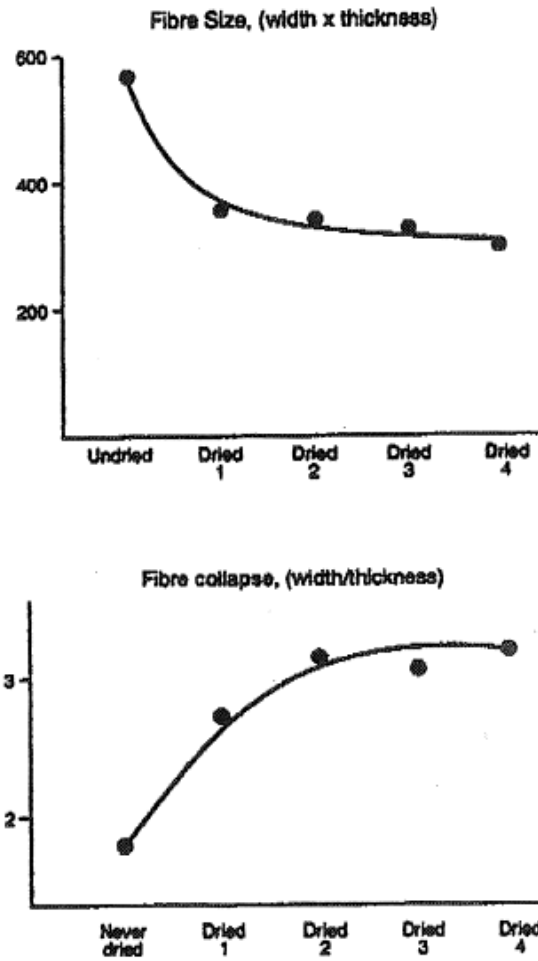


Figure 9: Fiber size (top) and fiber collapse (bottom) due to rewetting

The fiber collapse effectively levels off after two cycles of wetting and drying.

Hornification is traditionally measured by determining the reduction in the water retention value (WRV) of the pulp after a cycle of drying, although WRV measurement cannot reveal exactly how the fiber is changed. Table 3 presents some of the literature results of the degree of hornification observed on various pulp samples [102, 111].

Table 3: Degree of hornification observed in literature

Pulp	Recycling Level	WRV	Degree of Hornification (%)
Black spruce, bleached, kraft	Unrecycled	2.19	–
	1x Recycled	1.9	13.24
	2x Recycled	1.81	17.35
Hardwood, bleached, kraft	Unrecycled	1.92	–
	1x Recycled	1.10	42.71

In both of these studies, the pulps used were bleached kraft pulps, and a definite amount of hornification was observed. Such decreases in WRV are mirrored by decreases in sheet strength properties.

A decrease in tensile and burst strength, and an increase in tear strength, are observed in samples of refined, recycled kraft pulp (Figure 10 [61]).

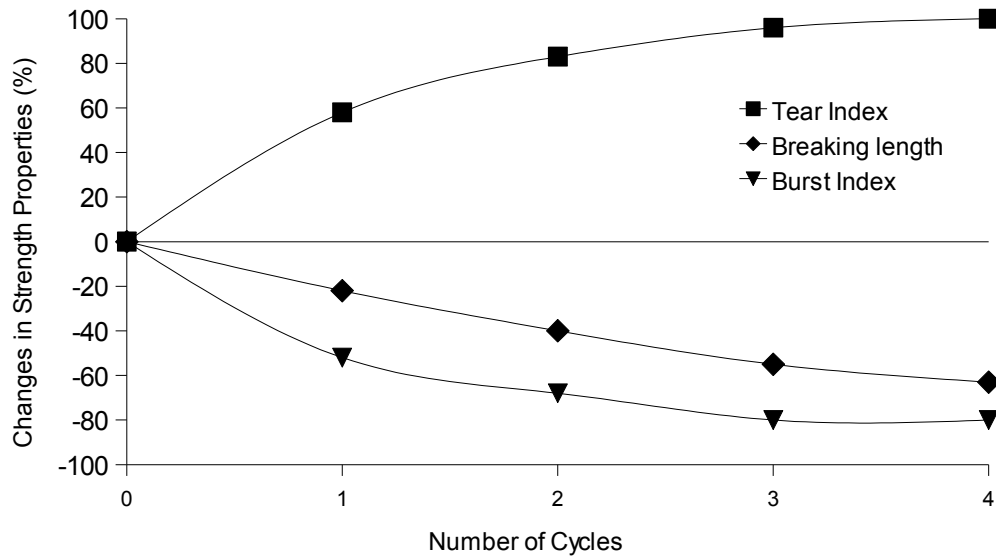


Figure 10: Effect of recycling on bleached kraft sheet properties

From this graph, it is seen that large decreases in tensile and burst strength, and accompanying increases in tear strength, occur due to recycling. Breaking length and burst index decrease due to poorer interfiber bonding, while tear index is

hypothesized to increase due to individual fiber reinforcement because of internal intrafiber bonding. The largest changes occur after the first recycle step, and level off after three recycle steps. This change in sheet properties mirrors the fiber collapse results, indicating a link between the loss of fiber swellability and the decrease in important sheet qualities.

It is known that low-yield (chemical) pulps undergo hornification to a greater degree than mechanical pulps [11, 48]. Studies of TMP routinely indicate that these mechanical pulps retain a higher degree of their initial water retention and sheet properties than kraft pulps. Figure 11 demonstrates the large variation between the relative breaking lengths TMP and kraft pulps upon recycling [35].

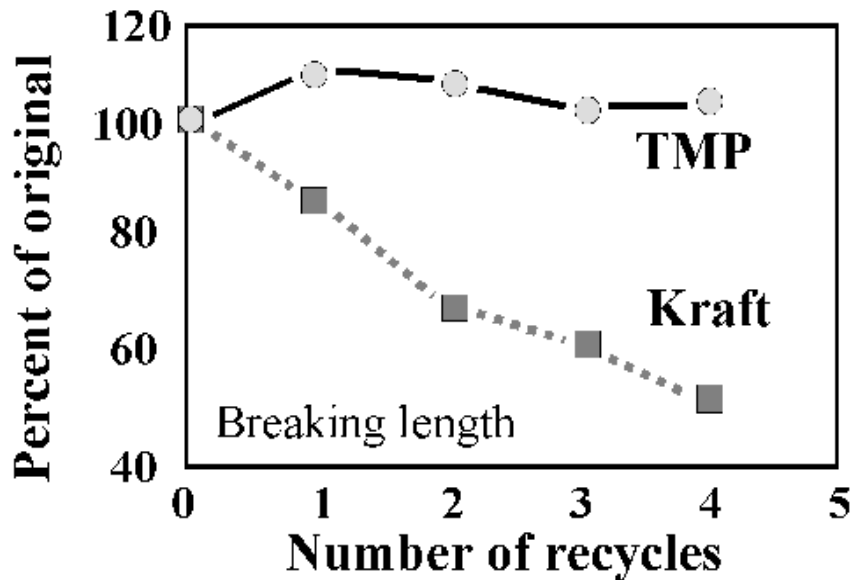


Figure 11: Comparison of TMP and kraft pulps upon recycling

While the kraft pulp lost roughly 50% of its initial tensile strength, the TMP lost no appreciable strength over the course of four recycling steps. Of course, mechanical pulps form weaker sheets than kraft pulps, so even though the kraft sheet loses a large

fraction of its strength after recycling, it still has a higher tensile strength than a sheet made from TMP [35].

It is also known that refining a recycled pulp can return the strength and water retention to the original levels. However, this is not a reversal of hornification. Rather, it is compensating for hornification by increasing the available bonding area, with a corresponding decrease in the rate of drainage [11]. As with all refining, there is an upper limit to the amount of strength increase that can be gained before the fiber is completely delaminated and destroyed.

2.4.2 Causes of Hornification

There are multiple hypotheses about the exact causes of hornification. Although all of the tests reveal similar decrease in sheet strength and water retention, the exact causes are still debated, and many of the hypotheses are contradictory. There is evidence to suggest that changes in cellulose are the primary cause of hornification. Hornification behavior is seen in cotton fiber, which consists of long cellulose chains (up to 5000 base units) [42, 48].

Some studies point to the resistance of mechanical pulps to hornification as evidence that hemicelluloses and possibly lignin inhibit any hornification effects. Hemicelluloses and lignin on the cellulose fiber surface may prevent intrafiber cellulose interaction [48, 87]. By blocking the functional groups on adjacent cellulose surface, the potential for hornification is reduced, and the rewet fiber retains a greater percentage of the available bonding strength it possessed before the initial drying. However, while hemicelluloses can aid in the development of paper strength [15],

lignin inhibits interfiber bond formation [16]. So, resistance to hornification does not automatically indicate the ability to manufacture a strong sheet with recycled fiber.

Initially hornification was thought to be caused simply by pore closure and fiber collapse, without any determination of why the pores failed to reopen when the fiber was rewet [75, 86, 99, 100]. Micropores and cracks (separations within the fiber wall) present in the never-dried fiber close completely upon drying [75, 100]. The average pore size is reduced upon drying due to the partial closure of larger pores that could never be fully restored [86, 99].

2.4.2.1 Irreversible Hydrogen Bonding

One proposed mechanism is simply an increase of intrafiber hydrogen bonding, holding the fibrils and microfibrils together, preventing the fiber from swelling, and reducing the number of potential interfiber bonding sites [86, 99]. Figure 12 is a model of fiber swelling developed to explain hornification behavior [48]. In this figure, state A represents a dry fiber, while state D represents a fully wet and expanded fiber. According to the hypothesis of irreversible hydrogen bonding, the microfibrils that make up the fiber would bond together during drying, and prevent expansion back to state D upon wetting, instead allowing only partial swelling to states B or C.

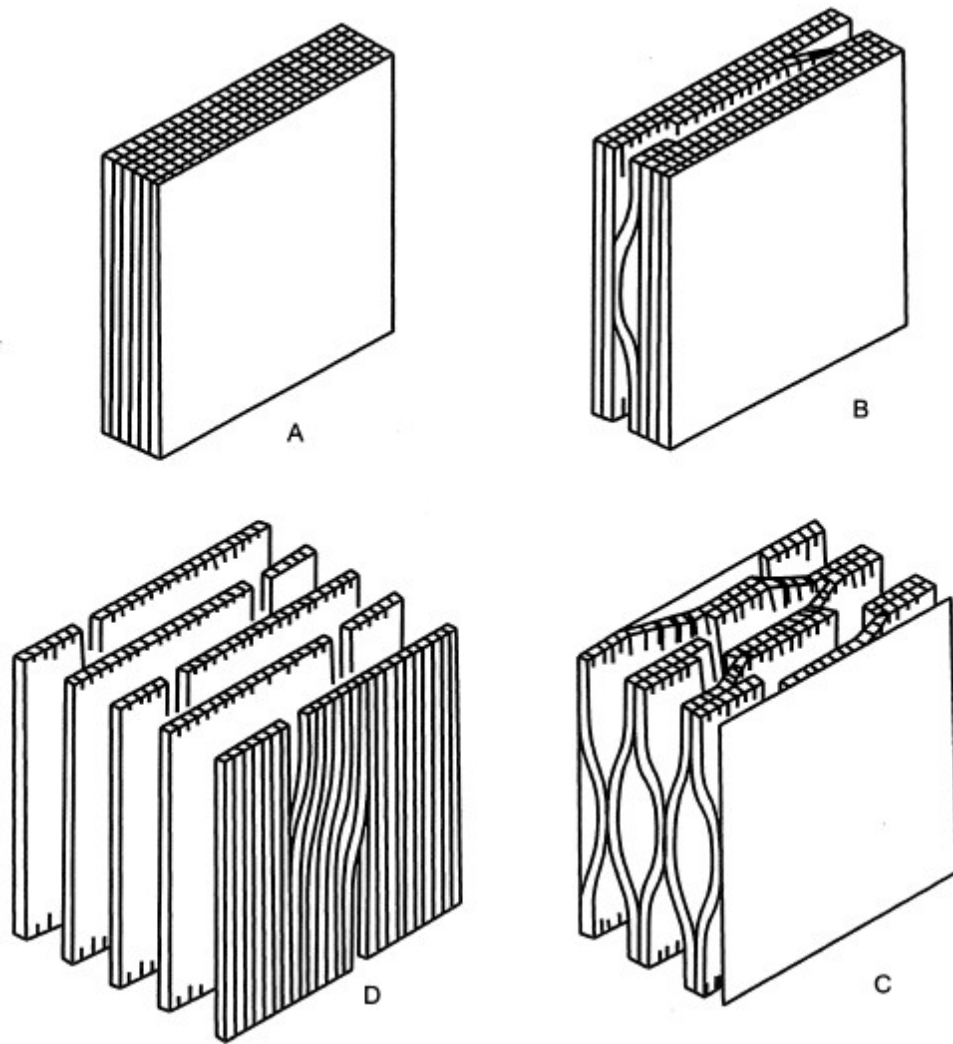


Figure 12: Fiber swelling model

A fundamental assumption of the irreversible hydrogen bonding hypothesis is that there are several types of hydrogen bonds, some of which are relatively weak and others that are fairly strong and capable of withstanding immersion in water without breaking [56, 59]. However, there is some question as to whether enough hydrogen bonds, even the strongest of which are relatively weak bonds, would remain unbroken and significantly prevent swelling when the fiber was rewet [26].

2.4.2.2 Formation of Covalent Bonds

A second hypothesis, that there are chemical changes occurring within the fibers, is also considered. Water can completely penetrate amorphous areas of a cellulose fiber by breaking hydrogen bonds, causing the swelling and flexibility that leads to good interfiber bonding [13]. However, covalent bonds that hold carbohydrate chains within the fiber together are not susceptible to such easy breakage [4, 5, 11, 26]. The removal of water brings neighboring cellulose chains into close proximity, allowing for a crosslinking reaction to occur [4, 11]. One such reaction is between a hydroxyl group and a carboxylic acid group, forming a lactone [26]. Similar reactions with aldehydes or ketones would form hemiacetals and hemiketals, respectively [11]. The lactone would remain unbroken after rewetting, and prevent the bound cellulose chains from separating and swelling. The effect of crosslinking has been demonstrated using extreme heat and catalysts to drive the crosslinking reaction, resulting in decreased fiber swellability, but also causing an increase in wet strength and a reduction of modulus of elasticity in the treated sheets [4, 11]. However, there is no direct evidence for the crosslinking reactions in hornified fibers, such as a decrease in the number of carboxyl groups present on the fiber to account for lactone formation [30, 63].

2.4.2.3 Fiber Crystallinity

An increase in the fiber crystallinity is a third popular hypothesis about the effect of hornification on the fiber structure. The crystalline cellulose in the fiber, being more highly ordered than the amorphous regions, is less susceptible to water penetration and has fewer available hydroxyl groups for interfiber bonding [13].

Several studies show an increase in the size and number of the crystalline regions within fibers due to drying and aging [16, 23, 34]. However, there is competing research that demonstrates a decrease in cellulose crystallinity with aging [56, 62]. There is some NMR evidence for cocrystallization as a mechanism for increasing the size of the crystalline regions during drying, causing an increase in crystal size without significantly reducing the size of the amorphous regions [63].

2.4.2.4 Hemicellulose Loss

While the majority of studies focus on the changes in cellulose due to hornification, there is also research into other possible effects. Hemicellulose loss, for instance, is one possible cause of the loss in water retention and bonding strength [34, 57, 83]. Hemicelluloses aid in fiber bonding and are the most hygroscopic of all the chemicals in pulp [10, 15, 48]. Removal of the hemicelluloses due to washing or chemical conversion would therefore have an adverse affect on pulp properties. Removal could occur simply due to hemicellulose dissolution in water [34]. However, chemical conversion of the hemicellulose, such as to a furfural polymer, is possible and would cause a drop in swelling and bonding potential [57, 83]. Hemicellulose behavior is complicated, and it is possible to remove or alter a significant amount of hemicellulose chains from pulp without perceptibly diminishing the paper strength [61]. The effects of hornification are too repeatable to be caused predominantly by hemicellulose-related factors.

2.4.2.5 Surface Inactivation

There is also some research into the inactivation of the cellulose fiber surface by extractives and fatty acids within the pulp. These chemicals remain trapped within

the fiber during the initial pulping process, but are then drawn to the surface over time and remain there during repulping [61, 91]. Much like lignin, these extractives could block the formation of hydrogen bonds and prevent interfiber bonding. However, this hypothesis does not explain the degree of hornification seen in chemical pulps, which have the majority of the extractives removed during the pulping process, and runs counter to the arguments that lignin inhibits hornification by preventing intrafiber cellulose interactions by blocking some of the cellulose fibers' bonding sites [87].

2.4.2.6 Cellulose Chain Cleavage

Hydrolysis of the cellulose chains, reducing the chain length (the average degree of polymerization) may be another contributing factor to the strength loss of recycled pulp. The failure mechanism in virgin paper is most often a failure of the interfiber bonds, while in recycled paper, the failure of individual fibers is also observed [46, 52, 53]. Direct analysis of single fiber tensile strength after artificial aging confirms a decrease in single fiber tensile strength [52]. Such cellulose chain cleavage is caused by hydrolysis of the cellulose polymer, and is aided by paper acidity [72]. However, while chain cleavage is seen in several studies, it is not a universally observed effect. It is seen most often in aging studies on dry paper samples, while studies on drying determined that standard drying rates and temperatures did not decrease the degree of polymerization of the cellulose fibers [84]. Hydrolysis is generally assumed to be a process more associated with aging, especially at elevated temperatures and humidities as seen in Figure 13, and does not

account for the degree of hornification seen in samples prepared without being aged [118].

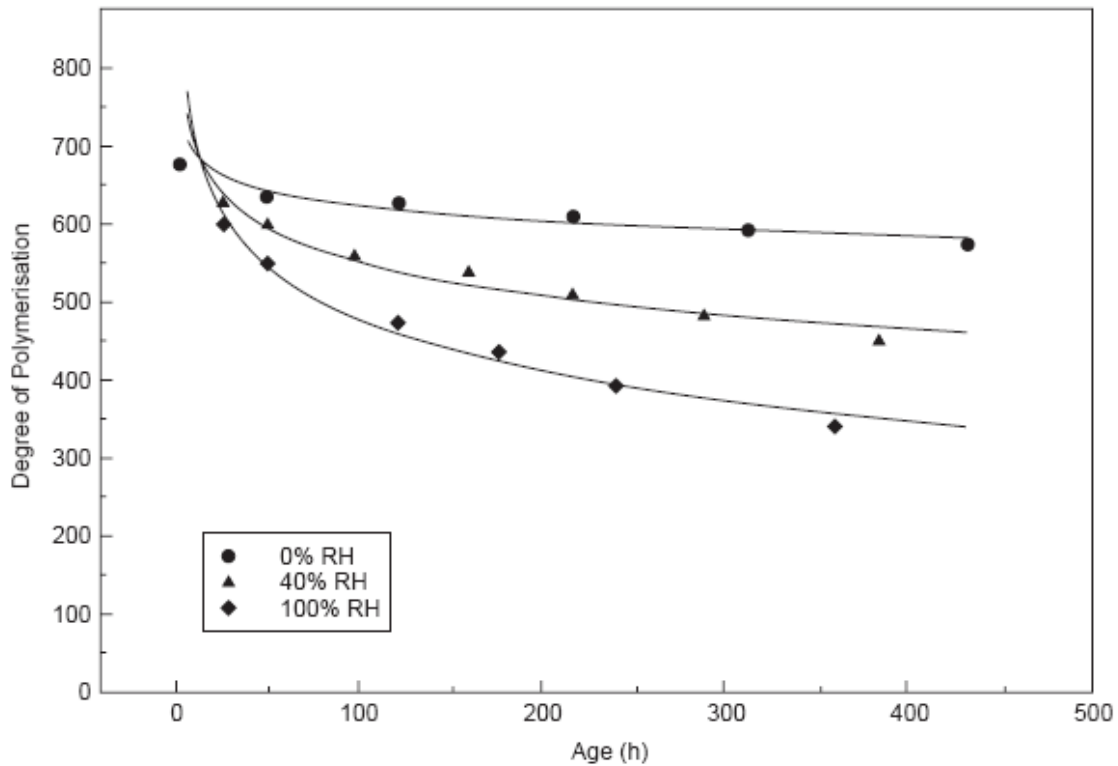


Figure 13: Chain scission due to aging at elevated humidity

2.4.3 Rate of Hornification

In order to better understand the mechanisms behind hornification, the triggering causes of hornification have also been researched. Measured by change in water retention, on a paper machine hornification begins initially during the pressing of the wet pulp, and continues through the drying of the sheet, while the sheet contains between 45%-60% solids [106]. Hornification can begin only after the amount of water in the fiber drops below the fiber saturation point, the volume of water needed to completely fill the fiber's pores, and stops once enough water has been removed to stop driving the hornification process. Temperature can play an

important role in hornification by increasing the rate of water removal. It has been shown that faster drying causes a greater degree of hornification than slower drying in a cooler environment [37, 85, 116]. However, it is not necessarily temperature, but rather an increase in the rate of water removal, that causes excess hornification [48].

2.5 Methods of Analysis

There are several standard methods of analysis used to define the properties of pulp in industry, including water retention value, freeness, and coarseness. Today, newer analysis methods offer more powerful insights into the nature and behavior of fiber and lead to a more exact understanding of the forces at work within a sheet of paper.

2.5.1 Water Retention Value

Water retention value (WRV) is a measurement of the affinity of pulp for water [38]. WRV is commonly referred to as a measure of “bound water,” water chemically attached to the fiber, although it is not. It is a measure of the water trapped within a fiber mat, both within individual fibers and the interfiber spaces, such as water trapped within fiber pores, which is held in place by capillary forces rather than chemical attachment to the fiber [38, 76]. WRV correlates to several important sheet properties. For example, it is known that, in refined pulps, an increase in WRV correlates to an increase in the sheet breaking length [76]. WRV is also used as a gauge of the swellability of a given fiber sample [106], and therefore it has become the method most commonly used to measure the degree of hornification in a pulp.

2.5.2 Freeness

Freeness is a measure of how quickly water is able to drain from pulp. A low freeness value indicates poor drainage and a slower sheet production speed in a paper mill [10, 81]. With better drainage a paper machine can operate at higher speeds, but there is a trade-off. Refining decreases freeness while increasing WRV. Refining processes are therefore a balance between increasing WRV, which represents an increase in sheet strength [76], and maintaining a high freeness in order to keep production speed at an acceptable level. The standard freeness test in North America, the Canadian standard freeness measurement, can be done rapidly with a small amount of fiber [106]. Because of this, freeness is the common method of determining the level of refining of a pulp sample.

2.5.3 Coarseness

While not as common as WRV or freeness measurements, fiber coarseness also measures an important variable: the weight of the fiber per unit length [18, 70, 79, 117]. Coarseness is affected by a range of variables, including fiber crosssection and cell wall thickness and density. Higher coarseness values indicate a thicker or denser cell wall and increased fiber strength [70]. Coarser fibers are less flexible when wet, which can inhibit fiber entanglement and the formation of interfiber bonds [117]. Pulps with high coarseness also have fewer fibers per unit weight, producing a paper sheet with larger void spaces and fewer interfiber bonds, leading to decreased sheet strength [117]. Coarser fibers also feel rougher to the touch, and are less suitable for printing because the rough surface does not take ink smoothly [70]. Less coarse fibers are used for printing paper and especially tissue, which needs a smooth

surface and high tensile strength at a lower basis weight [18]. All other variables being equal, fiber coarseness is inversely related to WRV, where fiber swelling is inhibited by the denser cell wall [70].

2.5.4 Fiber Length and Pulp Fines Content

Fiber length is dependent upon the species of wood, but is generally longer for softwood fibers than hardwood fibers [10, 81]. However, mechanical damage to the fibers from pulping and refining can cause small pieces of the fiber to break off, increasing the fines content of the pulp and decreasing the average fiber length [29, 32]. Monitoring both the fiber length and fines content is a method to determine the amount of mechanical damage to a fiber sample due to processing.

2.5.5 Tritium Tracer Analysis

The tritium tracer technique was developed by Dr. Frances Walsh to determine the bound water content of pulp samples [104]. Tritiated water is introduced into the pulp solution and allowed to reach equilibrium, then all free water is removed from the pulp sample by washing with acetone. The use of acetone washes ensures that all free water is removed from the pulp, and only bound water remains. The tritium containing pulp is then washed with water whereupon the tritium transfers to the water. The wash water is then counted for radioactivity with a scintillation counter and the level of tritium determined. The partition coefficient, the distribution of the tritium between the water and the pulp, is then determined. These partition coefficients allow the relative amount of bound water in multiple samples of pulp to be compared. Unlike WRV, this technique measures only bound water, water that

cannot be removed even with repeated acetone washes, and not pore water or water trapped in the fiber mat and held in place by capillary forces.

This technique has been used to determine the effect of refining on fiber surface area. Table 4 highlights some preliminary work using this method to measure the tritium distribution between pulp and water (K_{pw}) with a sample of bleached softwood kraft pulp.

Table 4: Tritium tracer analysis of refined pulp

Refining level (revolutions)	CSF (mL)	K_{pw}	WRV (g/g)
0	676	0.09	1.78
2500	464	0.22	2.14
5000	358	0.32	2.26
7500	261	2.09	2.31
10000	235	3.54	2.37

From this data, it is apparent that the tritium tracer technique can be used to track changes in the fiber due to refining. While freeness and water retention progress linearly, the K_{pw} measurements undergo a large change under 300 freeness. Dr. Walsh attributed this sharp increase to delamination of the fiber, an unraveling of the fibril and microfibril structure that unrefined fibers possess. This hypothesis was based on several pieces of supporting evidence: fiber saturation point and microscopy images of the fiber.

Fiber saturation point (FSP) measurements, another method of measuring bound water, also reveal this type of behavior when used to analyze refined fibers. FSP measurements do not measure water trapped within fiber pore structures like water retention measurements, but instead measures only the water bound to the fiber.

Historical measurements of FSP show a similar trend in refined fibers as these K_{pw} experiments, as shown in Figure 14 [76].

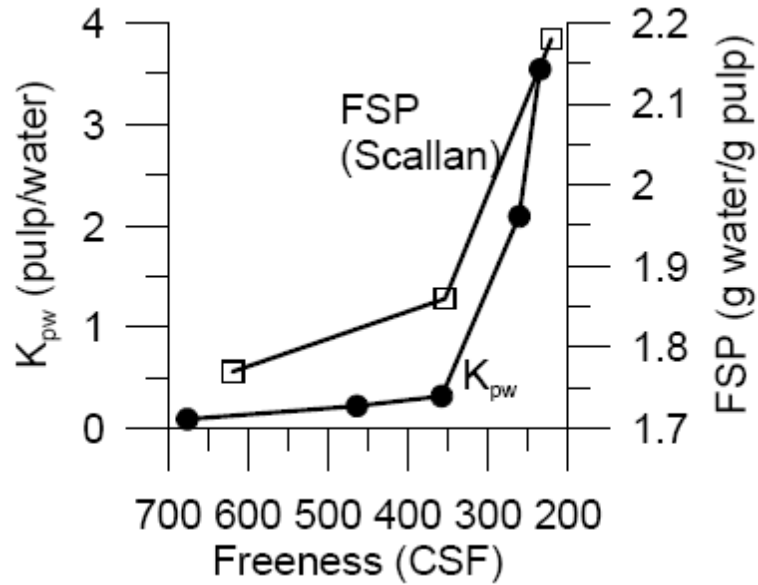


Figure 14: K_{pw} results compared to historical FSP data

Both the FSP and K_{pw} data indicate that the refined fibers undergo a drastic change after being refined to a freeness below 300 mL. Evidence of this change was further detected by taking light microscopy images of the refined fibers. The images of the fibers at freenesses of 358 and 261 mL reveal noticeable changes in the fiber.

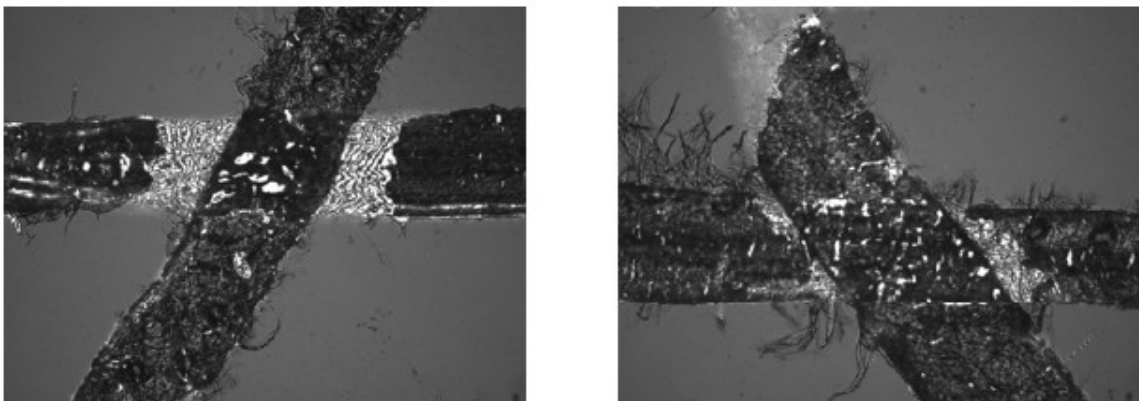


Figure 15: Light microscopy images of refined fiber at 358 mL CSF (left) and 261 mL CSF (right)

There is much more visible damage to the fiber at a freeness of 261 mL. This delamination increases the surface area of the fiber greatly, exposing more surface and allowing for greater interaction between the water and fiber, driving the increase in FSP and K_{pw} . However, the damaged areas of the fiber do not expose any complex pore structures that would drive a similar increase in the WRV measurements.

Further work revealed that there are three zones of refining, as shown in Figure 16, which shows the changes to fines content, K_{pw} , WRV, and FSP of bleached kraft pulp as it is refined from 700 mL CSF to less than 100 mL CSF.

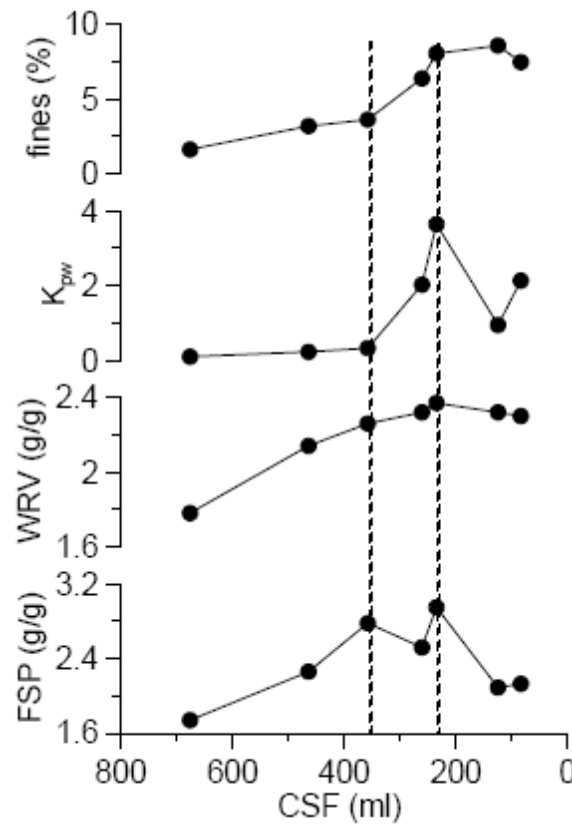


Figure 16: Effect of refining on FSP, WRV, K_{pw} , and fines content

There is an initial zone above 350 mL freeness that opens up the fiber surfaces, increasing the surface area without excessively damaging the fibers. However, continued refining causes the fibrils to delaminate, detected by sharp increases in K_{pw} and FSP, although WRV and CSF tests are not sensitive to the delamination effect. When destruction of the fiber begins, there is an increase in the fines content of the pulp as small bits of the fiber are worn away by the refining action. In this zone, the surface area of the fiber increases as large portions of the fiber delaminate, as shown in the SEM images of Figure 17.

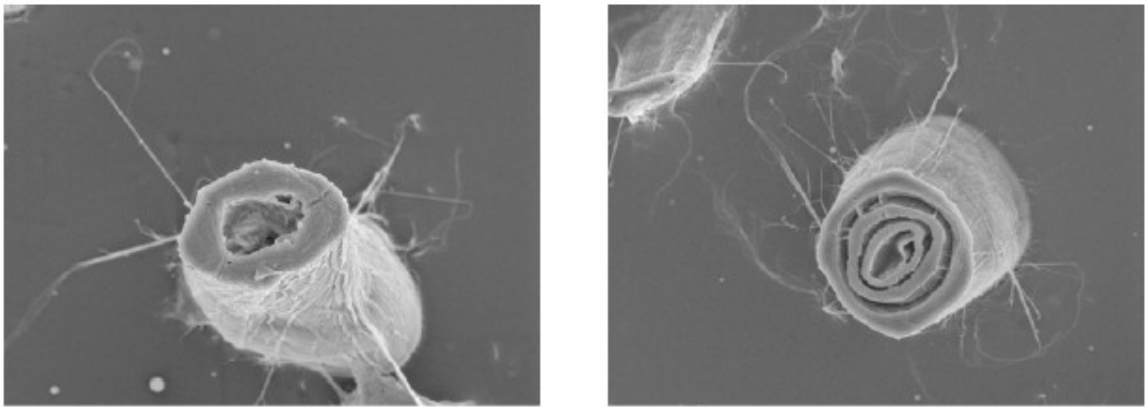


Figure 17: SEM images of refined fiber at 358 mL CSF (left) and 261 mL CSF (right)

The water between the delaminated layers is not merely bound, but contained. This containment gives the water a highly ordered structure and prevents its removal during FSP and K_{pw} analysis. Eventually, below a freeness of approximately 220 mL, further refining begins to cause complete destruction of the fiber structure and the loss of the areas of contained water, and the K_{pw} and FSP measurements drop while the WRV measurements level off.

2.5.6 Atomic Force Microscopy

The atomic force microscopy (AFM) technique was developed in 1986, and offers powerful insights into surface topography and chemistry [36]. By measuring the interactions between carefully manufactured probes and the sample surface, the surface can be mapped and the surface chemistry deduced [31]. An AFM probe is a cantilever with a tip of precisely determined chemistry and geometry [36]. Information about the sample is gathered by measuring the deflection of the cantilever as the tip interacts with the sample surface. The majority of modern atomic force microscopes use optical sensors, reflecting a laser off the back surface of the cantilever, to measure the deflection [31]. Figure 18 is a schematic of a typical AFM setup.

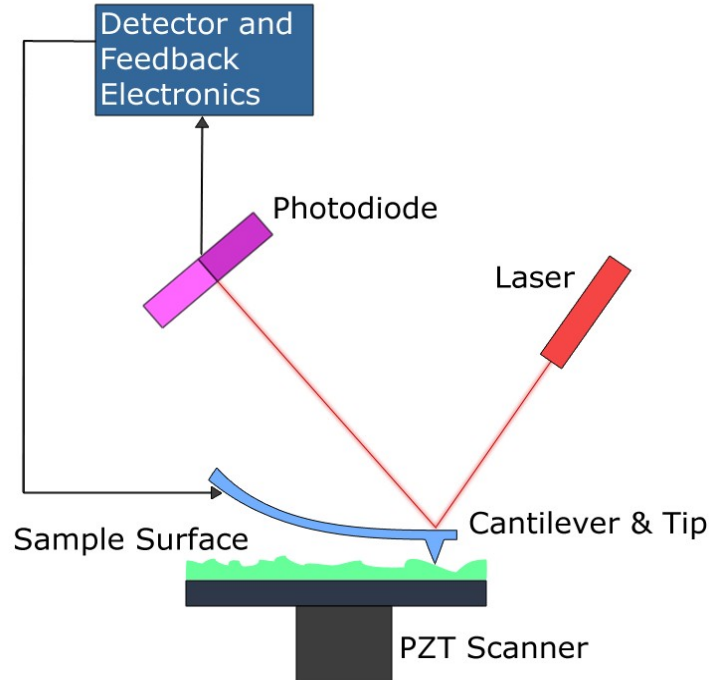


Figure 18: Schematic of typical AFM

2.5.6.1 Imaging

Topographic imaging of a sample surface can be carried out in different ways. The tip can be brought into contact with the surface and dragged across while maintaining a constant cantilever deflection, known as contact imaging [31]. The AFM raises or lowers the tip to keep the force constant, and draw a topographic map of the surface. However, damage to the tip and surface is common using this approach. Softer surfaces can be etched or distorted under the strain applied by the probe, and the probe itself can warp under the lateral forces applied [31]. In order to minimize surface and tip distortion, dynamic imaging is often used [28, 64]. The cantilever is allowed to oscillate at its resonant frequency and brought close to the sample surface, and the change in oscillation from interaction with the surface as the tip moves is used to draw the image. This prevents excessive wear on the tip due to continued surface contact [28].

The size and geometry of the AFM probe play an important role in the accuracy of any imaging, no matter which technique is used. The most accurate imaging is possible when only the end of the tip comes into contact with the surface of the sample. Small, sharp changes in the surface can cause extraneous contact with the sides of the tip, leading to inaccurate mapping of the surface. Figure 19 demonstrates how a sharp spike in the sample surface can be distorted [31].

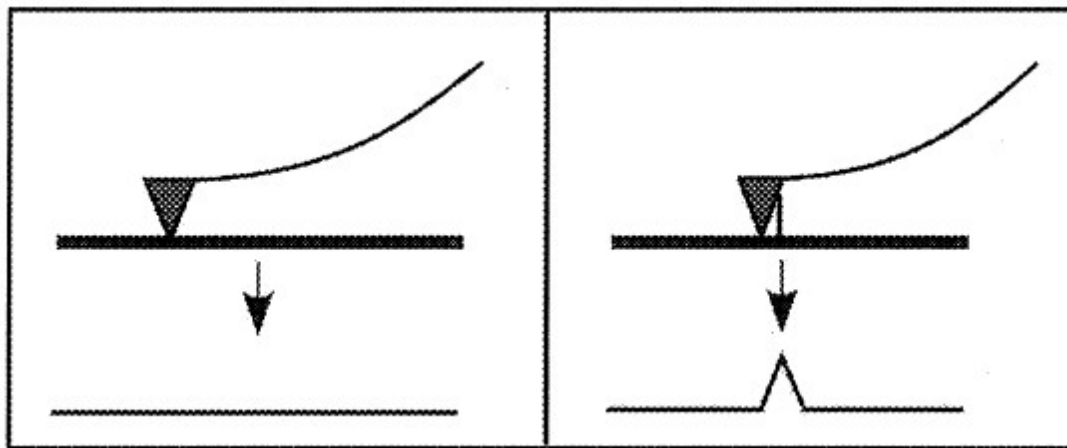


Figure 19: Image distortion during topographic mapping

Because the probe makes contact with the projection on its side rather than at the tip, the geometry of the spike is broadened. The spike is also smaller than the probe, so in effect the surface is imaging the probe [31]. In order to obtain accurate images, the AFM tip should be long and narrow to avoid surface contact with the side of the tip, and the radius of curvature at the end of the tip should be smaller than the surface features being imaged [31, 64].

2.5.6.2 Force Measurements

Measuring the strength of the interaction between the tip and surface is a common method to determine the chemical nature of the sample [31, 60]. Because the tip chemistry is controlled, the strength of the adhesion of the tip to sample surface can reveal information about the surface chemistry. Figure 20 shows a typical pull-off force curve, with the tip position shown [31].

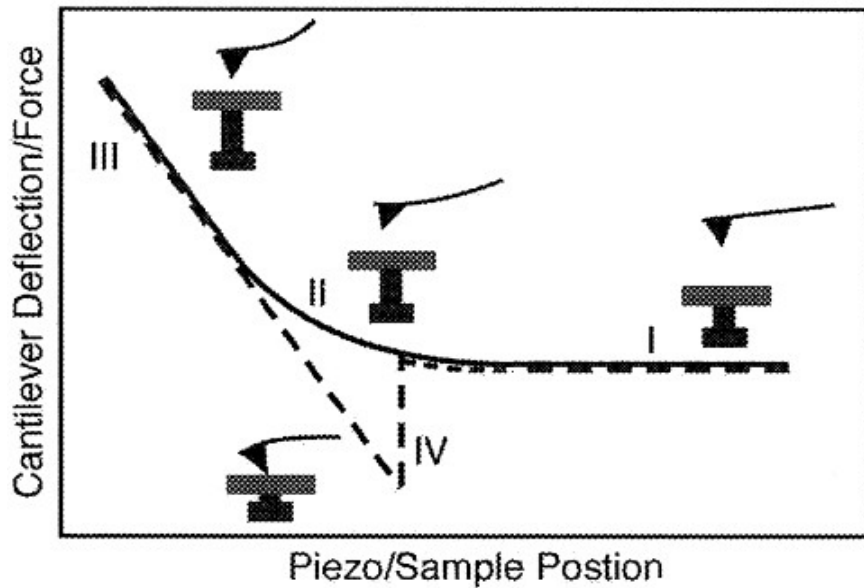


Figure 20: Typical force curve

The solid line indicates the probe's approach, far above the surface in region I. In region II, the tip approaches the surface and begins to interact, while in region III the tip is in contact with the surface and the deflection increases linearly as more force is applied. The dotted line indicates the retraction of the tip. The adhesion between the tip and surface causes the tip to deflect down until the force exerted by the cantilever exceeds the adhesive force, causing the tip to release. The adhesive force measurement is the difference between the tip at maximum deflection and the tip at rest. Figure 21 shows the dominant forces interacting between the surface and tip as a function of distance [49].

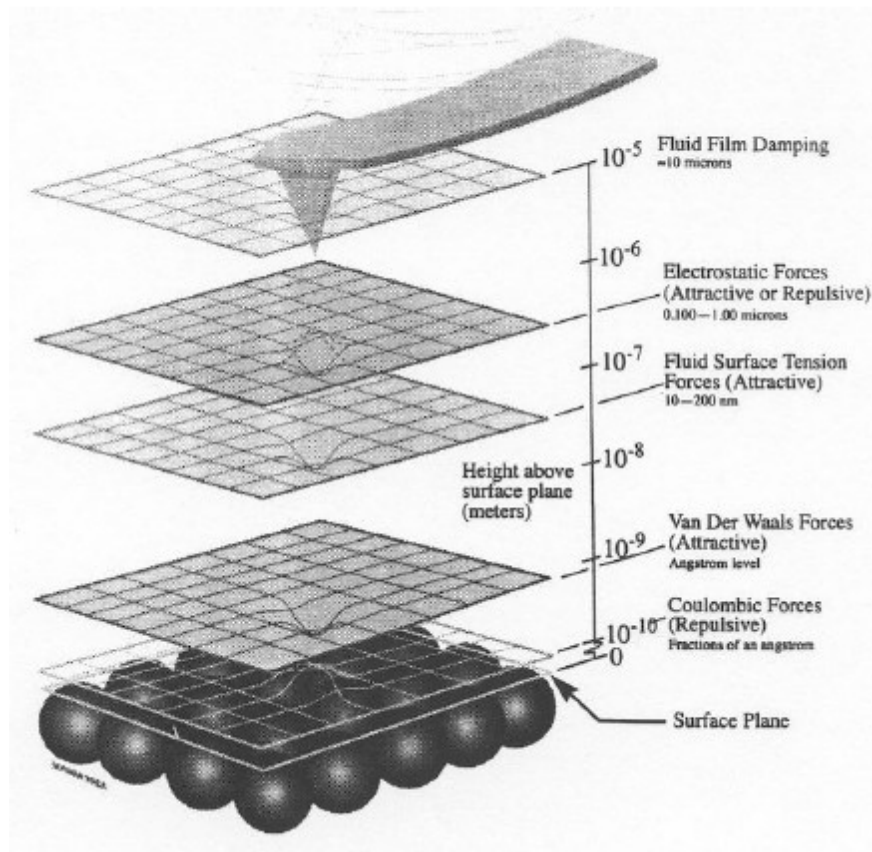


Figure 21: Tip-surface interaction forces as a function of separation

As can be seen from this diagram, different forces dominate tip-surface interaction as the tip approaches the sample surface. At a large distance, any interactions between the tip and surface are so weak that they are damped by the fluid medium around the sample, even air. Closer to the surface, any present electrostatic forces attract or repel the tip until the sample is within 200 nm of the surface, when surface tension effects dominate. When the sample is within an Angstrom of the surface Van der Waal's forces and Coulombic forces are present.

There are several variables that must be controlled in order to gather useful AFM data. Force measurements depend both on the chemistry of the interaction and

the contact area between the tip and surface [36, 61]. Tips of similar chemistry and varying radii of curvature have been used to demonstrate the dependence of the adhesion measurement on contact area [39, 40, 89, 115]. Without an accurate understanding of the sample surface, there is no way to distinguish a change in chemical interactions from a change in the area of contact.

For AFM measurements in air, humidity is one of the most important variables that affects the chemical interaction between the probe and sample [39, 45, 78, 89, 112, 113]. For hydrophilic surfaces, the most common effect of increased humidity is a tendency for water to condense at the point of contact between the tip and surface, forming a capillary bridge [39, 78, 112, 113]. As humidity increases, the amount of condensation will increase as well. For hydrophilic surfaces, the measured surface adhesion increases with humidity, as seen in Figure 22 [89].

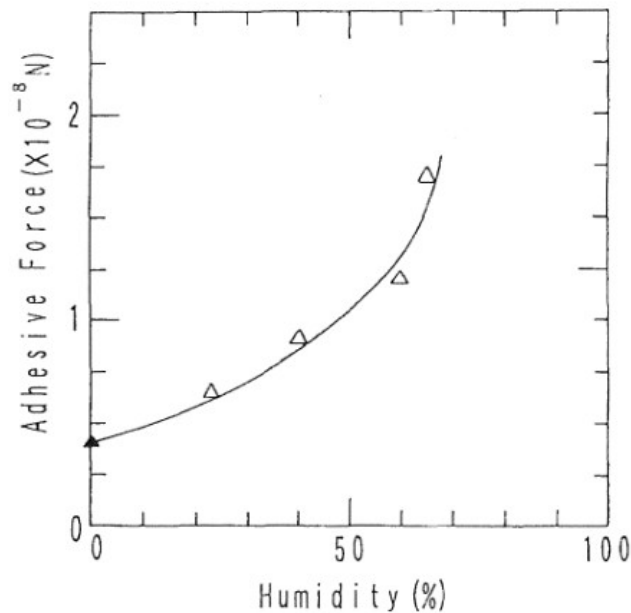


Figure 22: Surface adhesion vs. humidity using a silicon nitride tip and lithium fluoride crystal

At 0% RH, in this case in ultra-high vacuum, no water is present to form a capillary bridge. With increasing humidity more water condenses, a larger capillary bridge is able to form, and the force required to break the bridge increases. In order to remove the influence of capillary forces, samples must be analyzed without water present, such as in ultra-high vacuum, or completely submerged in water so that capillary bridges cannot form.

In addition to condensation effects, the presence of water can alter the structure of the surface, especially in extremely hygroscopic materials, such as hydrogels [45]. With increased humidity, hydrogel polymers absorb large amounts of water, greatly increasing in volume and becoming softer and more viscoelastic [113]. However, despite the variation in surface adhesion seen with alterations in humidity, adhesion measurements are demonstrably repeatable if humidity is held constant [39, 45, 78, 89, 112, 113].

2.5.6.3 AFM Analysis of Cellulose and Paper

Since the AFM has been introduced, several studies have been conducted using plant matter and paper fibers [68, 69, 114]. Several different studies used AFM imaging techniques to determine the structure of cellulose fibers and the interaction of cellulose, hemicellulose, and lignin. One study on straw revealed a complex interweaving of these compounds in straw cell walls [114].

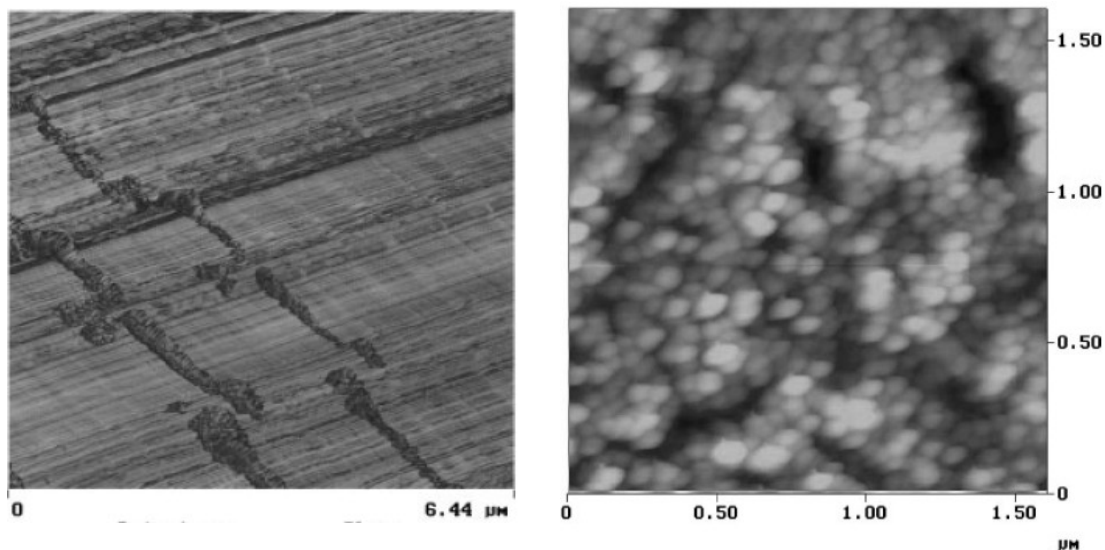


Figure 23: Structure of straw cell walls (left) and enlarged image of deposited lignin (right)

Within the cell wall, the cellulose exists in long, parallel bands interspersed with deposits of lignin, seen in the image on the left as irregular deposits running perpendicular to the cellulose. The lignin, seen here after being extracted from the cellulose and deposited on a film for imaging, is a mass of amorphous polymer deposits. While these images are of straw cells that have not been pulped, these same structural arrangements can be seen in cellulose pulp samples. Pulped fibers, imaged using AFM, show these same structural features [69].

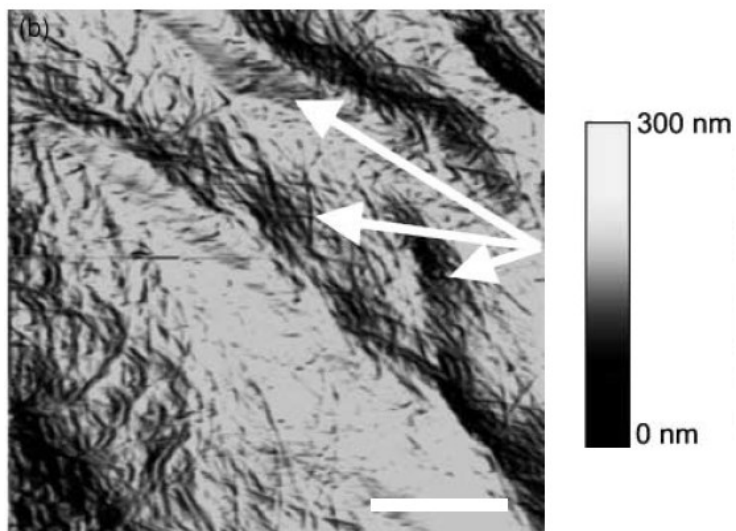


Figure 24: AFM image of bleached kraft fiber, arrows highlight visible wrinkling (inset bar = 500 nm)

In this image of the surface of a single bleached kraft fiber, long arrays of microfibrils are visible. The arrows highlight indentations that occur on the fiber surface. Unbleached fibers demonstrate the same pattern of microfibrils, but also possess lignin deposits [69].

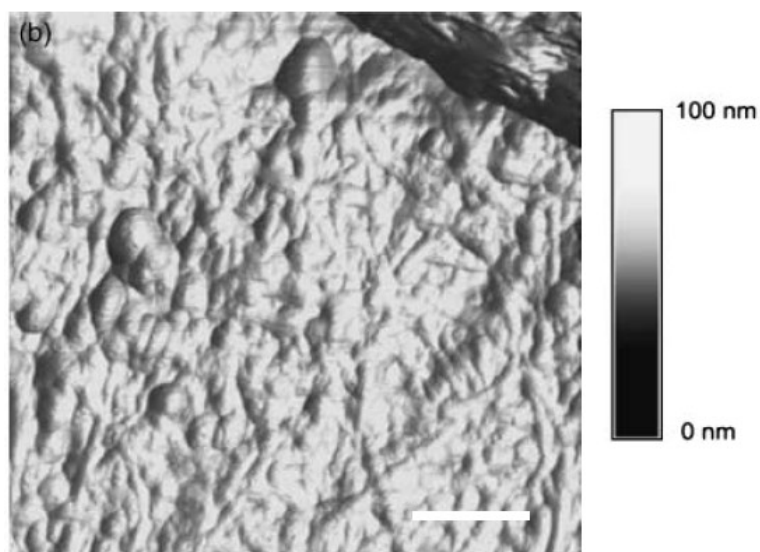


Figure 25: AFM image of unbleached kraft fiber (inset bar = 250 nm)

There are visible globular lignin deposits present on the unbleached fiber. The bleaching process oxidizes and removes this lignin. The pulping process can also cause mechanical deformation of the fiber, delaminating the surface and exposing more ordered regions, as seen in Figure 26 [69].

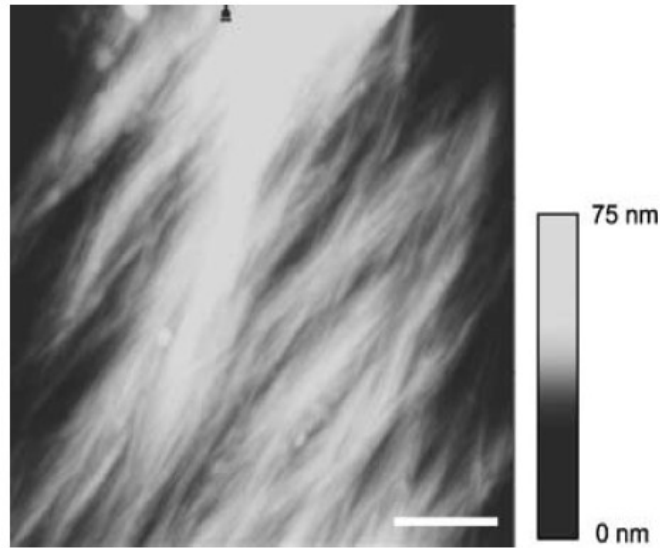


Figure 26: AFM image of cellulose fiber with oriented structure (inset bar = 200 nm)

In the previous two images, the microfibrils were not aligned in a parallel structure. However, in this image, the majority of the microfibrils are parallel. These regions of higher order are present internally in native fiber, and are often exposed during the pulping process [69]. Refining also exposes these inner areas, as the fiber is mechanically opened to expose more surface area for bonding.

AFM has been used to analyze the effect of aging on paper [68]. Samples of library materials, essentially printed pages, were aged and analyzed using AFM. Some samples were inoculated with mold spores before the aging process to determine the effect of biological degradation on the sheet, while other samples were

aged using only heat and humidity to drive the degradation. Analysis of these samples revealed cellulose degradation, visible as fiber fragmentation and pitting on the fiber surface in 25 μm^2 images, demonstrated in Figure 27.

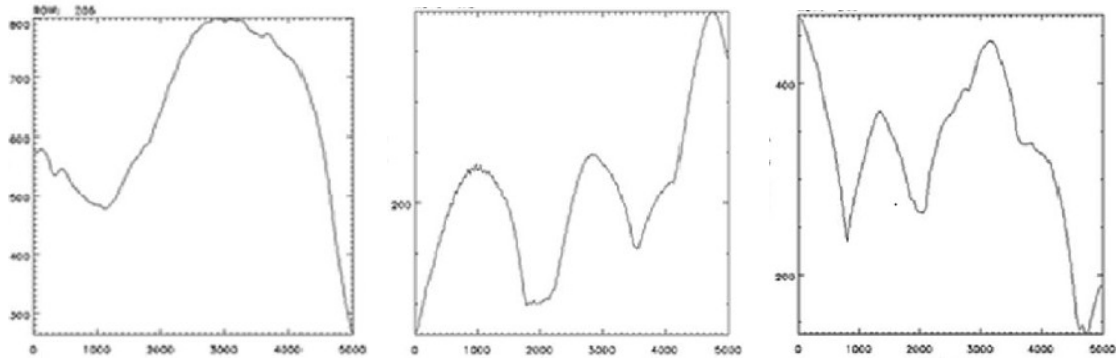


Figure 27: Height traces of unaged sheet (left), aged without mold (center), and aged with mold (right)

These three images each represent the change in height across a 5 μm crosssection of the fiber surface. The height trace analysis of the paper samples reveals the increase in pitting caused by aging. Non-cellulosic material, including bacterial byproducts, could also be identified and differentiated from the fiber.

CHAPTER III

THESIS OBJECTIVES

The goal of this thesis was to further increase the understanding of the mechanisms that contribute to hornification. To do this, atomic force microscopy techniques were used to examine the sample surface and compare the results with other, more traditional methods of pulp and paper analysis.

Initial experiments conducted on lab-recycled paper compared data from industry-standard test methods (water retention value, freeness, coarseness, fiber length, fines content, and tensile strength) to AFM results. After this initial experimentation only WRV, the commonly used measure of the degree of hornification in pulp, was monitored in conjunction with AFM. In addition to these recycling experiments, a study on refining was also conducted to determine if AFM was sensitive to any surface changes that occur during refining. In addition to WRV and AFM, a tritium tracer analysis was conducted on the refined samples to determine if any changes in bound water content could be detected upon recycling. Finally, recycled paper samples from a paper mill were analyzed using these AFM techniques to compare the lab-recycled pulp samples to machine-produced paper.

The specific objectives of this thesis were to:

1. Develop a method for quantifying paper surfaces using AFM and compare AFM data to standard industry techniques

2. Analyze recycled and refined pulp samples using AFM to determine the nature of any changes to the fiber surface
3. Use gathered data to form a hypothesis about the nature of the changes fiber undergoes during recycling, and compare this to the existing hypotheses on the mechanism of hornification
4. Use AFM analysis to compare lab-produced paper samples to mill samples and to attempt to trace the history of the fibers in the mill samples

CHAPTER IV

MATERIALS AND METHODOLOGY

Chapter IV reviews the materials used throughout this thesis, and provides a detailed overview of the methods and techniques used to collect data.

4.1 Materials

4.1.1 Bleached Kraft Softwood

The bleached kraft softwood pulp used for this research was northern softwood supplied by Stora Enso's Wisconsin Rapids mill. It was shipped and stored in slush form and kept refrigerated to prevent degradation. This pulp was supplied unrefined with a freeness of 675 mL (CSF) and a WRV of 1.89.

4.1.2 Bleached Kraft Hardwood

The bleached kraft hardwood pulp used for this research was northern hardwood supplied by Stora Enso's Wisconsin Rapids mill. It was shipped and stored in slush form and kept refrigerated to prevent degradation. This pulp was supplied unrefined with a freeness of 715 mL (CSF) and a WRV of 1.71.

4.1.3 Thermomechanical Pulp

The thermomechanical pulp used for this research was southern pine supplied by Augusta Newsprint's TMP mill. It was shipped and stored in slush form and kept refrigerated to prevent degradation. This pulp was supplied unrefined with a freeness of 250 mL (CSF) and a WRV of 1.11.

4.1.4 Mill Samples

Samples of newsprint produced from recycled paper (fiber source: de-inked pulp, ONP) were supplied by Augusta Newsprint. These samples were conditioned and stored at TAPPI standard conditions following TAPPI procedure T 402 sp-03 once received [94].

4.2 Sample Preparation

4.2.1 Handsheet Preparation

Handsheets (1.2 g OD weight) were produced for testing. These handsheets were produced following the TAPPI T 205 sp-06 procedure [95]. Samples for AFM and tensile strength analysis were air dried to TAPPI standard conditions, except for samples that were heat treated as described in section 4.2.4 below. Samples for water retention value, fiber quality analysis, and tritium tracer analysis were partially prepared following this test method, but were couched and stored wet in sealed and refrigerated bags rather than pressed and dried.

Handsheets for recycling were prepared and stored in a similar manner, except that the amount of pulp used for air-dried recycling was increased to approximately 3.5-4 g (OD weight). These heavy sheets were allowed to dry for at least 48 hours in the conditioning lab to ensure they achieved equilibrium moisture content throughout. The heat-treated sheets prepared for recycling weighed 1.2 g (OD).

4.2.2 Refining Method

The beating of pulp was carried out in a Valley beater, shown in Figure 28, using the TAPPI T 200 sp-06 procedure [96].



Figure 28: Valley beater

23 liters of 1.57% consistency pulp was introduced into the Valley beater and allowed to mix without beating for several minutes. A sample of the unrefined pulp was withdrawn and stored refrigerated to use as high freeness pulp for experimentation. The remaining pulp was beaten to two consistency levels, medium freeness (approximately 400 CSF) and low freeness (approximately 250 CSF). Samples of pulp were drawn at intervals to determine the raw Canadian standard freeness (without correction) until the target levels of beating were reached. Full freeness determinations were carried out on each sample before being made into handsheets for testing and recycling.

4.2.3 Recycling Method

Handsheets made for recycling were stored at TAPPI standard conditions until processing. These handsheets were repulped using a British disintegrator. Roughly 6 g of the handsheets were disintegrated in 2 L of water for 30,000 revolutions to fully disintegrate the handsheet and produce a pulp slurry of approximately 0.3%

consistency. After the samples were disintegrated, they were again made into handsheets following established procedures for further testing or recycling.

4.2.4 Drying Methods

In addition to air-drying, samples were also dried at accelerated rates by both hot plate and microwave. Wet 1.2 g (OD weight) handsheets were couched and pressed following the TAPPI T 205 sp-06 procedure [95]. Samples were then dried on an Emerson Speed Dryer (Model 130) set at 105°C, or in an Emerson 1,000-Watt microwave (Model MW8119SB) set on high. Each handsheet was dried to a total weight of no more than 1.3 g (therefore possessing a maximum of 8% moisture). After drying, these handsheets were stored at TAPPI standard conditions for 24 hours before testing or recycling.

4.3 Experimental Procedures

4.3.1 Water Retention Value

WRV was measured using a modified version of the TAPPI UM 256 procedure [98]. Approximately 0.6 g (OD weight) of pulp at 0.5% consistency were drained onto a fine mesh screen in a centrifuge cup and placed in a centrifuge at 900g for 30 minutes to remove all free water. The “wet” pulp (s) was weighed, then dried and the dry pulp (p) weighed again to determine the amount of bound water. Water retention was calculated as the weight of bound water per unit of dry pulp, using Equation 1 [98].

Equation 1: Water retention value

$$WRV = \frac{s - p}{p}$$

This test was repeated four times for each sample, and the average value and standard deviation were calculated.

Degree of hornification was calculated by determining the percentage decrease in the WRV of the recycled samples from the unrecycled samples, using Equation 2.

Equation 2: Degree of hornification

$$\text{Degree of hornification} = \frac{WRV_{RO} - WRV_{RX}}{WRV_{RO}} * 100$$

4.3.2 Freeness

Canadian standard freeness was measured using the TAPPI T 227 om-04 test method [92]. A schematic of a CSF tester is shown in Figure 29 [10].

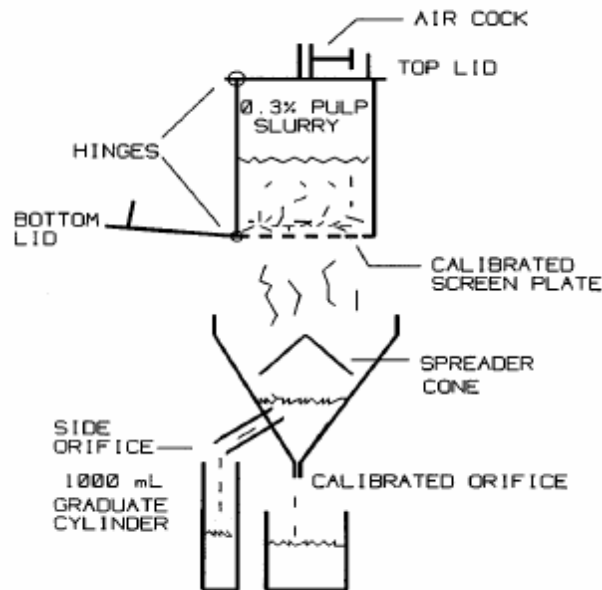


Figure 29: Schematic of CSF tester

The exact consistency and temperature of the sample were measured in order to correct for small variations from the test standard using Equations 3 and 4.

Equation 3: Temperature corrected freeness

$$CSF_T = CSF_U + 4.6(20 - T) \left[1 - \frac{(400 - CSF_U)^2}{61000(CSF_U)^{0.25}} \right]$$

Equation 4: Fully corrected freeness

$$CSF = CSF_T + 590(C - 0.3) \left[1 + \left(\frac{0.4 - C}{0.2} \right) \left(\frac{CSF_T}{1000} \right) \right] \left[\frac{1 - (CSF_T - 390)^2}{87000(CSF_T)^{0.2}} \right]$$

4.3.3 Coarseness, Fiber Length, Fines Content

Optical fiber quality analysis was used to determine coarseness, fiber length, and fines content of virgin and recycled pulp using an OpTest Fiber Quality Analyzer and a modified version of the TAPPI T 271 om-07 test method [66, 93]. A pulp solution of less than 0.0002% consistency was prepared. A 600 mL sample of this pulp solution with a known weight of fiber (maximum 1.2 mg) was run through the FQA, which uses an optical sensor to measure the length and width of each fiber in the sample, and calculates the coarseness, length-weighted fiber length, and fines content (by weight), defining a fine as a piece of fiber between 0.07 mm and 0.20 mm in length. Figure 30 shows the fluid flow through the FQA and an image of the optical analysis, with four discrete fibers highlighted.

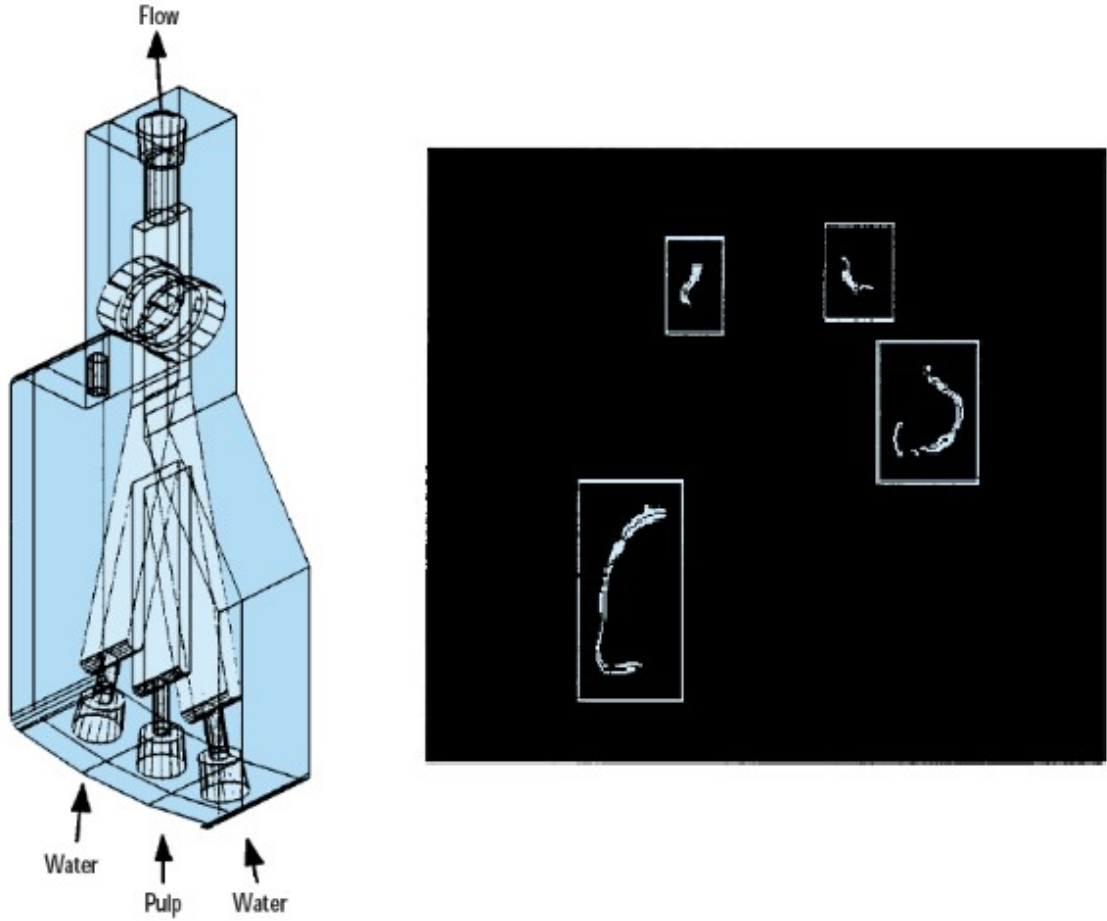


Figure 30: FQA fluid flow diagram (left) and optical image representation (right)

Coarseness was calculated by dividing the total mass of fiber (m) by the product of the arithmetic mean length (l_n) and the total number of fibers (n), as showing in Equation 5 [101].

Equation 5: Coarseness

$$C = \frac{m}{nl_n}$$

The length-weighted fiber length was determined by grouping the fiber into length classes (designated l_i) and determining the number of fibers in each class (n_i), then using Equation 6 [93].

Equation 6: Length-weighted fiber length

$$l_{lw} = \frac{\sum_i n_i l_i^2}{\sum_i n_i l_i}$$

The FQA test was repeated twice for each pulp sample, and the results of each test were averaged.

4.3.4 Tensile Strength

Tensile strength was measured using a L&W Alwetron and following the TAPPI T 220 sp-06 procedure [97]. Two 15 mm strips were cut from two handsheets prepared for testing, for a total of four strips. The results of each test were averaged and the standard deviation was calculated.

4.3.5 Tritium Tracer Analysis

Tritium tracer analysis was conducted following the procedure for determining the fiber:water partition coefficient using tritiated water, developed by Dr. Frances Walsh [104]. Wet pulp (1.2 g OD weight) was diluted to 8% consistency and placed in a Buchner funnel with a fritted glass filter attached to a low vacuum to facilitate drainage. 25 mL of water containing 20 μ Ci of tritium was added to the pulp, stirred for 30 seconds with a glass stirring rod, and allowed to equilibrate for 1 minute. The fritted glass filter ensured that the majority of the water remained with the pulp slurry until the vacuum was applied after the equilibration period. Excess water was removed from the fiber by washing the pulp with successive 25 mL aliquots of anhydrous acetone until the radioactive material in the acetone measures less than 1000 dpm when measured by scintillation counter. After the acetone washes, the pulped was further washed with 25 mL of water twice more.

The activities of the initial water, the acetone washes, and the final two water washes were determined using a Perkin-Elmer Tri-Carb 2800 TR scintillation counter. A 100 μ L aliquot from each wash was withdrawn and mixed with 10 mL of Scintiverse-E scintillant. The distribution of the tritium between the pulp and water (K_{pw}) was determined by calculating the activity of the water bound to the fiber (dpm_p) and the activity of the water that was not bound (dpm_w).

Equation 7: Partition coefficient

$$K_{pw} = \frac{dpm_p}{dpm_w}$$

The activity of the bound water was calculated by measuring the total activity in the final two water washes, which represents the amount of tritium that remained with the fiber after all free water was removed by acetone (D_p), and dividing by the weight of the pulp (p), as shown in equation 8. The activity of the free water was determined by subtracting the activity of the bound water from the initial activity of the water sample introduced to pulp (D_i), and dividing by the total weight of the initial water (q_i), as shown in Equation 9.

Equation 8: dpm in bound water

$$dpm_p = \frac{\sum D_p}{p}$$

Equation 9: dpm in free water

$$dpm_w = D_i - \frac{\sum D_p}{q_i}$$

The partition coefficients of the samples provided a method to compare the amount of bound water present in each pulp. This test was repeated four times for each sample, and the results were averaged and the standard deviation was calculated.

4.3.6 Atomic Force Microscopy

Atomic force microscopy measurements were taken using an Asylum Research MFP-3D SA AFM, using IGOR Pro controller software [2].

4.3.6.1 Sample Preparation

Samples for AFM analysis were secured to clean glass slides, which were held in place by magnets to prevent movement during testing. For analysis of paper samples, 1 cm² test squares were cut from the sheets and secured to the slide using double-sided tape. For single fiber experiments, dilute fiber solutions were run through a filter paper, trapping fibers onto the filter surface. A clean glass slide was then pressed to the filter paper so that some fiber adhered to the glass surface. The slide was dried at TAPPI standard conditions, securing the fibers in place.

4.3.6.2 Humidity Control

In order to control the ambient humidity during experimentation conducted in air, the Asylum Research Closed Fluid Cell, as shown in Figure 31, was used [1].

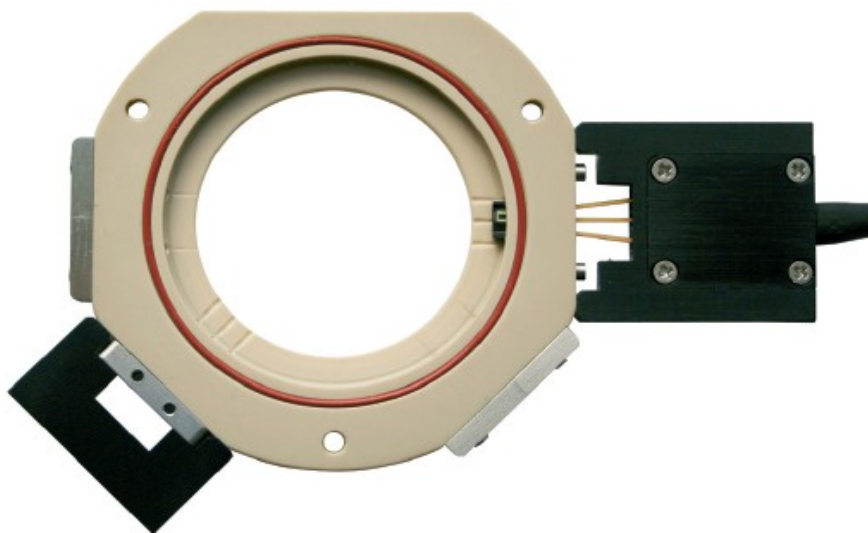


Figure 31: Closed fluid cell

The samples is mounted on the glass side within the recessed area and the cantilever assembly is sealed in place on top, allowing for a closed environment of approximately 3 cc in volume to be created around the sample. Two streams of nitrogen gas, one bone dry and one saturated with water vapor, were mixed together in precise volumes (measured by Aalborg GFM171 flowmeters) and introduced into the fluid cell in order to regulate the humidity. Samples were allowed to equilibrate for one hour at the desired humidity before testing. Except for experimentation to determine the effect of humidity on AFM measurements of cellulose fiber, all samples measured in air were kept at 50% RH throughout testing.

4.3.6.3 Force Curves

Adhesion measurements were collected using AC240TS silicon cantilevers manufactured by Olympus Group and purchased through Asylum Research, which have a nominal spring constant of 2 N/m and a tip radius of curvature of 10 nm [65]. An SEM image of the cantilever is shown below in Figure 32 [65].

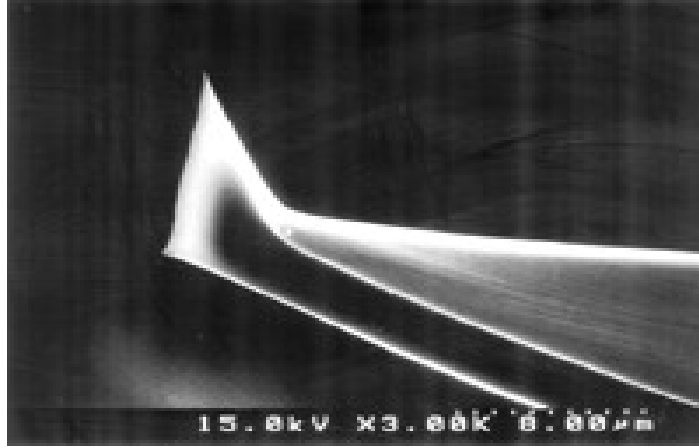


Figure 32: AC 240 TS cantilever SEM image

The exact spring constant of each cantilever was calculated by the IGOR Pro software using Equation 10, the Sader equation [74].

Equation 10: The Sader equation

$$k = 0.1906 \rho_f b^2 L Q_f \Gamma_i(\omega_f) \omega_f^2$$

The Sader method uses the length (L) and width (b) of the cantilever (provided by the manufacturer), along with the thermal quality factor (Q) and the thermal resonant frequency (ω_f) measured by the AFM. There are two constants based on the fluid medium surrounding the probe: ρ_f , the density of the fluid, and $\Gamma_i(\omega_f)$, a hydrodynamic function based on the Reynolds number of the fluid. With the spring constant of the probe determined, the AFM software automatically calculates the adhesion force from the measured cantilever deflection.

For the force measurements conducted during these experiments, the tip was deflected up 100 nm after being brought into contact with the surface. This helped to ensure adequate contact between the tip and surface. At each test point, the adhesion force was measured twice, and if the two values were within 10% of each other, they

were averaged together and this value was recorded as the adhesion measurement. Measurements that differed by more than 10% were discarded, because it was assumed that surface irregularities prevented the tip from making consistent contact with the surface. The following images are samples of force measurements taken during experimentation.

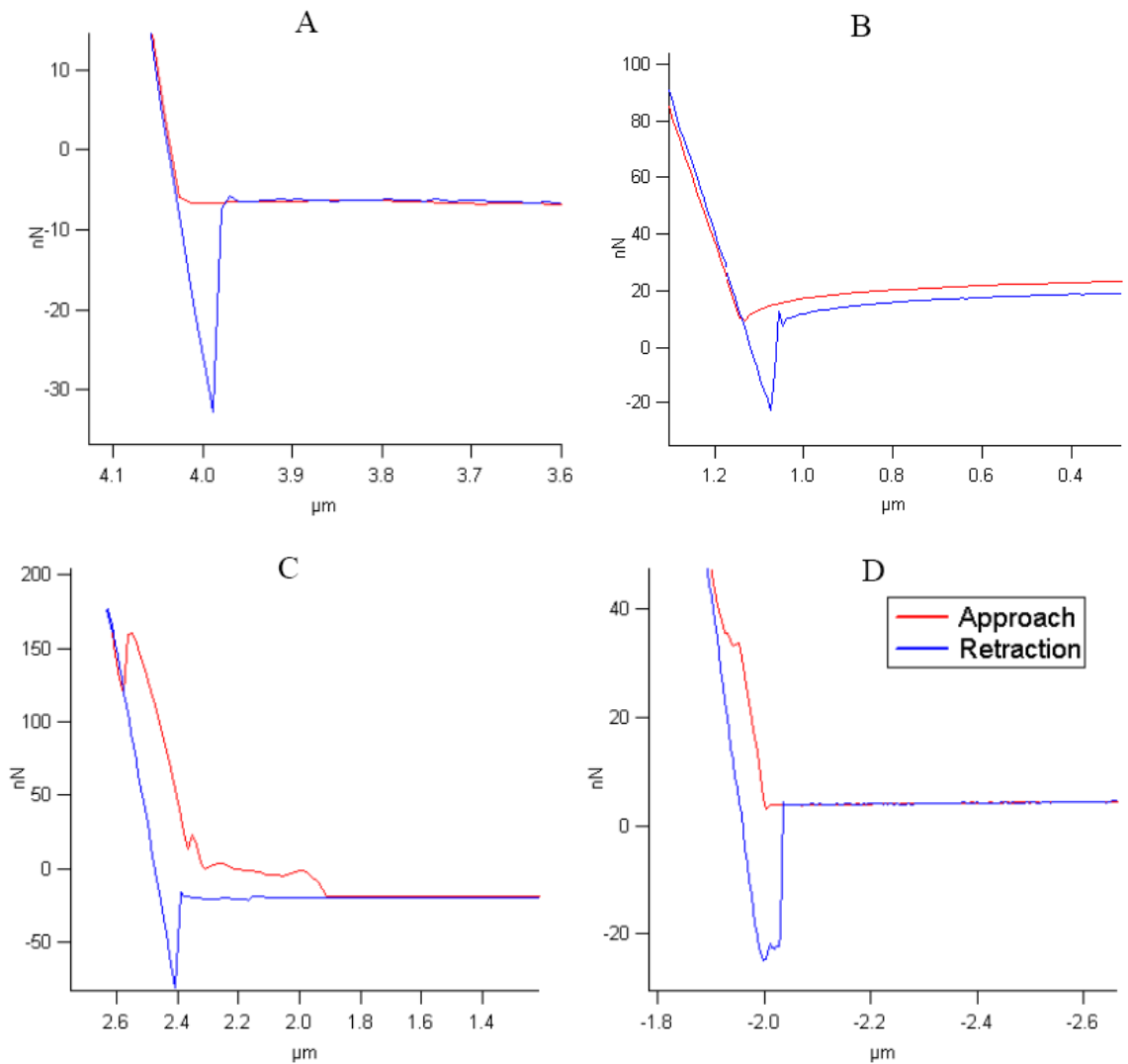


Figure 33: Sample AFM force curves

Force curve A represents an ideal force measurement. There is a single, distinct peak indicating where the separation of the tip and surface occurred as the tip retracted.

This force curve most accurately matches the ideal as shown in Figure 20. Image B, however, demonstrates a slight hysteresis. After tip-surface separation, the tip does not return fully to its initial rest position. Image C demonstrates the effect that surface deformation may have on the initial deflection of the tip. Ideally, once the tip and surface make contact, the cantilever will deform linearly as it presses into the surface. However, if the surface deforms as more force is applied, a non-linear approach curve is generated. Finally, force curves that resemble image D occur when the tip and surface do not separate cleanly as the tip retracts. In this image, two distinct peaks are visible in the retraction curve, indicating that there were two points of adhesion between the tip and surface. As the tip retracted, there were two sequential separations. In all of these images, the adhesion force is determined by calculating the change from the maximum deflection to the rest position of the retraction line.

Throughout the refining and recycling experiments conducted on lab-prepared handsheets, at least 60 adhesion measurements were gathered for each sample, using test squares from multiple handsheets. During the single fiber analysis experiments, 40 adhesion measurements were taken on a single fiber at each stage of wetting and drying. In order to analyze the mill samples, which had higher sample variability than the lab samples, 100 to 150 adhesion measurements were taken from multiple test squares from each sample provided.

4.3.6.4 Imaging

Sample imaging experiments were conducted using Hi'RES-W tungsten probes, manufactured by MikroMash, with a radius of curvature of 1 nm at the tip, shown in Figure 34 [58].

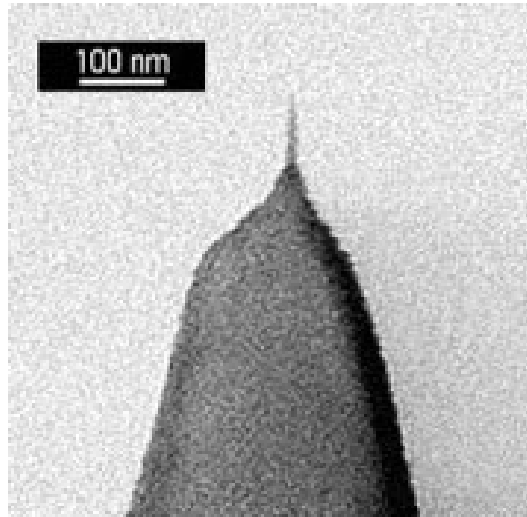


Figure 34: Hi'RES-W cantilever SEM image

The small radius of curvature allowed for precision imaging of the surface at extremely high resolution. Imaging experiments were conducted in intermittent contact mode to prevent damage or deformation of the tip and sample surface. Images ranged in size from $400\text{ }\mu\text{m}^2$ to 250 nm^2 . Root mean square (RMS) roughness of the surface was calculated by the IGOR Pro software as required. At least 20 separate images of the same size were taken of all samples where the average RMS roughnesses of two different samples were compared.

4.3.6.5 Probe Contamination and Damage

Probe contamination and damage is a constant possibility while conducting atomic force microscopy experiments. In order to determine that no contamination or

damage occurred, at least ten adhesion measurements were taken against a clean glass slide before and after selected tips were used to take force measurements or image fiber. If the average adhesion values between the tip and glass differed after the tip was used on the fiber surface, then contamination or damage of the tip had occurred and the data collected using that tip was invalid. Throughout all experimentation, there was no evidence of tip contamination or damage.

CHAPTER V

RESULTS AND ANALYSIS

In order to study the effect of hornification on cellulose fiber surfaces, the adhesion between the AFM probe and fiber was measured using the experimental procedures outlined in Chapter IV and compared to other experimental data to determine the changes in the fiber samples. In this chapter, AFM studies of the three fiber types processed in the lab and samples procured from a recycle paper mill are presented.

5.1 Unrefined Recycling

Sample handsheets of unrefined bleached kraft softwood, bleached kraft hardwood, and thermomechanical pulp were made and recycled using the procedures outlined in section 4.2.1. Samples were recycled up to three times, producing four sets of handsheets for each type of pulp.

5.1.1 Bleached Kraft Softwood

Samples of unrefined bleached kraft softwood pulp were recycled in the lab, and the resulting sheets were analyzed for water retention, tensile strength, fiber length, fines content, coarseness, bound water content, and surface adhesion. Loss of tensile strength and decrease in water retention are commonly accepted effects of hornification in the pulp and paper industry, and these tests provided a baseline for the other changes seen in the fiber throughout the recycling experiment. Fiber length,

fines content, and coarseness were measured using FQA to determine if the fibers were being physically damaged by the recycling procedure.

Table 5: Bleached softwood kraft recycling

	WRV	Tensile Strength	Mean Length	Fines Content	Coarseness	Surface Adhesion
	(sd)	kN/m (sd)	mm, lw	%, lw	mg/m	nN (sd)
Never Dried	1.89 (0.08)		2.07	0.60	0.14	
Unrecycled	1.79 (0.02)	2.13 (0.06)	2.05	0.63	0.16	27.55 (4.82)
1x Recycled	1.73 (0.03)	1.91 (0.05)	2.06	0.62	0.16	68.26 (7.79)
2x Recycled	1.65 (0.02)	1.79 (0.06)	2.04	0.63	0.16	84.96 (8.57)
3x Recycled	1.64 (0.02)	1.69 (0.04)	1.90	4.62	0.2	93.98 (6.74)

WRV and tensile strength experiments showed the expected trends, a relatively large initial decrease, followed by progressively smaller decreases with each additional recycle step, as shown in Figure 35.

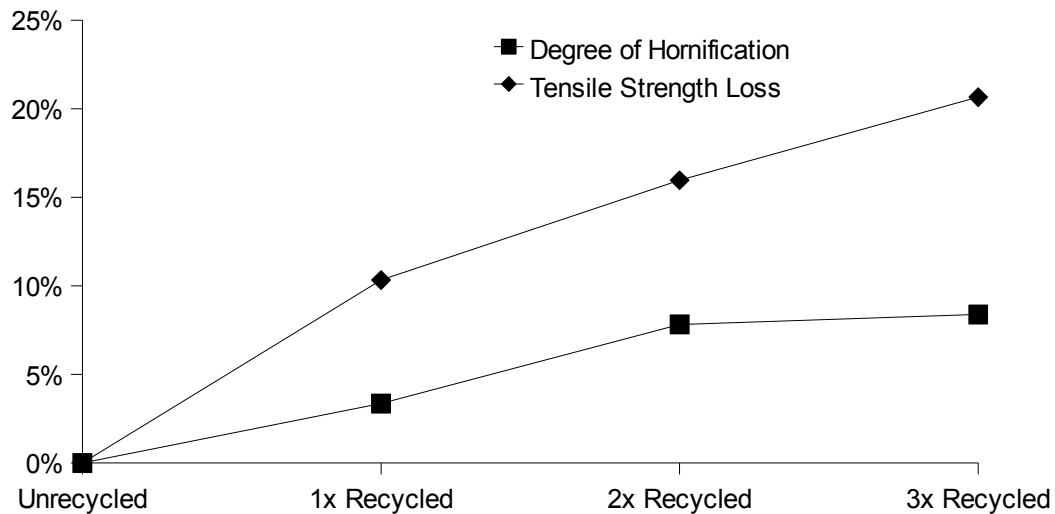


Figure 35: Degree of hornification and tensile strength loss as a function of recycling for bleached softwood kraft pulp

Both WRV and tensile strength showed almost 50% of the final decrease after the first phase of recycling. As seen in the literature reviewed in section 2.4.1, these decreases level off after several iterations of recycling, as expected [35, 61, 102, 111]. The magnitude of the degree of hornification and loss of tensile strength are lower

than those seen in the literature, which is to be expected because these analyses were done using unrefined pulp. The degree of hornification is known to increase with the degree of refining of the initial pulp sample, as shown in Figure 36 [82].

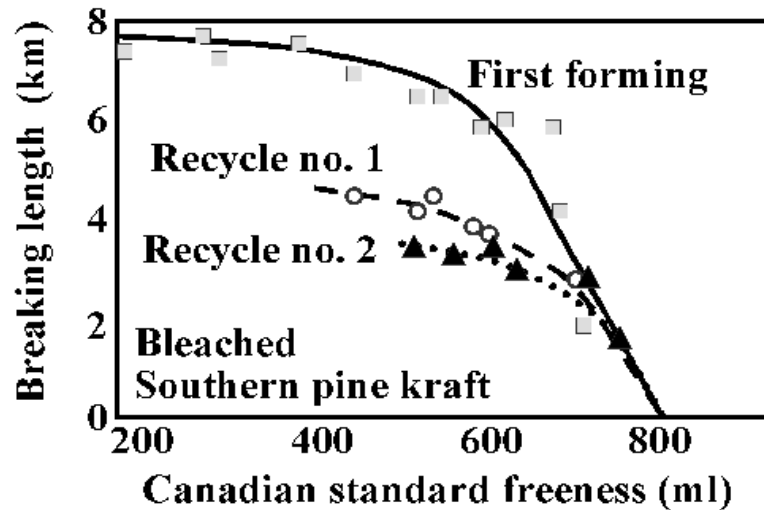


Figure 36: Effect of refining on breaking length

With increased refining (decreased freeness), the breaking length increases, but the magnitude of strength loss due to recycling also increases.

Mean length remained constant from the never-dried fiber through the first recycle steps, with a slight drop after the last repulping process. This indicates that, at least initially, the recycle procedure did not cause physical damage to the fibers during the repulping process. However, between the second and third recycle, fiber length decreased by almost 0.15 mm, which is a significant change. Research has demonstrated the link between WRV and fiber flexibility, and a loss of pore volume in the fiber causes an increase in fiber stiffness [14, 27]. It may be that these stiffer fibers are more likely to break under shear forces rather than bend like more flexible fibers, causing mechanical damage to the fiber during the repulping [118]. This effect

is most often seen during aging, but some aging does occur during the ongoing recycling process. Similarly, fines content increased after the final recycling step, as mechanical damage to long fibers resulted in the formation of a large number of fines. Coarseness increased as swellability of the fibers decreased, as expected [70]. However, these effects occurred only after several recycle steps, when changes to WRV, tensile strength, and surface adhesion had leveled off, indicating that these chain scission effects do not contribute to the hornification process.

The surface adhesion measured by the AFM increased, indicating that the surface became more hydrophilic with progressive recycling. Loss of tensile strength indicates that the interfiber bonding within the sheet decreased, which is often attributed to a loss of fiber flexibility and increasing hydrophobicity of the surface that prevents the formation of strong interfiber bonds [11, 48]. But over the course of multiple recycling steps, the surface apparently became more than three times as hydrophilic as the unrecycled sheet. However, the adhesion between the AFM probe and sample surface is dominated by both chemical interactions and contact area [31, 36]. Given the nature of cellulose fiber, which is composed of long polymer chains with a large number of hydrogen bonds, it is unlikely that such an increase could be due to a chemical change of the fiber surface. If the surface hydrophilicity actually increased, then there should have been a matching increase in the tensile strength due to the formation of an increased number of hydrogen bonds, which is the opposite of what is observed. Therefore such a change must be due to some other factor such as better tip-surface contact.

5.1.1.1 Sheet Surface Adhesion by Test Location

The surface adhesion measurements from the recycling experiments are all taken from several different test squares from several different handsheets. There is no way to use handsheets to simulate recycling and analyze the same fiber at different points in the process, so in order to demonstrate the regularity of the pulp samples, the following breakdown of surface adhesion by handsheet and test site for unrecycled bleached kraft softwood pulp is given.

Table 6: Surface adhesion by test location

	Handsheet 1		Handsheet 2		Handsheet 3		Total
	Site 1	Site 2	Site 1	Site 2	Site 1	Site 2	
# Measurements	19	19	16	17	18		89
Mean Adhesion (nN)	26.87	26.09	28.68	28.44	27.89		27.55
Standard Deviation	4.74	5.43	4.36	4.30	3.87		4.82

There was no measurable difference between the adhesion measurements taken from any of the test squares. Throughout the experimentation, there was no indication of irregularity between samples of the same pulp taken from different test sheets for the handsheet samples recycled in the laboratory.

5.1.1.2 Humidity

For all experiments done in air, humidity was controlled and kept to TAPPI standards. However, a small analysis of the effect of humidity on adhesion measurements was conducted using samples of the recycled bleached kraft softwood. Samples were moved from storage at standard conditions to the test chamber, where they were analyzed at 50% RH. The humidity was then lowered to 20% RH and the sample was allowed to equilibrate for several hours. Then the humidity was raised to 80% RH and again allowed to equilibrate.

Table 7: Humidity control results

		Mean Surface Adhesion (nN)	Standard Deviation
Unrecycled	20% RH	25.98	3.66
	50% RH	30.21	3.25
	80% RH	32.47	6.23
3x Recycled	20% RH	79.63	8.12
	50% RH	97.42	7.47
	80% RH	108.42	15.21

As expected for hydrophilic materials, the presence of increasing amounts of humidity caused an increase in the adhesion measured between the tip and surface [45, 78, 89, 112, 113]. In humid environments, contact between the tip and surface causes a small amount of condensation and the formation of a capillary bridge between the tip and surface. At higher humidities, increased condensation causes a larger capillary bridge to form, which increases the force required to separate the tip and surface upon retraction of the probe. Figure 37 illustrates the effect of humidity on the surface adhesion measurements.

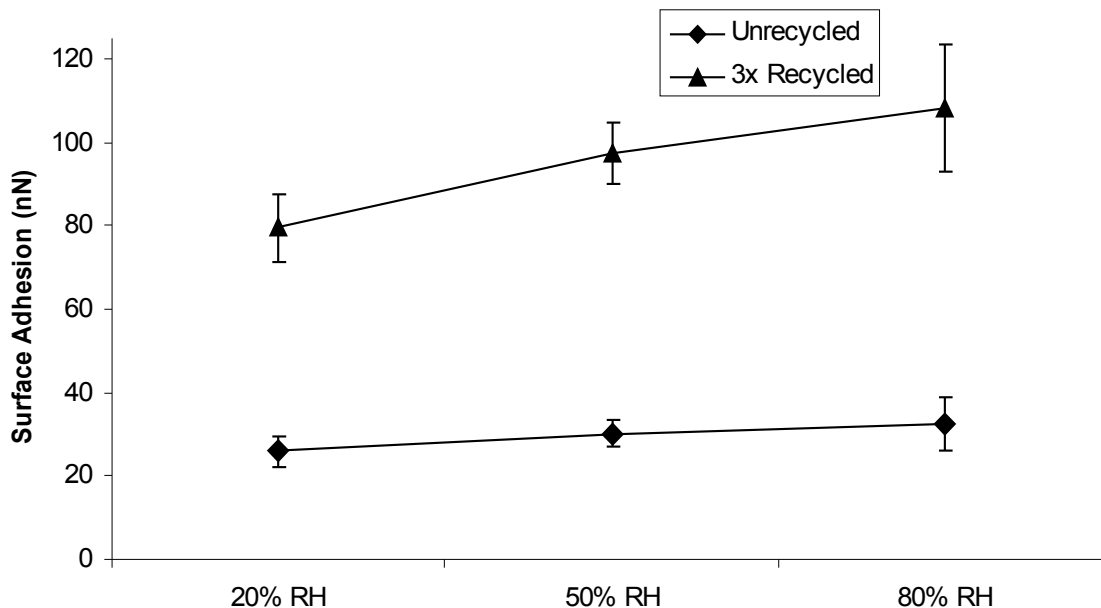


Figure 37: Surface adhesion as a function of relative humidity

While the magnitude of the surface adhesion increase due to increasing humidity is four times greater upon recycling, proportionally the increases are similar. The increase in surface adhesion from 20% RH to 80% RH is approximately 25% for the unrecycled samples and 35% for the recycled samples. This relative increase is most likely due to the increased size of the water layer on the surface because of the surface topography change.

5.1.2 Bleached Kraft Hardwood

For the bleached kraft hardwood pulp, WRV and FQA data were collected and compared to the AFM adhesion measurements.

Table 8: Bleached hardwood kraft recycling

	WRV	Mean Length	Fines Content	Coarseness	Surface Adhesion
	(sd)	mm, lw	%, lw	mg/m	nN (sd)
Never Dried	1.71 (0.10)	1.31	0.74	0.09	
Unrecycled	1.60 (0.05)	1.32	0.75	0.10	28.09 (6.43)
1x Recycled	1.33 (0.03)	1.31	0.72	0.10	65.23 (7.30)
2x Recycled	1.30 (0.03)	1.28	1.25	0.11	76.33 (8.91)
3x Recycled	1.32 (0.07)	1.26	1.95	0.10	82.62 (11.14)

The bleached hardwood kraft samples showed the same trends as the softwood pulp. Again, the degree of hornification roughly followed the expected trend: an initial large increase followed by progressively smaller changes, as shown in Figure 38.

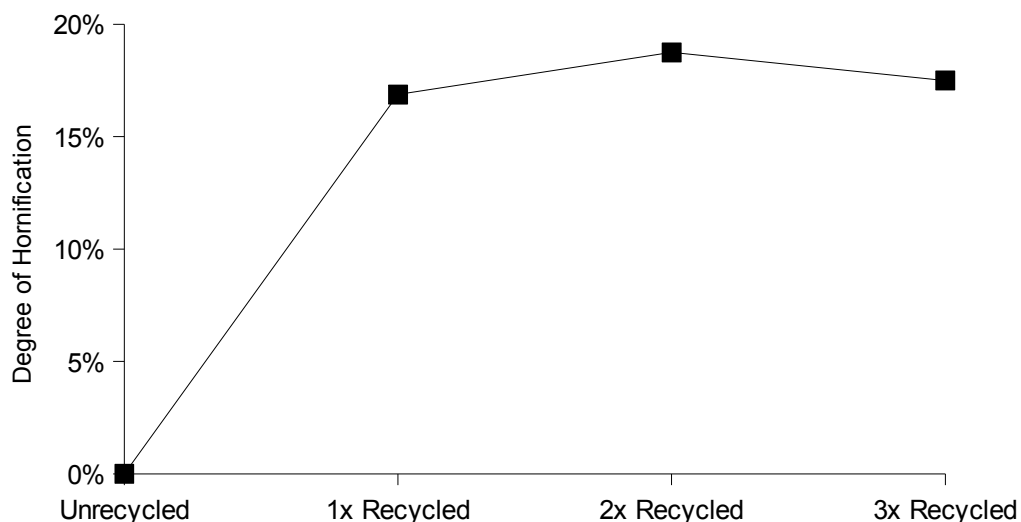


Figure 38: Degree of hornification for bleached hardwood kraft pulp

In this instance, the majority of the hornification occurred after the first recycle step, with only marginal increases over the following two cycles.

As with the softwood pulp, the decrease in WRV was mirrored by increases in the surface adhesion. Decrease in WRV is explained by the decrease in pore volume seen with cycles of wetting and drying, but the increase in surface adhesion again

goes against conventional wisdom: that the poorer sheet qualities are due to a decrease in sheet hydrophilicity.

Similar to the softwood kraft pulp, in the initial recycling steps of the hardwood pulp, no change was seen in fiber length or fines content, indicating that no mechanical damage occurred due to the repulping process. But as the recycling progressed, analysis of the fibers revealed slight shortening and a small increase in the fines content, indicating that the fibers became more susceptible to damage due to increased stiffness and decreased fiber strength [118]. Coarseness remained fairly constant and lower than the coarseness for softwood; again, an expected result as hardwood fibers are shorter and less coarse than softwood fibers [70, 117].

5.1.2.1 Accelerated Drying

Samples of hardwood pulp were also used in experiments to determine the effect of accelerated drying of handsheet samples. Samples dried at higher temperatures undergo a higher degree of hornification, but this is due to a faster rate of water removal rather than being directly related to temperature [48]. The rate of water removal seems to adversely affect pore size because the pores close to greater degree to try to reach thermodynamic equilibrium the faster the water within the pores evaporates. The drying rate was increased by drying sample handsheets on a hotplate and in the microwave.

Table 9: Accelerated drying of hardwood pulp

		WRV	Surface Adhesion
		(sd)	nN (sd)
Unrecycled	Air Dried	1.60 (0.05)	25.58 (5.73)
	Microwave	1.16 (0.06)	33.93 (6.56)
	Hot Plate	1.33 (0.06)	33.95 (7.44)
1x Recycle	Air Dried	1.33 (0.03)	55.71 (8.88)
	Microwave	1.05 (0.11)	69.71 (8.01)
	Hot Plate	1.11 (0.05)	71.19 (7.99)

While the surface adhesion values increased slightly in the samples that were dried at accelerated rates, the change did not approach the magnitude of the changes seen in the WRV. The water retention of the heat-dried sheets decreased to a greater extent than seen during the entirety of the progressive recycling experiment conducted with air-drying.

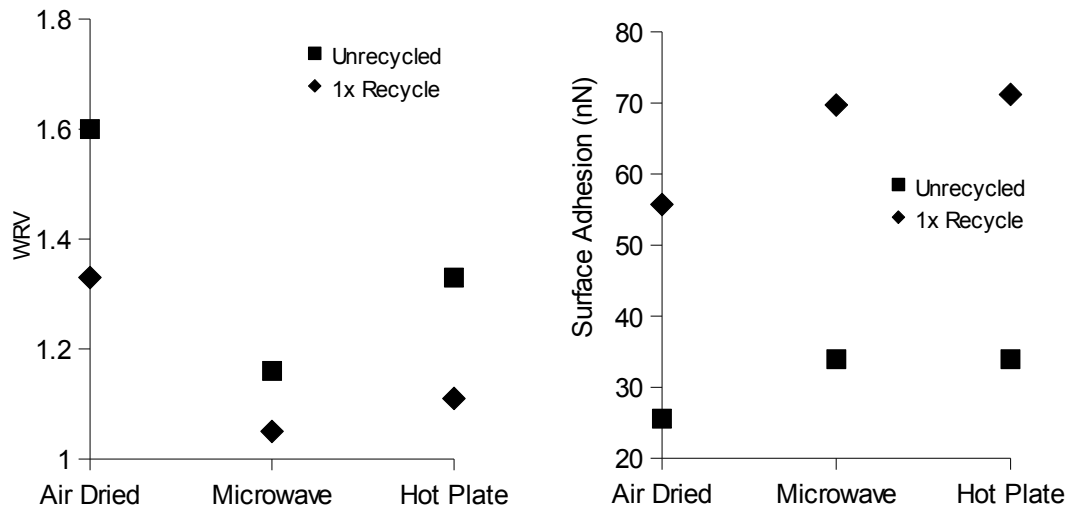


Figure 39: Accelerated drying WRV and surface adhesion measurements

Increasing the rate of drying had only a minimal effect on the surface adhesion of the fiber compared to the effect of recycling the sheet, while WRV was more affected by the drying rate than recycling. The surface adhesion measurements are affected mainly by changes in topography, while the water retention is affected by loss of pore volume. The disconnect between these experimental data suggests that while

hornification causes both pore volume loss and surface topography changes, the two effects are not directly linked to each other. A clear contrast is drawn between accelerated drying and recycling. WRV decreases for both operations, but the surface adhesion is only affected by recycling. The root cause is that the porosity changes in WRV are of a scale too large for the AFM to observe.

5.1.2.2 Inhibition of Hornification

Hornification of fiber can be inhibited by the introduction of a material with a large number of hydrogen bonds to the pulp [33]. By adding a high dose of sucrose or glycerol to the pulp, the degree of hornification due to recycling can be reduced. Experiments were conducted to determine the effect of the addition of sucrose (20 g per 100 mL) to the surface adhesion measurements of the recycled sheets. These experiments were conducted with the unrefined bleached kraft hardwood pulp samples. The pulp for each handsheet (1.2 g OD weight) was disintegrated in 500 mL of water and added to 4.5 L of water with the appropriate concentration of sucrose. The pulp was mixed to ensure even dispersion of the fibers, then introduced to the handsheet mold for handsheet forming.

Table 10: Inhibition of hornification

	WRV		Surface Adhesion	
	Normal	with Sucrose	Normal	with Sucrose
	(sd)	(sd)	nN (sd)	nN (sd)
Unrecycled	1.60 (0.05)	1.54 (0.06)	28.09 (6.43)	23.07 (7.33)
1x Recycled	1.33 (0.03)	1.47 (0.10)	65.23 (7.30)	34.81 (9.98)
2x Recycled	1.30 (0.03)	1.43 (0.11)	76.33 (8.91)	46.70 (11.12)
3x Recycled	1.32 (0.07)	1.38 (0.03)	82.62 (11.14)	59.89 (16.32)

The addition of sucrose helped to maintain the swellability of the recycled fiber and retarded the increase of the surface adhesion. However, dosing the pulp in this manner only affects one paper-making cycle before the sucrose washes out of the sheet entirely [33]. Because the sucrose washed away upon repulping, in order to maintain better fiber properties high doses of sucrose (>20 g per 100 mL pulp) needed to be added to the pulp before each handsheet forming process. Figure 40 shows the progression of the degree of hornification and surface adhesion measurements in the pulp with and without sucrose.

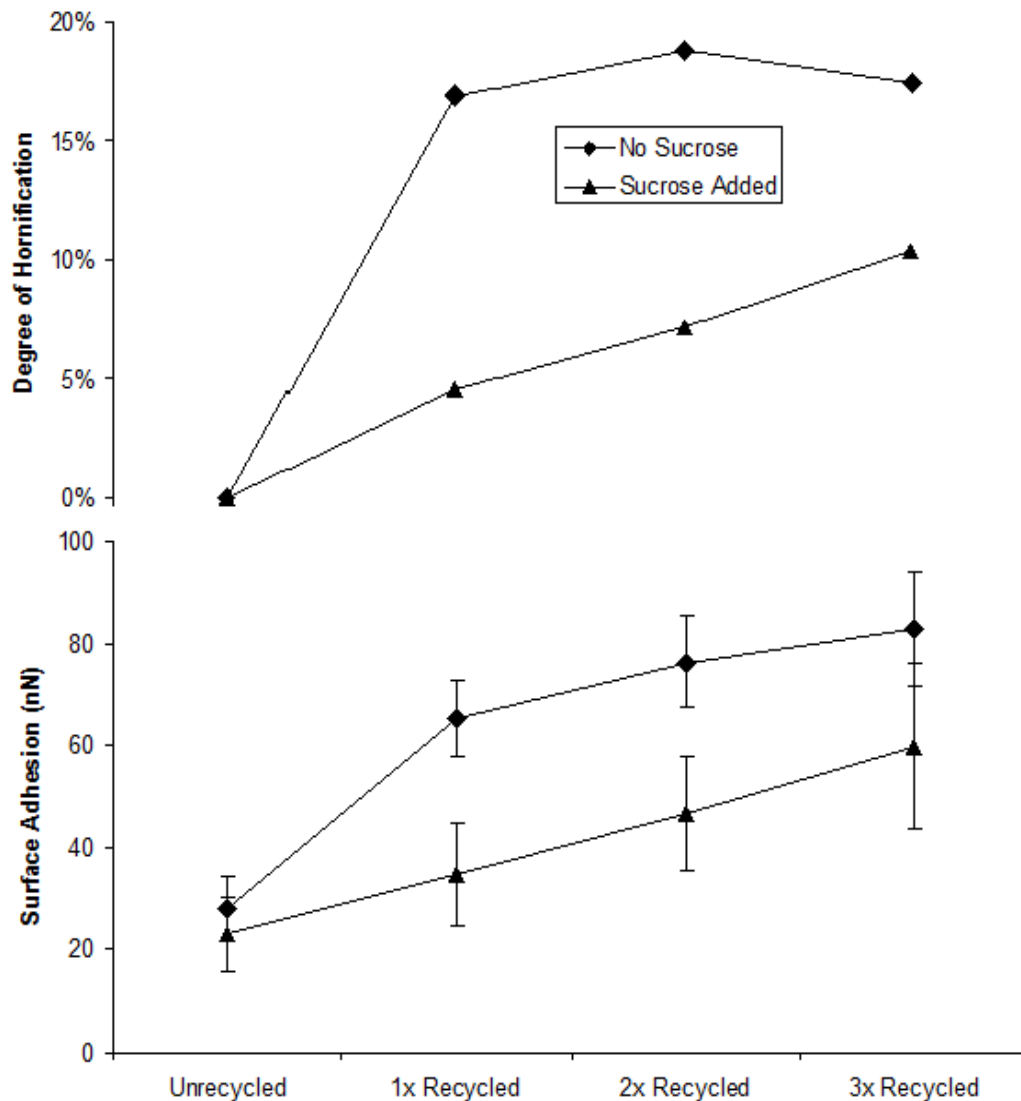


Figure 40: Effect of sucrose on recycling hardwood pulp

From this graph, it is apparent that the sucrose partially reduces the effect of hornification on recycled fibers, but does not completely eliminate it. With each cycle of wetting and drying, the surface adhesion and degree of hornification of the pulp with sucrose increases, but to a much less drastic degree than the pulp without sucrose. After three recycle steps, the degree of hornification of the pulp with sucrose is still increasing linearly, rather than leveling off. If the recycling were continued,

the pulp with sucrose would most likely reach the same ultimate degree of hornification than the regular pulp, although this would take several more steps. The addition of sucrose, which is rich in hydrogen bonds, prevents some of the intrafiber bonding that occurs upon drying, but cannot stop all of it.

5.1.3 Thermomechanical Pulp

Thermomechanical pulp, which has a much higher yield than kraft pulp and contains a large fraction of lignin and extractives, is known to experience the effects of hornification to a much lesser degree than kraft pulps [48]. The WRV analysis of the TMP used for these recycling experiments verifies this.

Table 11: TMP recycling

	WRV	Mean Length	Fines Content	Coarseness	Surface Adhesion
	(sd)	mm, lw	%, lw	mg/m	nN (sd)
Never Dried	1.11 (0.04)	2.07	2.4	0.23	
Unrecycled	1.00 (0.06)	2.04	2.56	0.23	18.17 (3.20)
1x Recycled	1.01 (0.03)	2.05	3.21	0.24	23.25 (7.21)
2x Recycled	0.95 (0.04)	1.95	4.15	0.28	33.27 (3.86)
3x Recycled	0.93 (0.04)	1.98	3.93	0.27	33.29 (5.00)

The initial WRV of the never-dried TMP was much lower than either of the kraft pulps, which was expected because thermomechanical pulps have a much lower swellability than kraft pulps due to the difference in the pulping methods [43, 80]. The degree of hornification, shown in Figure 41, agreed with the data from the literature.

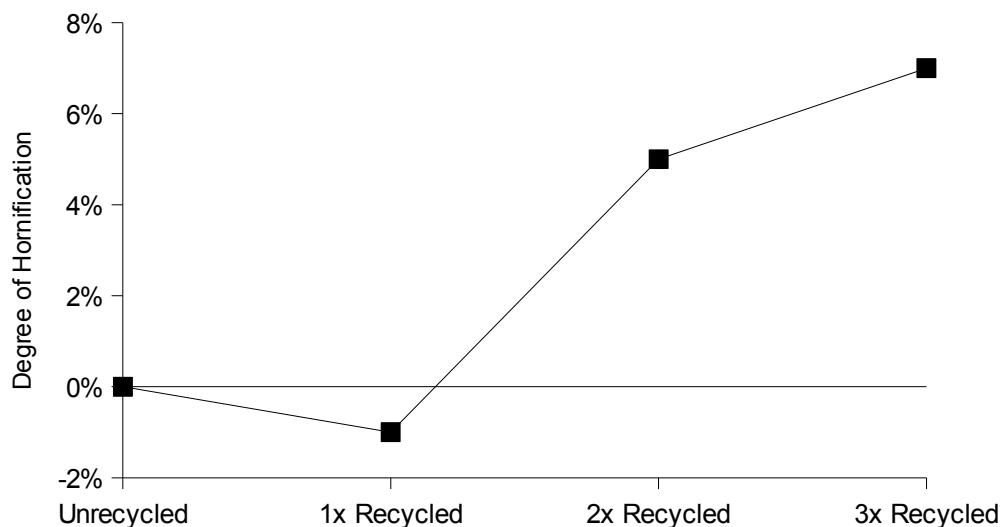


Figure 41: Degree of hornification for TMP

The relative decrease in the WRV seen over the course of the progressive recycling process was lower for the TMP than either of the kraft pulps. Most noticeably, there was no appreciable loss of water retention due to the first recycling step. Similarly, the surface adhesion increased due to recycling, but to a much lower extent than seen in the kraft handsheets. The mechanical pulping process used to make TMP generates coarser, stiffer fibers that result in the formation of weaker paper, but these fibers retain a greater percentage of their initial properties upon recycling than the higher quality kraft fibers [11, 48].

5.1.4 Handsheet Recycling Summary

Recycling handsheets in a laboratory allowed for precise control of the environmental variable to which the sheets were exposed. Unlike mill recycling, no additional chemicals were used, nor was the pulp degraded by age or adverse environmental factors such as heat or excess humidity. Because these factors were controlled, the effects of hornification caused solely by cycles of wetting and drying

were able to be observed. The decreasing trend in the water retention of hornified pulps was already known [8, 11, 61, 73], but the surface adhesion data from all three types of fiber was unexpected. Common hypotheses held that the fibers became more hydrophobic upon recycling, causing a decrease in the tensile strength of recycled paper due to the loss of potential interfiber bonding sites. However, this study demonstrated that the fibers apparently became more hydrophilic upon recycling, as seen in Figure 42.

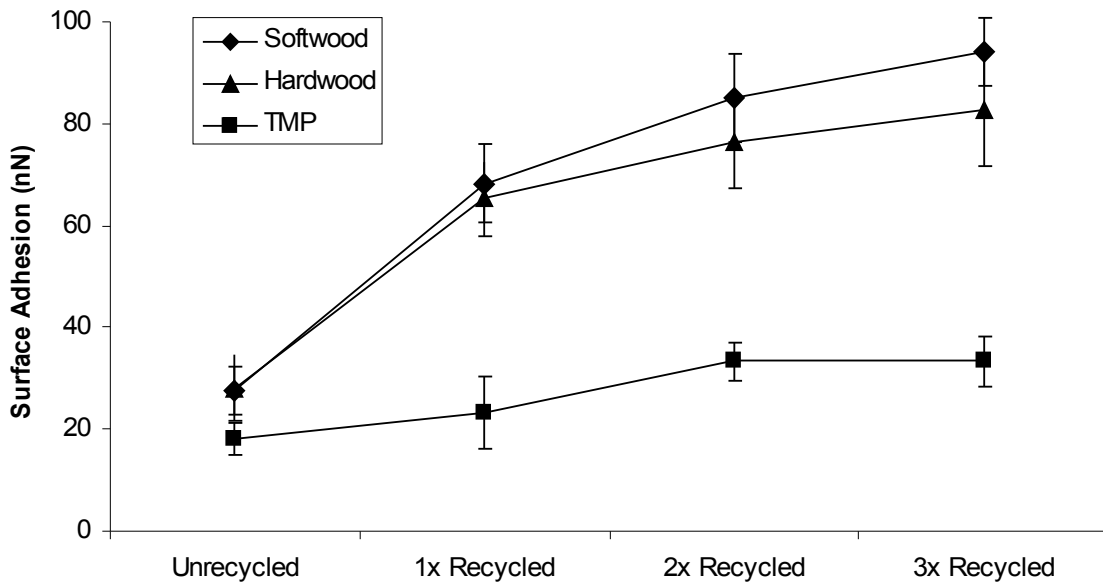


Figure 42: Surface adhesion data for recycled handsheets

The surface adhesion increased by approximately 300% for the kraft pulps by the ultimate recycling step. While the magnitude of these changes were larger for the kraft pulps than the TMP, the increase was still significant even in thermomechanical pulp. It is unlikely that the fiber surface became more hydrophilic due to a chemical change, as virgin cellulose fiber is covered with a high number of hydroxyl groups.

Therefore, the AFM must have measured increased surface adhesion because of increased surface-tip contact area.

Compared to the regularity of the AFM results, the WRV results do not show such clear trends. While WRV decreased with recycling, the degree of hornification was different for each type of fiber, as seen in Figure 43.

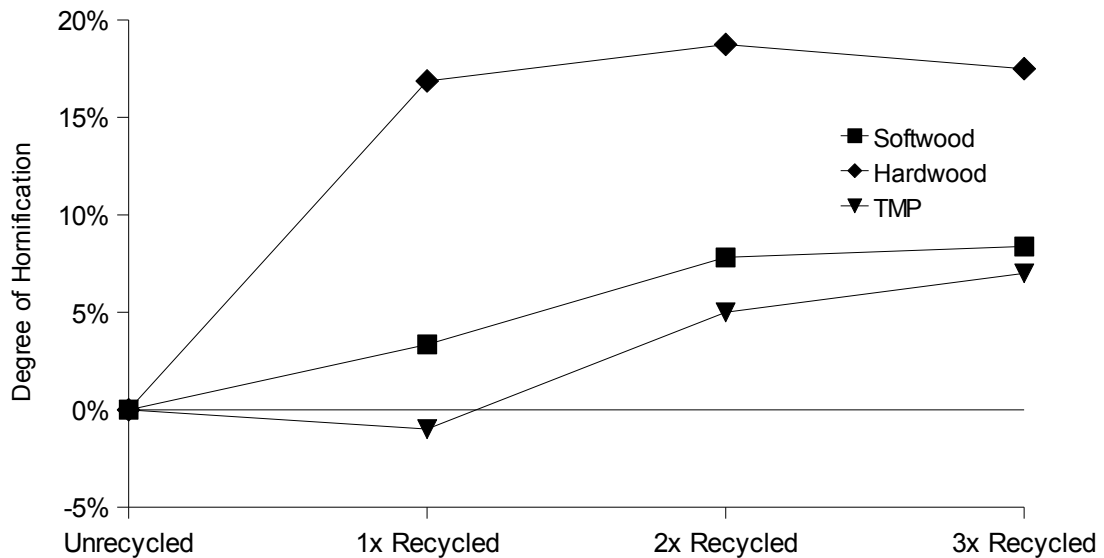


Figure 43: Degree of hornification data for recycled handsheets

Despite the similarity between the AFM measurements of the two kraft pulps, the degree of hornification is much higher for the hardwood pulp than the softwood pulp. The softwood pulp undergoes almost the same degree of hornification as the TMP, even though the change in surface adhesion was much higher for the softwood pulp than the TMP sample. The degree of hornification is expected to be higher for kraft pulps than TMP pulps [35, 61]. However, because this fiber was unrefined, the pulp samples differed significantly from samples traditionally used in papermaking. Degree of hornification in kraft pulps increases with the amount of refining [82].

Because these samples were unrefined, they did not show the expected drop in water retention, although the WRV measurements did decrease slightly for the softwood and significantly for the hardwood. Comparison of the surface adhesion measurements and the degree of hornification calculations indicates that the surface changes measured by the AFM are not directly related to irreversible closure of the fiber pores, which is the main contributor to the decrease in WRV.

These data conflict with several of the hypothesized causes of hornification. While pore closure is a demonstrated effect of wetting and drying cycles in pulp [75, 86, 99, 100], several hypotheses have been advanced to explain the reason for pore closure and the other effects of hornification [38, 46, 52, 53, 61, 72, 76, 84, 118]. One such hypothesis concerns the formation of covalent bonds on the fiber surface during drying. This hypothesis states that during drying, adjacent functional groups on the fiber surface react, forming covalent structures such as lactones and preventing fibers from swelling to their original size when rewet [4, 5, 11, 26]. However, such structures are more hydrophobic than hydroxyl groups and, using a hydrophilic AFM probe, the measured surface adhesion between the tip and sheet would decrease if the number of hydrophobic groups on the surface increased. No such decrease in the surface hydrophilicity was seen here.

Similarly, the hypothesis that the surface became inactive due to extractive coating is also unlikely. This hypothesis states that extractive compounds and fatty acids trapped within the interior of the fibers work their way to the surface due to the cycles of wetting and drying [61, 91]. Again, the presence of an increased amount of hydrophobic compounds on the fiber surface would have been detected by AFM

analysis and resulted in lower surface adhesion measurements as the recycling progressed.

No evidence of cellulose chain cleavage as a mechanism for hornification was seen during this experiment, according to the data gathered by FQA. Degradation of the cellulose chain, making fibers weaker and more prone to damage, results in shorter fibers [46, 52, 53]. However, the largest decreases in water retention and increases in surface adhesion in all of the handsheet samples were seen after the first recycle process when there was no evidence of fiber damage, which manifests itself as a decrease of fiber length and increase in fines content. It is known that cellulose chain cleavage is affected more by aging, especially at high humidities and temperatures, than by cycles wetting and drying [84, 118]. As the recycling experiments progressed, the increased fiber damage might have been due to cellulose chain cleavage, but at the time this damage occurred the changes in WRV and surface adhesion were far less pronounced than they were at the beginning of the experiments.

5.2 Single Fiber Wetting and Drying

While the bulk of this study was conducted using handsheet samples, a separate study was done using single fibers mounted on a glass slide. By wetting and drying the fibers directly on a slide, the effect of hornification on a single fiber could be determined. In addition, because the fibers were mounted to the slide and not part of the sheet matrix, analysis could be conducted in an aqueous environment. Figure 44 shows how single fibers reacted to cycles of wetting and drying.

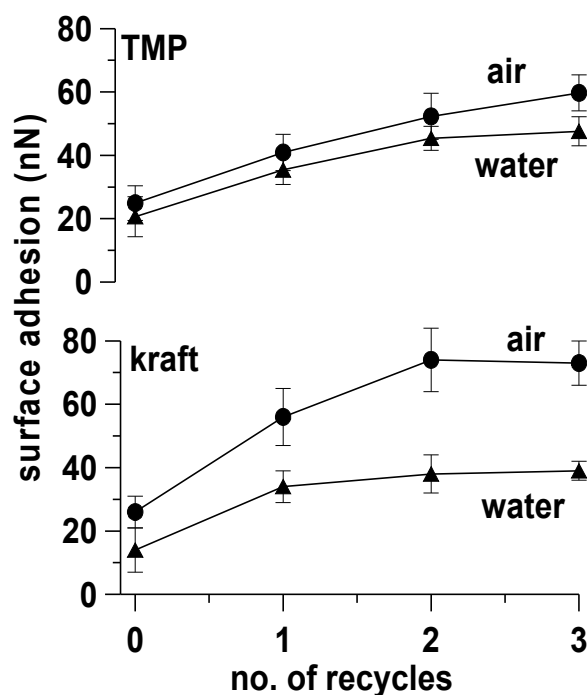


Figure 44: Effect of recycling on the surface adhesion of single fibers

The data from the two single fiber experiments follow the same general trends as the recycled samples in the handsheet experiments. Initially, the surface adhesion increased upon wetting and drying, but then the change levels off after the first few cycles. In both cases, the adhesion measured was lower for the sample in water than in air, which can partially be explained by the lack of capillary action between the tip and surface when the measurements were conducted in an aqueous environment [39, 89]. This difference can also partially be attributed to fiber swelling. Fibers swell upon rewetting, taking in water and expanding. A wet, swollen fiber has fewer potential bonding sites per unit surface area than it would in its dry, collapsed state, lowering the adhesive forces that attract the AFM probe. Because the kraft fibers had a higher swellability than the TMP, this effect was more pronounced in the kraft experiments.

5.3 Refining

After analysis of the effect of recycling on unrefined fiber surfaces, a study was conducted using the bleached softwood kraft pulp to determine the effect of refining on the fiber surface as observed by AFM, and to determine if there were any additional effects due to the recycling of the refined fibers. Refining is an important part of the papermaking process, used to increase the tensile strength of the paper sheet by increasing the surface area of the fiber available for bonding [32]. Samples were analyzed to determine their freeness (CSF), WRV, monolayer bound water (K_{pw}) and surface adhesion.

Table 12: Refining experiment data

		CSF mL	WRV	Kpw (sd)	AFM nN (sd)
Unrefined	Unrecycled	676	1.79	0.11 (0.08)	27.55 (4.82)
	1x Recycle	677	1.73	0.21 (0.05)	68.26 (7.79)
	2x Recycle	672	1.65	0.18 (0.05)	84.96 (8.57)
	3x Recycle	670	1.65	0.12 (0.02)	93.98 (6.74)
Medium Refining	Unrecycled	415	2.06	1.02 (0.4)	34.62 (3.67)
	1x Recycle	428	1.48	0.43 (0.4)	68.80 (9.53)
	2x Recycle	424	1.38	0.46 (0.03)	93.46 (9.93)
	3x Recycle	424	1.38	0.65 (0.4)	106.39 (9.35)
High Refining	Unrecycled	222	2.41	0.72 (0.3)	28.56 (6.39)
	1x Recycle	245	1.73	0.83 (0.3)	82.16 (8.55)
	2x Recycle	247	1.64	0.69 (0.4)	92.55 (8.84)
	3x Recycle	246	1.66	0.82 (0.4)	98.02 (7.73)

In this study, the freeness of the fiber was not affected by recycling the unrefined or the refined pulp samples. Freeness was fairly constant at all levels of recycling, indicating that the drainage of the fibers was not affected by hornification.

However, WRV was affected by both refining and recycling. The WRV increased for the unrecycled pulp as the level of refining increased. At each level of

refining, the WRV also decreases with progressive recycling steps. However, this decrease is much smaller for the unrefined pulp than either of the refined pulps, as shown in Figure 45.

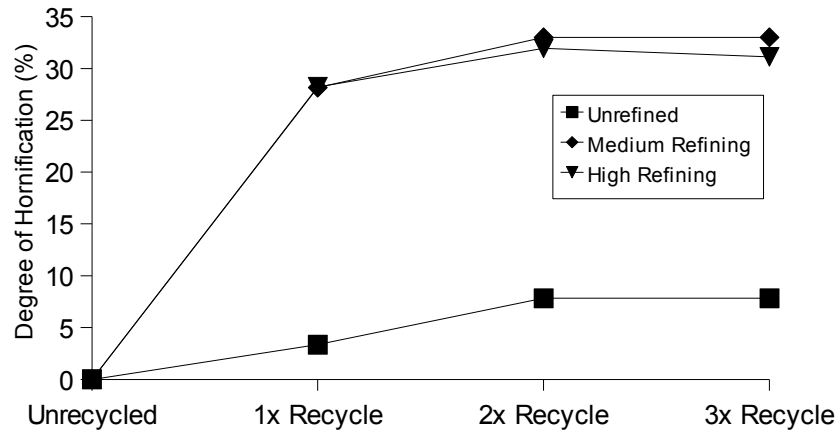


Figure 45: Effect of refining on degree of hornification

Going from the virgin sheet to the first recycle, the degree of hornification of the unrefined pulp is less than 4%, and the degree of hornification is less than 8% after the final recycle step. However, for the refined samples, the degree of hornification is almost 30% after the first recycle process, and remains roughly constant at approximately 30% during the following recycling steps. The WRV decreases much more sharply than expected at the medium level of refining. Degree of hornification should increase with refining [82], however the observed degree of hornification was equivalent for the medium and highly refined pulps. There are any number of factors that could affect the WRV measurements, such as an increase in the rate of drying. In general, however, the higher degrees of hornification seen in the refined samples more closely agree with the data from the literature presented in section 2.4.1 [102, 111].

Refining exposes the interior of the fiber, increasing surface area and allowing a greater number of interfiber bonds to form, strengthening the resulting sheet [32]. But the increase in surface area exposes a greater number of the fibers' internal pores, allowing for more water retention initially but also causing a greater observed degree of hornification as the pores close during drying [75, 100].

The analysis of monolayer bound water (as measured by K_{pw}) is complicated by the relatively large degree of error seen in the results. This large error has been noted before for highly refined pulps, due to experimental uncertainty [105]. The sample used for monolayer bound water analysis is relatively small (1.2 g OD weight of fiber), and the fiber damage caused by refining is not uniform. It is likely that small differences in the degree of damage to the fiber samples result in large differences in K_{pw} measurements, due to the sensitivity of the test. However, it appears that the degree of monolayer bound water is affected by refining but not recycling, as has been noted earlier [104]. With the exception of the K_{pw} measurement of the unrecycled medium refining sample, K_{pw} increases with the level of refining, but it remains fairly constant at all levels of recycling. The exposure of more surface area allows for an increased amount of bound water, but this does not decrease with recycling as WRV does. WRV, although often considered to measure bound water, does not accurately measure monolayer bound water. It measures both bound water and water trapped in pores by surface tension [38, 76]. The disparity between these two sets of data indicate that while additional surface area is exposed during refining, none of this surface area is lost as the fiber is recycled, even though

the newly exposed pores are subject to the expected shrinkage and closure as the fiber is subjected to cycles of wetting and drying.

The AFM data are also of interest. The refining process had no significant effect on the surface adhesion measurements, as seen in Figure 46.

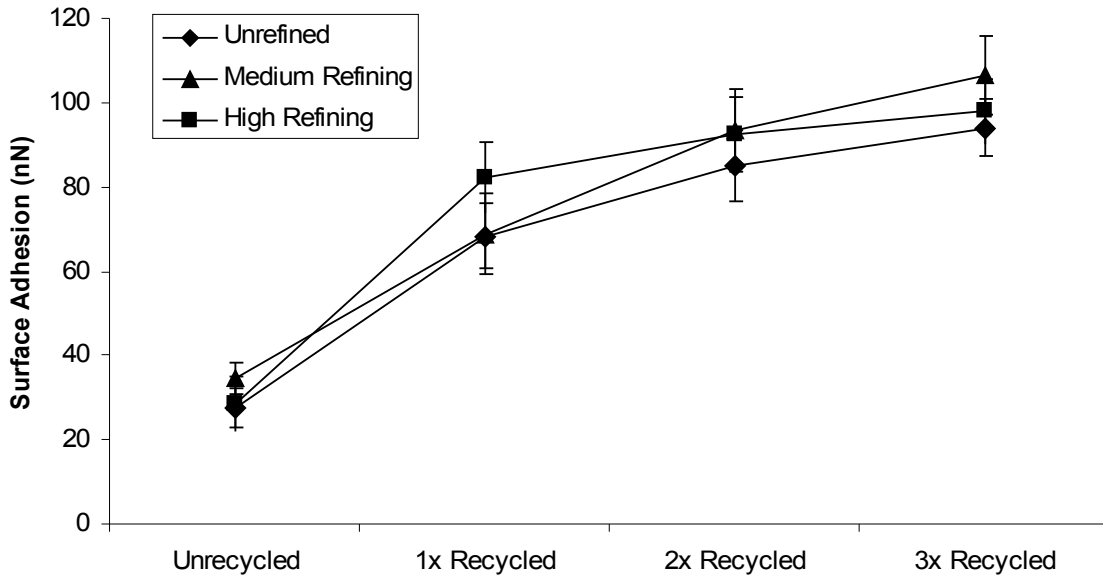


Figure 46: Refining and recycling surface adhesion measurements

Together with the WRV and K_{pw} data, this indicates that while refining exposes more of the fiber and increases the surface area, the refining process does not affect the surface of the fiber. The total amount of exposed surface does not affect AFM measurements, although they are sensitive to the chemistry and topography of the surface. Refining is essentially a macro-scale effect, causing changes in the fiber on a scale too large to be observed through AFM analysis.

Again, as with the heat treatment study, a disconnect between water retention and surface adhesion is observed. The adhesion measurements are unaffected by refining, while the degree of hornification measurements are not.

5.4 AFM Imaging of Fiber

The AFM was used to image the fiber surface in addition to measuring surface adhesion. If the changes in adhesion were caused by a surface topography change, then such a change should be detectable as a change in the surface roughness. The first step to quantifying the fiber surface was to obtain clear images of the fiber surface.

These images ranged in size from 250 μm^2 to 2500 nm^2 . Because the changes in surface adhesion were obtained using an AFM probe with a radius of curvature of 10 nm at the tip, the changes to the fiber must have occurred on a scale smaller than 10 nm for the result to be measurable using such a probe. A tip with a radius of curvature of 1 nm was used to image the fiber. However, changes on a nanometer scale, while the most likely cause for the change in surface adhesion, were not the only possible changes. The loss of fiber volume due to fiber collapse is a known effect of hornification, and this imaging study was run across a range of sizes to determine if there were large-scale surface changes occurring on the fiber surface. However, due to the roughness and variability of the fiber surface, there was no discernible pattern visible with the larger images. Sample images are shown below, while more images are given in Appendix A. The images presented in this section are all from the same test location from an unrecycled hardwood kraft handsheet.

5.4.1 25 μm^2 Images

The following images are samples of the 25 μm^2 images that were taken of unrecycled kraft fibers.

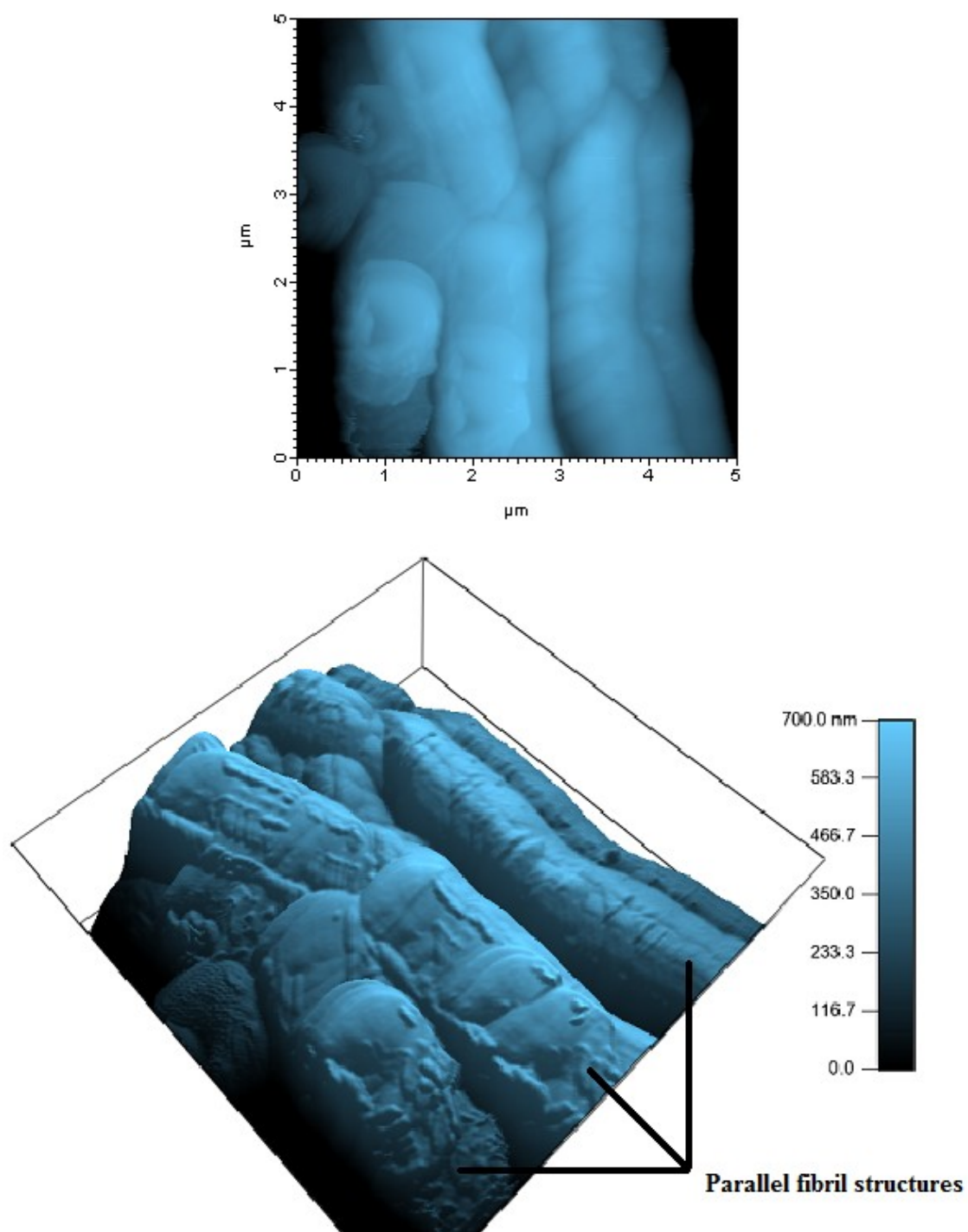


Figure 47: 2D and 3D rendering of 25 μm^2 unrecycled kraft fiber

On this scale, the surface roughness is dominated by large, irregular features. In this particular image, several different fibrils are shown bound together in parallel. The following chart demonstrates the problem of variability, which obscure any trends in surface roughness.

Table 13: RMS roughness results for 25 μm^2 images

	Kraft		TMP	
	Unrecycled	3x Recycled	Unrecycled	3x Recycled
RMS Roughness (nm)	295.2	322	243.8	274.8
Standard Deviation	118.9	96.99	145.2	125.3

There are no visible trends of surface roughness on this scale. There were no larger variations in roughness discernible, and any small variations were lost due to the surface irregularity.

5.4.2 0.25 μm^2 Images

The following images are samples of the 0.25 μm^2 images that were taken of unrecycled kraft fibers.

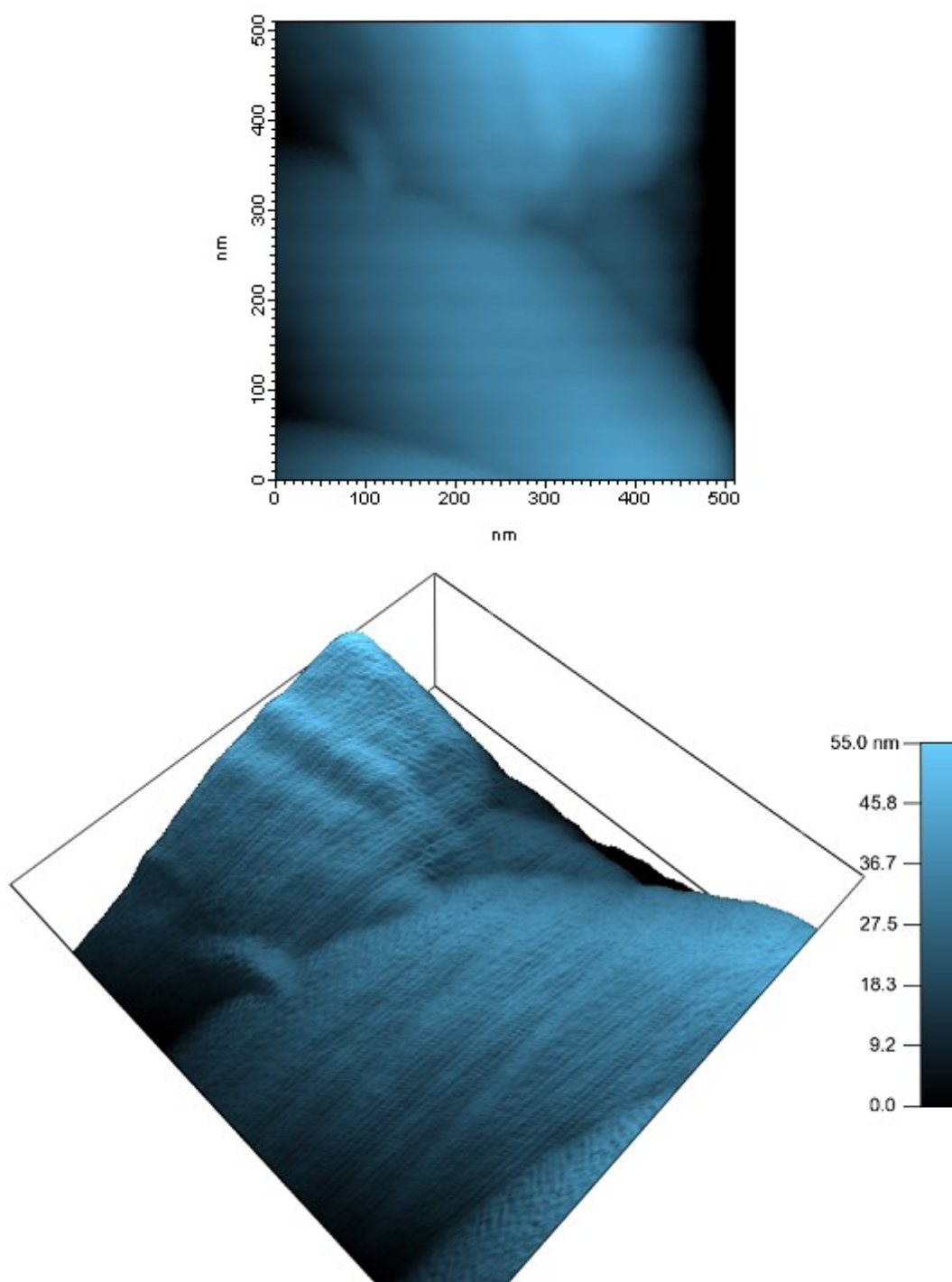


Figure 48: 2D and 3D rendering of $0.25\mu\text{m}^2$ unrecycled kraft fiber

Large features are still evident on this scale. This image appears to show one microfibril overlapping another. Again, the irregularity apparent in these samples on

this scale does not allow for accurate comparisons between the unrecycled and recycled pulps, as shown in the image analysis data given in Table 14.

Table 14: RMS roughness results for 0.25 μm^2 images

	Kraft		TMP	
	Unrecycled	3x Recycled	Unrecycled	3x Recycled
RMS Roughness (nm)	16.08	16.99	14.07	14.26
Standard Deviation	6.3	7.1	5.94	3.87

5.4.3 2500 nm^2 Images

The following images are samples of the 2500 nm^2 images that were taken of the unrecycled kraft fiber surfaces.

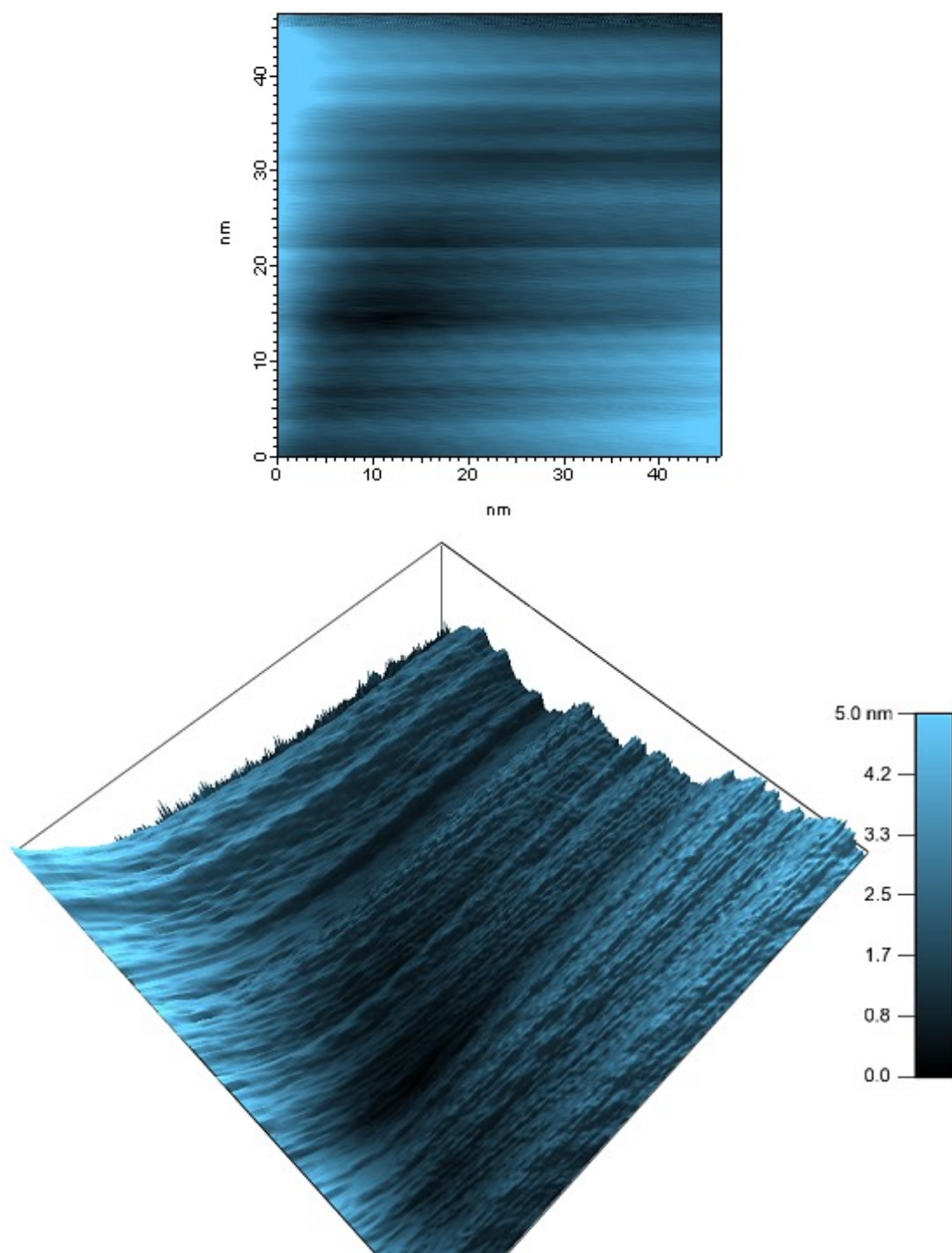


Figure 49: 2D and 3D rendering of 2500 nm² unrecycled kraft fiber

At this much smaller scale, the surfaces were regular enough that a noticeable change was apparent between the unrecycled and recycled kraft fibers.

Table 15: RMS roughness results for 2500 nm² images

	Kraft		TMP	
	Unrecycled	3x Recycled	Unrecycled	3x Recycled
RMS Roughness (nm)	1.36	0.81	1.41	1.36
Standard Deviation	0.6	0.29	0.43	0.67

For the kraft pulp, a decrease in the surface roughness, which indicates that a smoother surface resulted after multiple recycle steps, was apparent after analyzing the images. For the TMP samples, however, no such pattern was discernible. Given that the kraft pulps demonstrated a much higher susceptibility to hornification, with a much larger increase in surface adhesion, it is most likely that any changes the TMP fibers underwent were too subtle to determine through this type of image analysis. A 300% increase in surface adhesion for the kraft pulp was measured, despite only a 40% decrease in these RMS roughness measurements.

The decrease in surface roughness causes an increase in tip-surface contact area. As the surface becomes smoother, the AC 240 probe is able to contact more of the active bonding sites on the fiber surface, increasing the tip-surface adhesion and causing the apparent increase in surface hydrophilicity due to recycling.

5.5 Mill Sample Analysis

Several samples of newsprint made from recycled fiber at the Augusta Newsprint mill were analyzed using AFM. Surface adhesion measurements were taken from four paper samples from four different days' production from June and July of 2006 and compared to the adhesion data from the TMP samples that were recycled in the laboratory.

Table 16: Surface adhesion analysis of mill newsprint samples

	Lab Sample	Mill Samples			
	1x Recycle	22-Jun	28-Jun	29-Jun	3-Jul
Surface Adhesion (nN)	23.25	31.67	12.75	18.21	33.65
Standard Deviation	7.21	25.00	6.94	15.87	22.98

The mill samples showed a much higher degree of variability than the lab sample, due to both the irregularity of the feed stock used to make recycled newsprint and the chemical load used, including filler, brightness enhancers, de-inking chemicals, and any chemicals that might have been in the feed stock before the recycling process. A histogram of the surface adhesion measurements from the four mill samples is provided below to illustrate the variability of the samples.

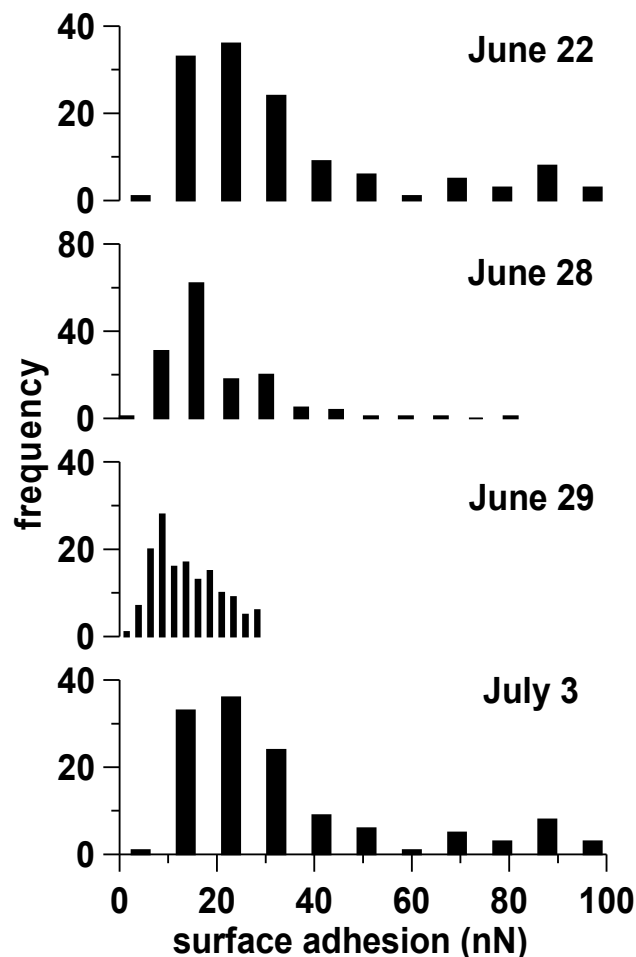


Figure 50: Mill newsprint histogram

From this breakdown, it is apparent that the four paper samples were very irregular. In particular, the June 29 sample was wildly different from the others. For the other three days, the most common surface adhesion measurements were between 15 and 35 nN, which matches that of the lab-recycled TMP fibers, with a smaller incidence of points at a much higher surface adhesion, possibly some hydrophilic materials mixed in with the fiber. However, on June 29, all of the measurements were below 30 nN, and the highest frequency was in the 8-10 nN range, well below that of any fiber measurements gathered during the laboratory experiments. It is most likely that the pulp that day contained a hydrophobic contaminant that coated the fiber surface,

resulting in the discrepancy. It is interesting, however, that all four of the samples met the mill's production specifications for optical properties (such as opacity and brightness) and tensile strength. This indicates that, at least in some instances, AFM can prove to be an overly sensitive tool.

5.6 Summary

Several noticeable trends became apparent during the course of study. While some of the effects of hornification are known, the exact mechanisms that cause these changes are complex and hard to decipher. Two separate effects were observed during this study. First, the loss of fiber swellability, as measured WRV, which followed the expected trends that have been observed by researchers studying hornification and workers in the recycling industry. Second, the changes in the tip-surface adhesion and the fiber surface roughness, which were not directly related to the decrease in water retention.

In several instances, WRV was seen to change to a much greater degree than the surface adhesion measurements. During the heat treatment experimentation, WRV decreased greatly, despite relatively small increases in the tip-surface adhesion. During the refining experiments, it was seen that WRV and degree of hornification were influenced by the amount of refining the fiber samples underwent, while the surface roughness was not measurably affected. K_{pw} , however, was unaffected by recycling, indicating that the monolayer bound water content remained relatively constant. The amount of monolayer bound water is a function of exposed surface area - recycling did not cause a detectable decrease in the exposed surface area of the fibers.

Surface adhesion as measured by AFM is affected by surface chemistry and tip-surface contact area. Because drastic alterations in surface chemistry that would result in large increase in fiber hydrophilicity are unlikely, the surface topography must be changing. The loss of surface roughness indicates that the contact area has increased, allowing for more interaction between the active groups on the fiber surface and the AFM probe.

It is likely that the fiber surface is collapsing in on itself as it goes through cycles of wetting and drying. Microfibrils on the surface of a fiber laminate together, smoothing the surface, and preventing the joined microfibrils from forming interfiber bonds. Decreases in surface roughness due to this lamination effect would have little effect on the overall fiber pore and void volume, while collapse of the pores and voids would not affect the fiber surface except at the surface directly adjacent to these sites. Figure 51 illustrates these changes to the surface.

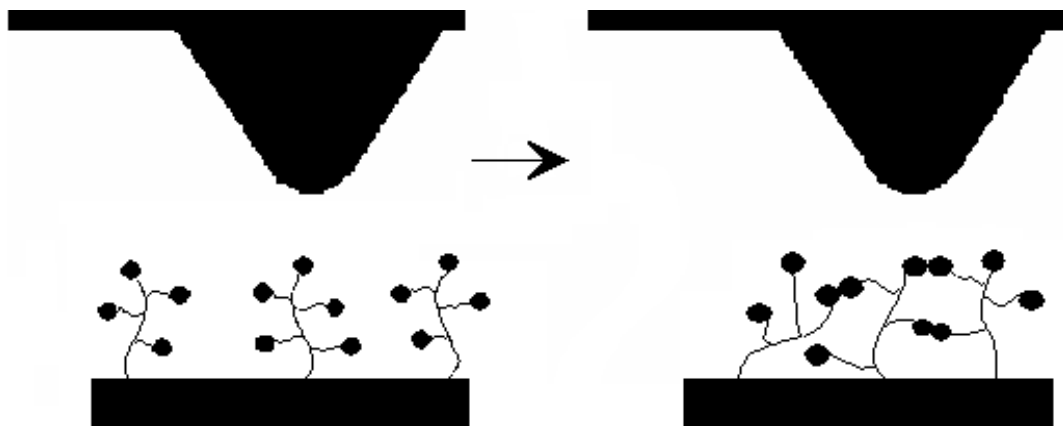


Figure 51: Illustration of surface laminating effect from virgin fiber (left) to recycled fiber (right)

The apparent conflict arises because the different techniques measure different attributes of the fiber. The lower WRV results from a collapse of the pores, which

reduces the water-carrying capacity of the fiber. Hence, the AFM responds more to changes in the packing density of the surface than to changes in surface chemistry. Lamination of the surface causes the active sites to draw towards one another and smooth out the surface, resulting in a higher surface adhesion measurement. A higher concentration of these active sites, along with loss of fiber flexibility due to pore closure, explain the decrease in tensile strength, because interfiber entanglements and bonding are inhibited when these active sites on adjacent fibers can no longer come into contact as easily.

CHAPTER VI

CONCLUSIONS AND RECOMMENDATIONS

This thesis evaluates the use of atomic force microscopy to study the effects of hornification on cellulose fiber surfaces. This work demonstrates that there are apparently two separate effects that occur during the hornification process. It is known that hornification causes a decrease in the water retention of recycled pulp, but the change in surface roughness on a nanometer scale has not been previously observed.

The WRV analyses performed during these experiments confirmed the observed behavior seen in the literature. With progressive recycling, cellulose fibers lose their ability to retain water due to collapse of the fiber and loss of pore volume. However, the secondary effect of hornification was observed using AFM. The force of adhesion between a hydrophilic AFM probe and the fiber surface increased upon recycling, indicating that the surface of a hornified fiber was more hydrophilic than that of an unhornified fiber, which contradicts conventional wisdom. It had been assumed that the lower tensile strength of a recycled paper sheet was due to an increase of hydrophobicity on the fiber surfaces.

This research demonstrated that the surface of a cellulose fiber becomes smoother after being recycled, increasing the contact area between the probe and fiber surface and causing an apparent increase in sheet hydrophilicity. Furthermore, the refining experiments and heat treatment experiments demonstrated that the changes in

surface roughness and water retention are not directly linked. It is possible to make large changes in the water retention value of the refined and recycled pulps without affecting the surface adhesion measurements drastically. The fiber delamination effects of refining and the pore closure that contributes to a decrease in water retention occur on a scale too large to be observed using AFM. The AFM apparently observes changes in the surface caused by the interaction of adjacent microfibrils and free cellulose chains on the surface, which becomes smoother as intrafiber hydrogen bonding laminates the bonding sites on the surface together.

6.1 Recommendations For Future Work

With an understanding of how the fiber surface changes due to recycling, a more effective method of measuring the effects of hornification is now available. Changes in fiber surface topography not only change how fibers interact with each other, but how they interact with the chemical additives that are common in the pulp and paper industry. The following paths are potential research avenues that might yield both theoretical and practical knowledge about hornification.

1. **Controlled analysis of the effect of chemical additives on hornification:**
Commercial paper products contain a variety of polymers, fillers, and other additives that bond strongly with cellulose fibers. A study of the effect of these chemicals on surface adhesion and roughness would determine if these chemicals have an impact on this surface lamination effect.
2. **Polymer adhesion study:** Loss of surface roughness and concentration of the active groups would change how polymers interact with the fiber surface.

Polymers of different size and charge density may be more effective on recycled fibers, with the differing surface topography.

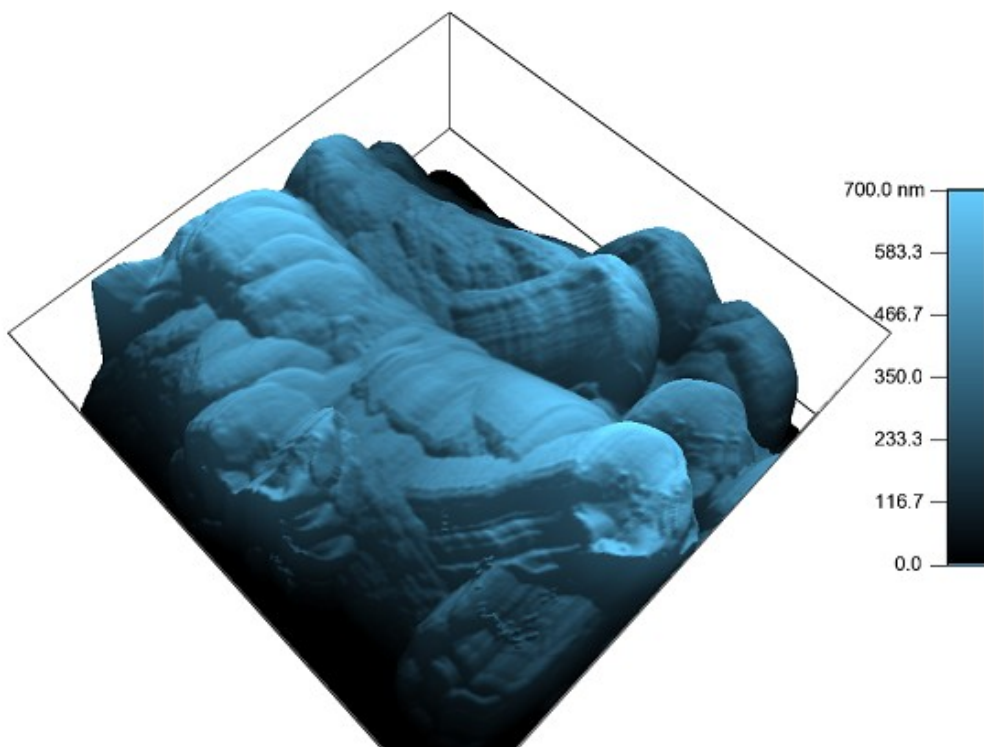
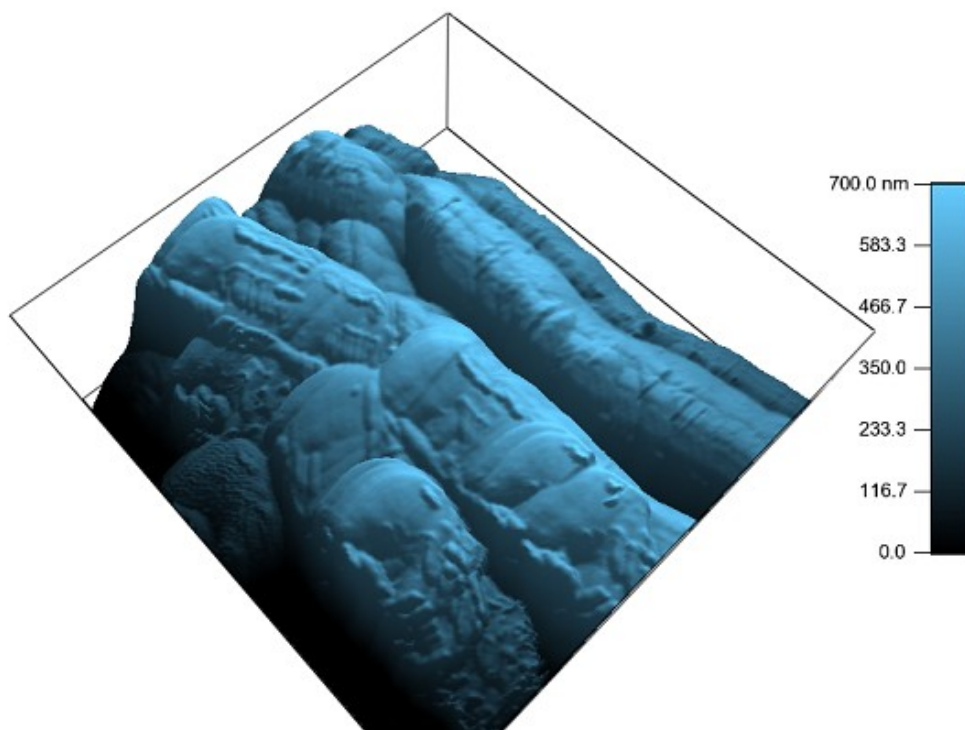
3. **Determine effect of surface roughness loss on tensile strength:** Tensile strength is traditionally thought to be affected by fiber flexibility, which in turn is affected by fiber pore volume. This research demonstrated that decrease in surface roughness and loss of pore volume are not directly linked, and therefore that fiber flexibility can potentially be altered without affecting surface roughness. Further study can be conducted to determine the effect of fiber surface roughness on sheet tensile strength.
4. **Inhibition of hornification study expansion:** The use of sucrose to inhibit hornification retarded both the increase in surface adhesion and the loss of WRV, however the concentration of sucrose required, and the fact that it needs to be added to the pulp each time it is recycled, does not make it cost-effective for industry use.
5. **Mill trial expansion:** The initial study of samples from a paper mill revealed that the AFM as used in this thesis is over-sensitive to the common variations inherent in an industry setting. However, further work should be done to determine if the AFM can be adapted for use in problem analysis and troubleshooting for a mill environment.

APPENDIX A

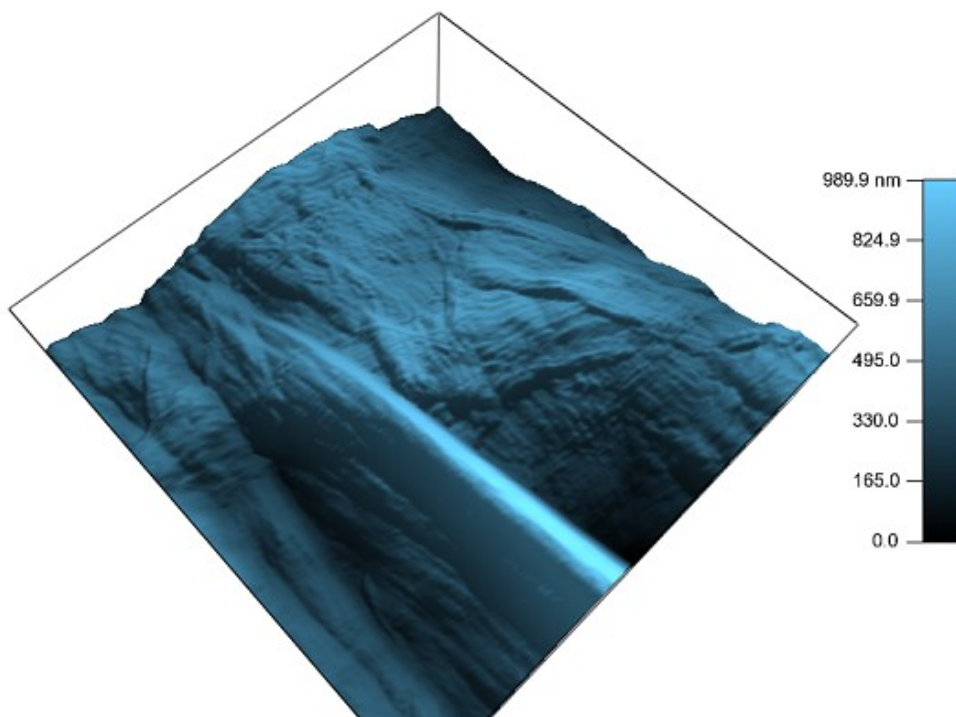
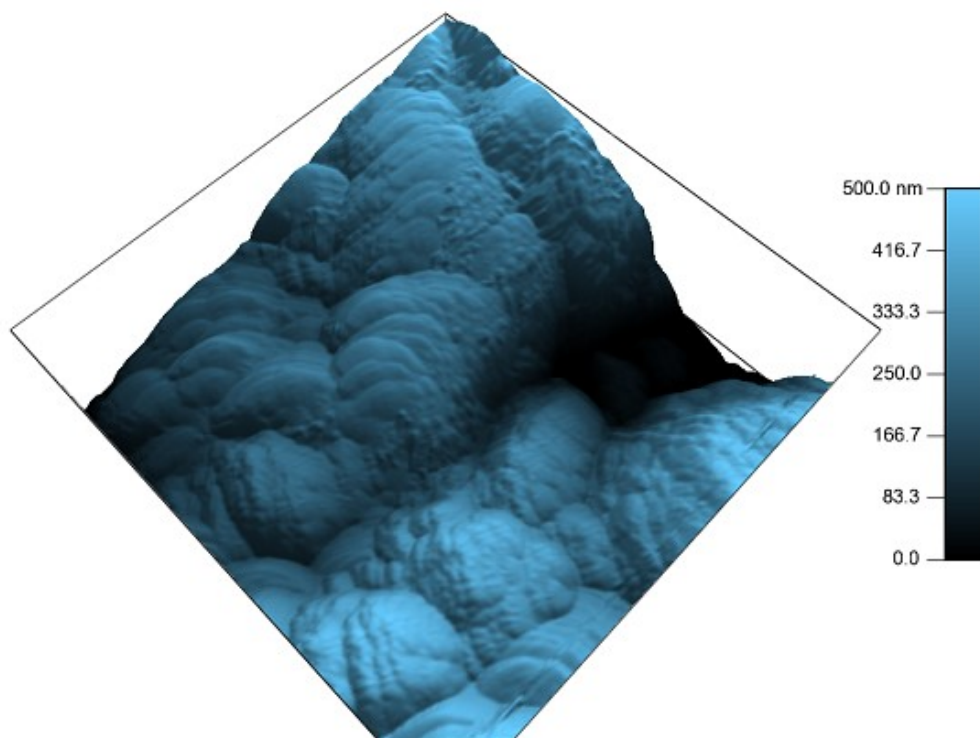
ADDITIONAL FIBER AFM IMAGES

The following images are 3D renderings of unrecycled and recycled kraft and TMP fiber surfaces at various sizes.

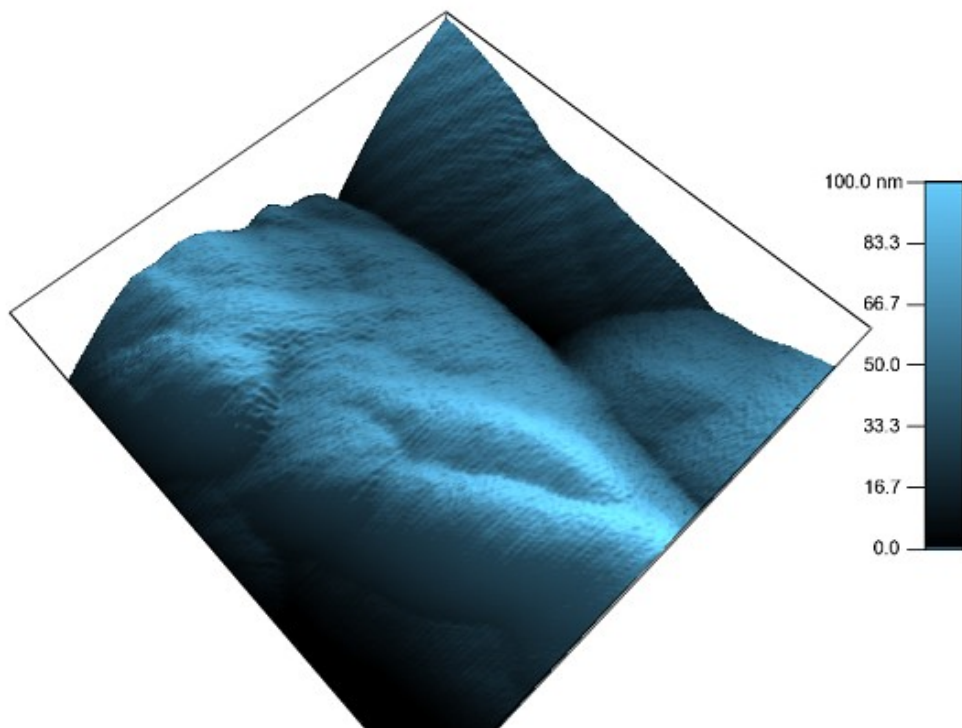
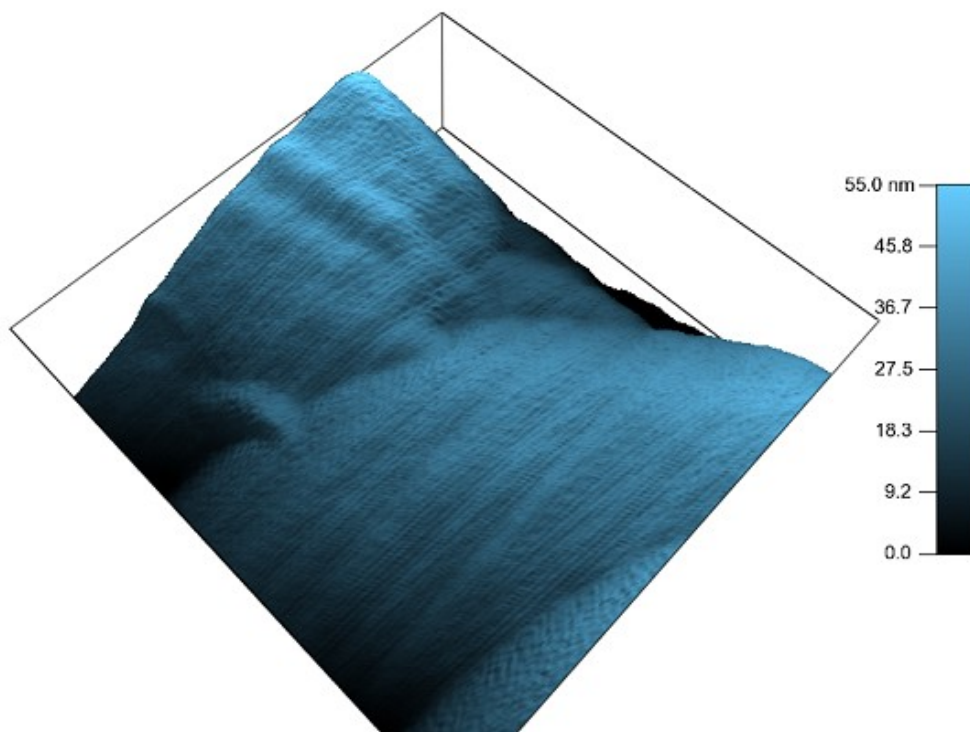
Unrecycled kraft, 25 μm^2



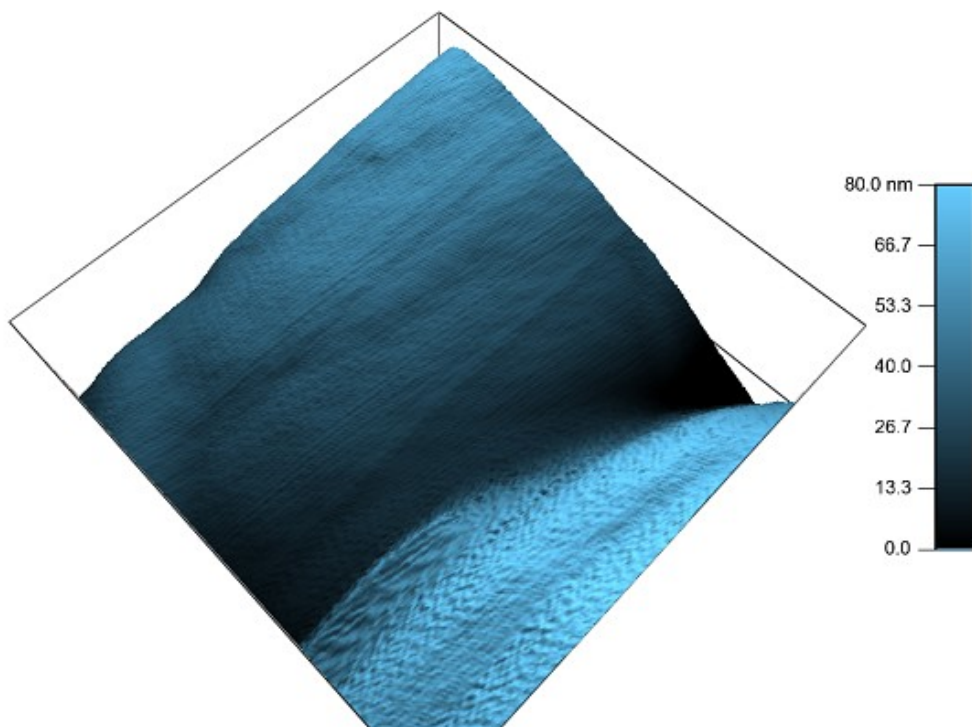
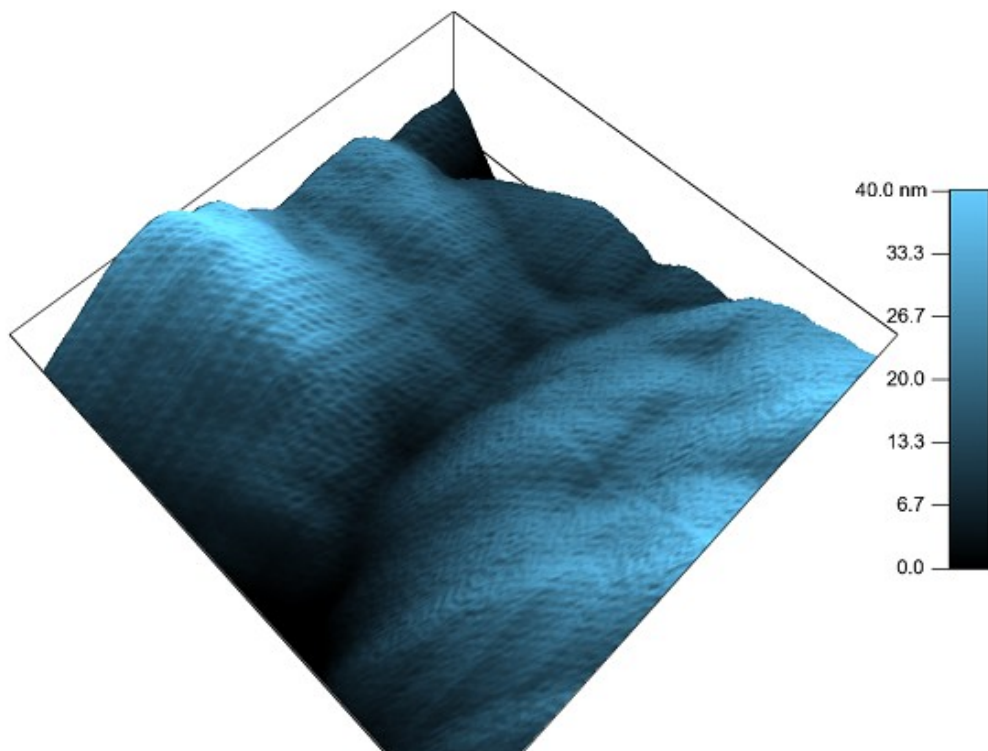
Recycled kraft, 25 μm^2



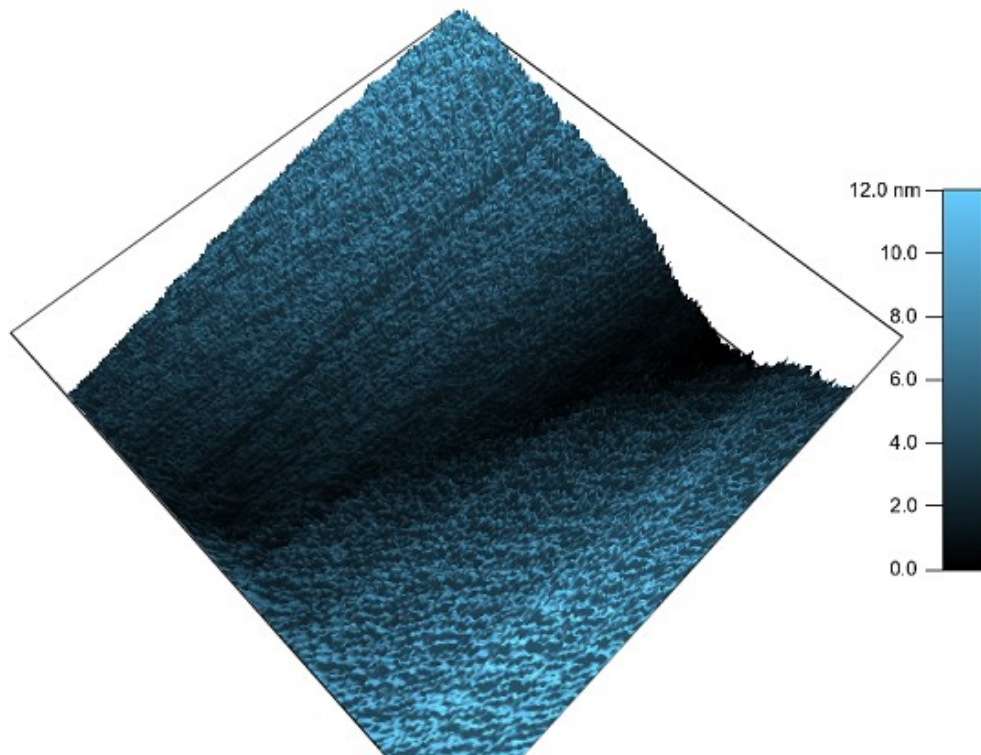
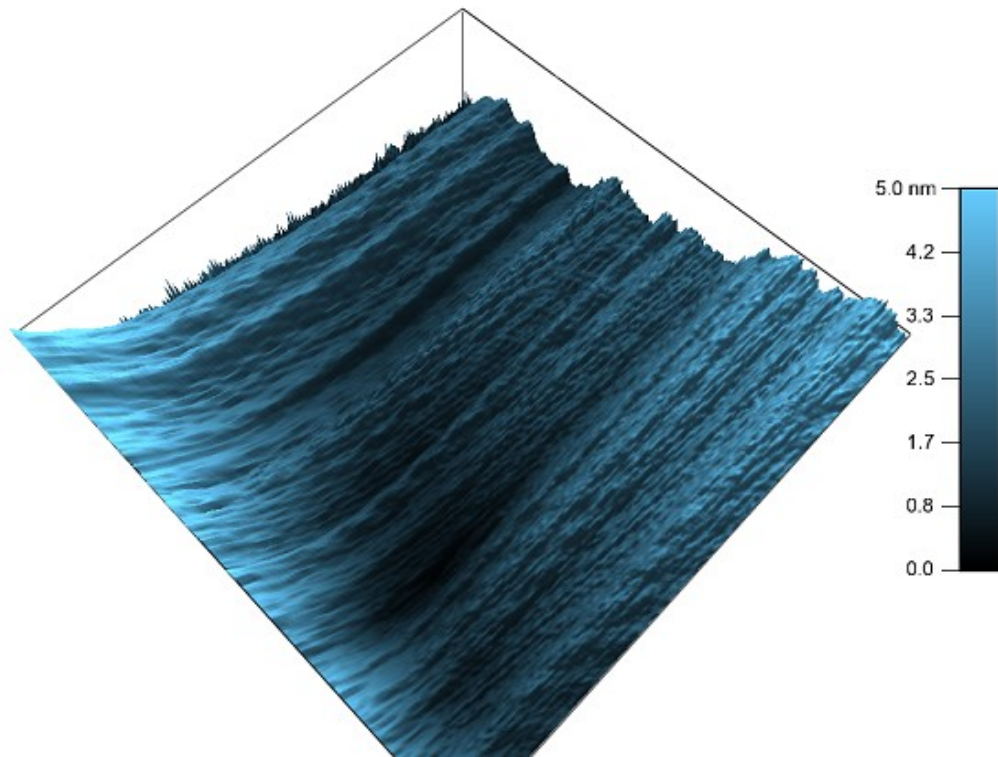
Unrecycled kraft, 0.25 μm^2



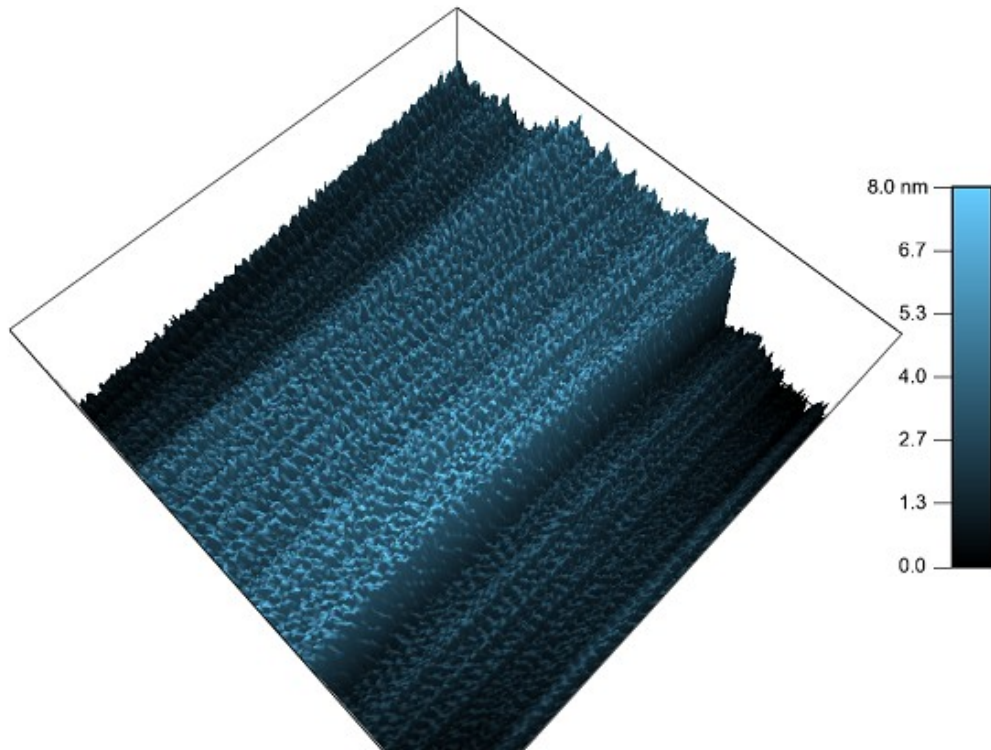
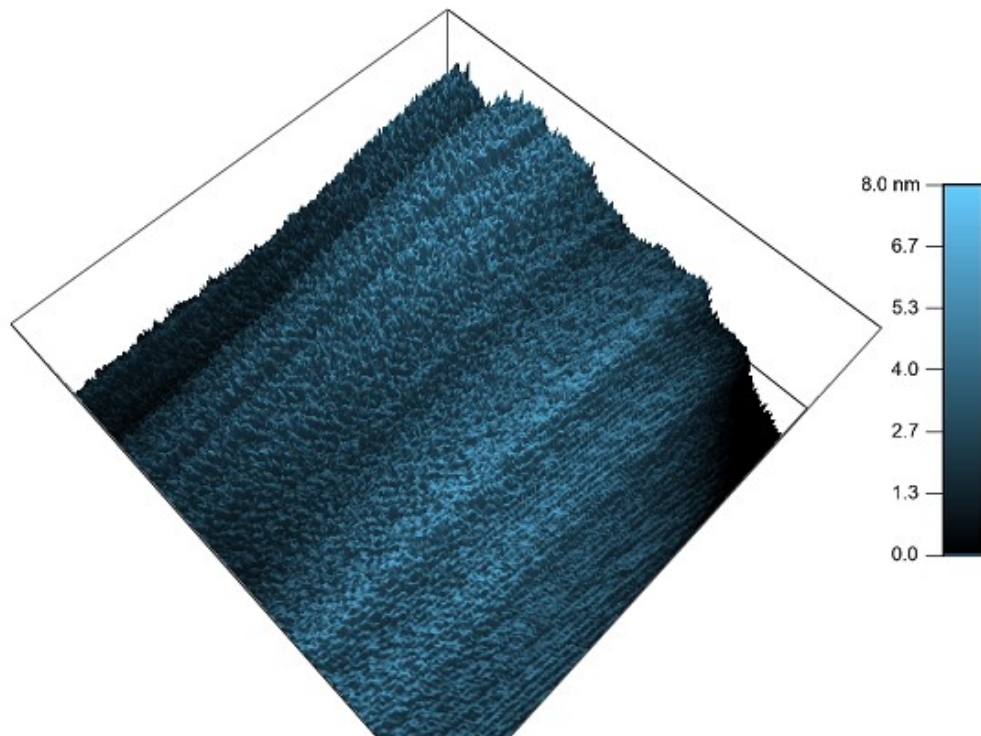
Recycled kraft, 0.25 μm^2



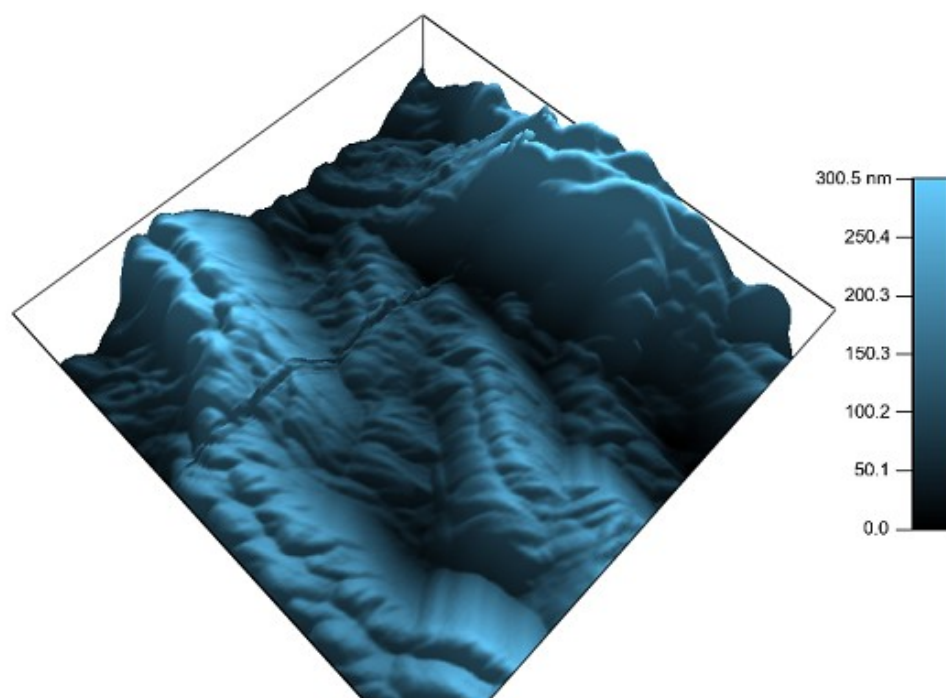
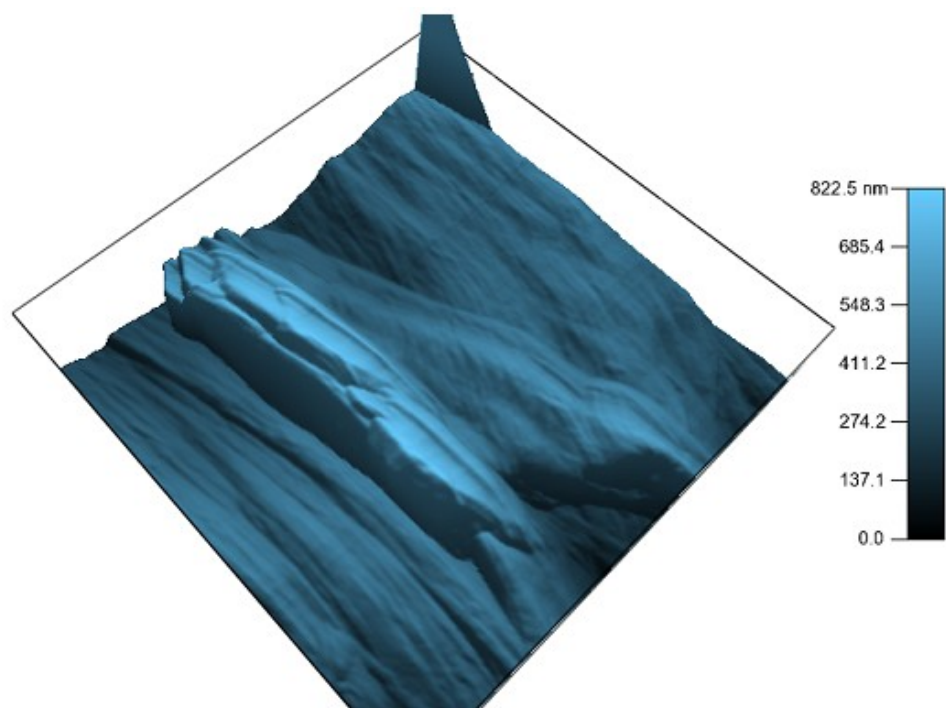
Unrecycled kraft, 2500 nm²



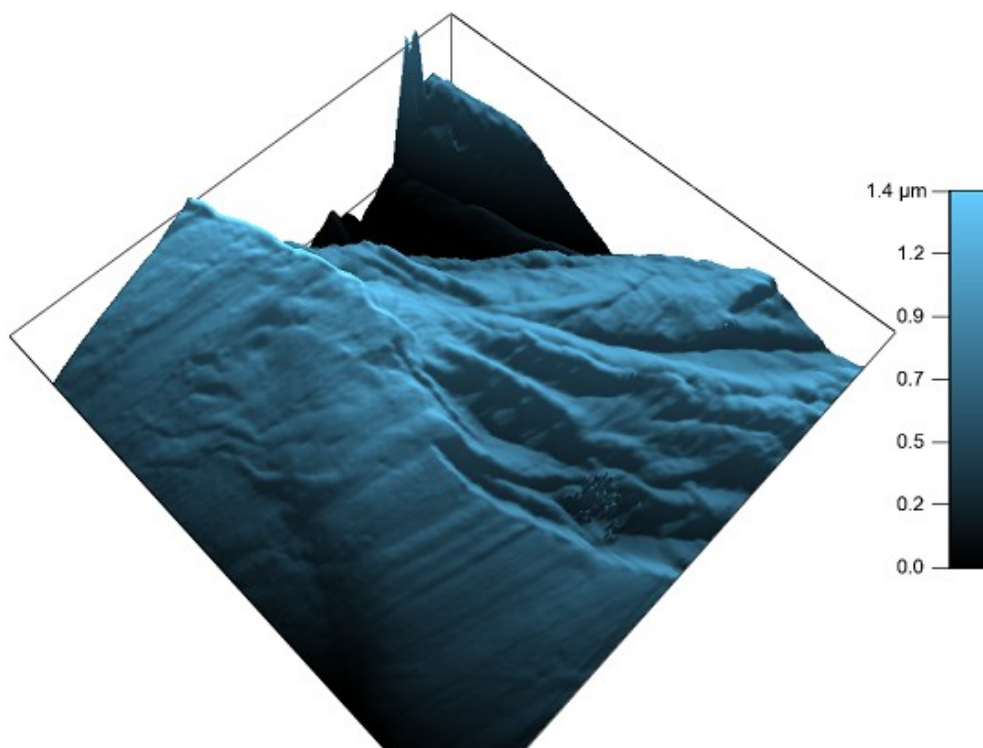
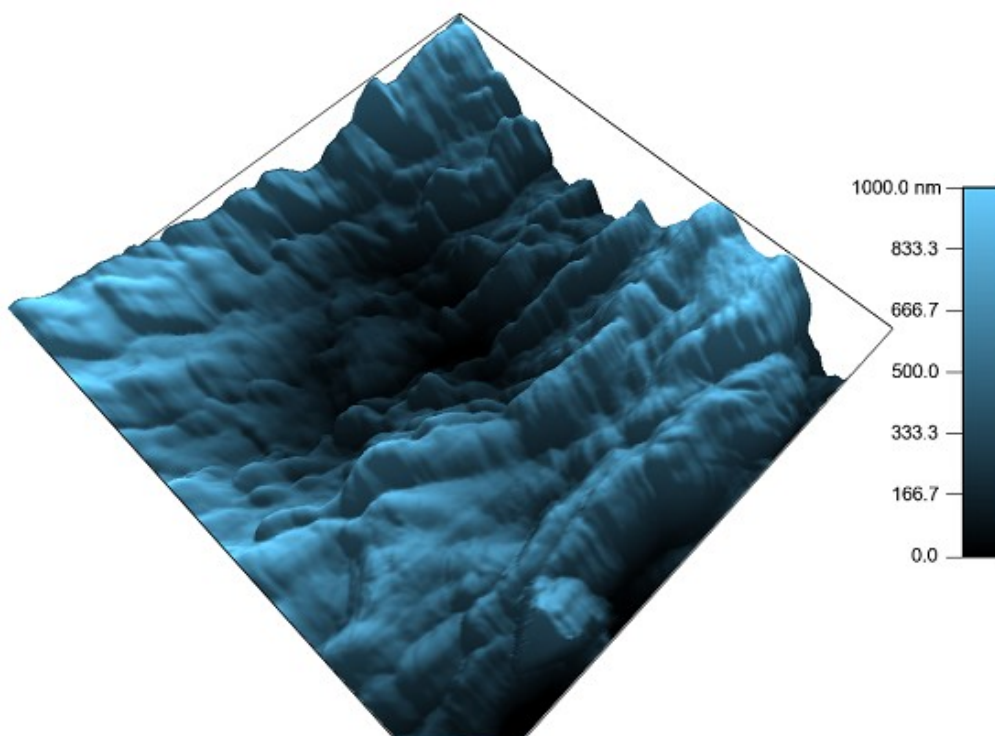
Recycled kraft, 2500 nm²



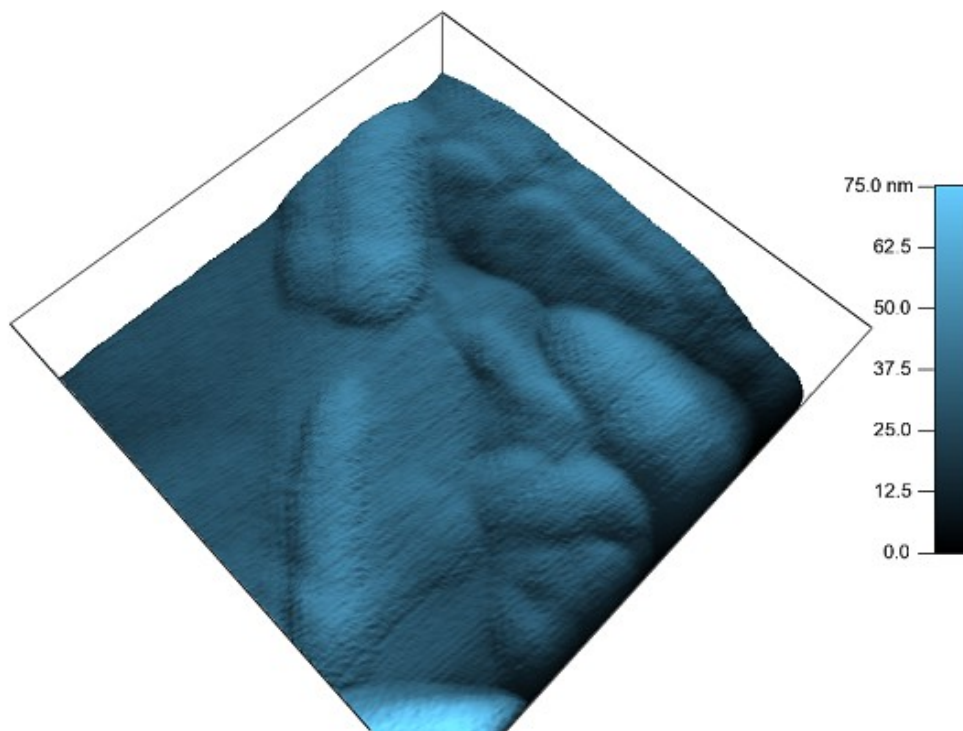
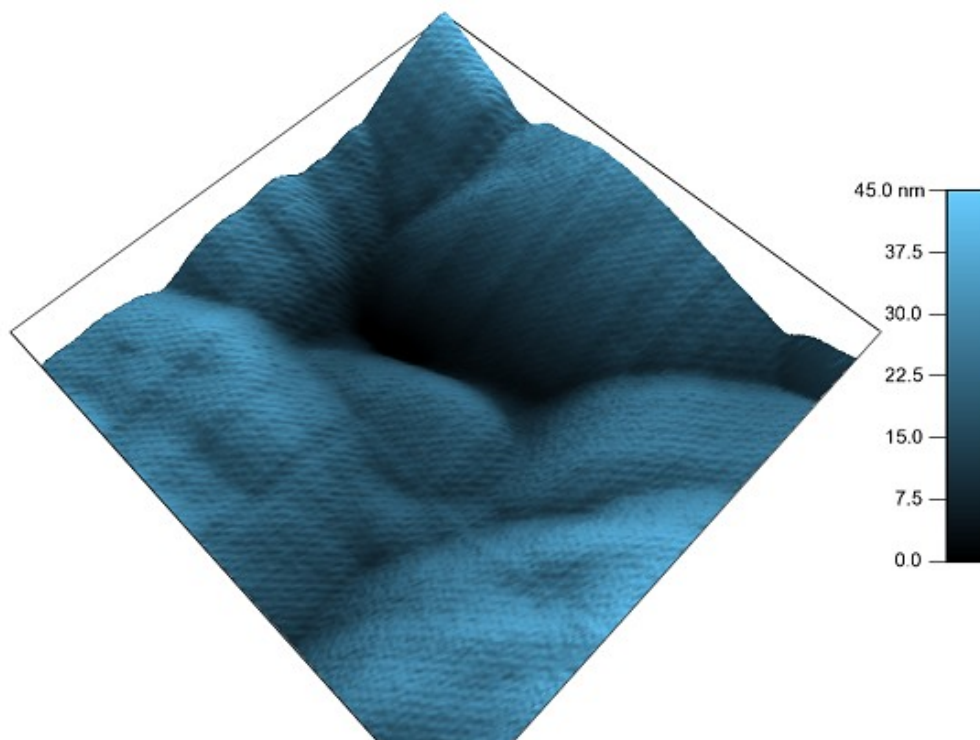
Unrecycled TMP, 25 μm^2



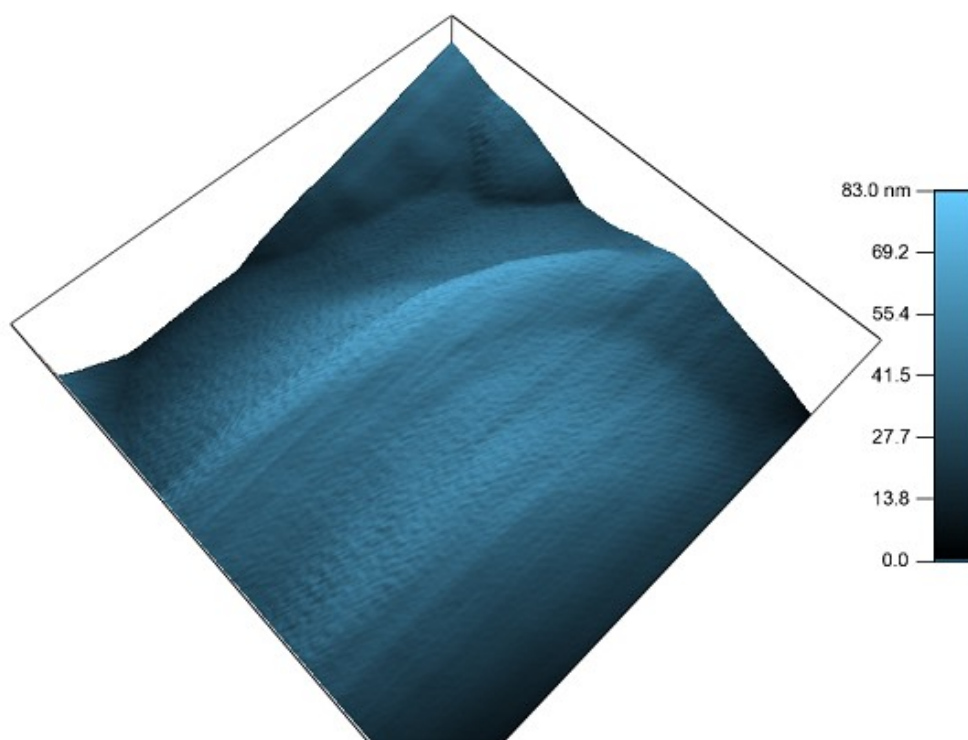
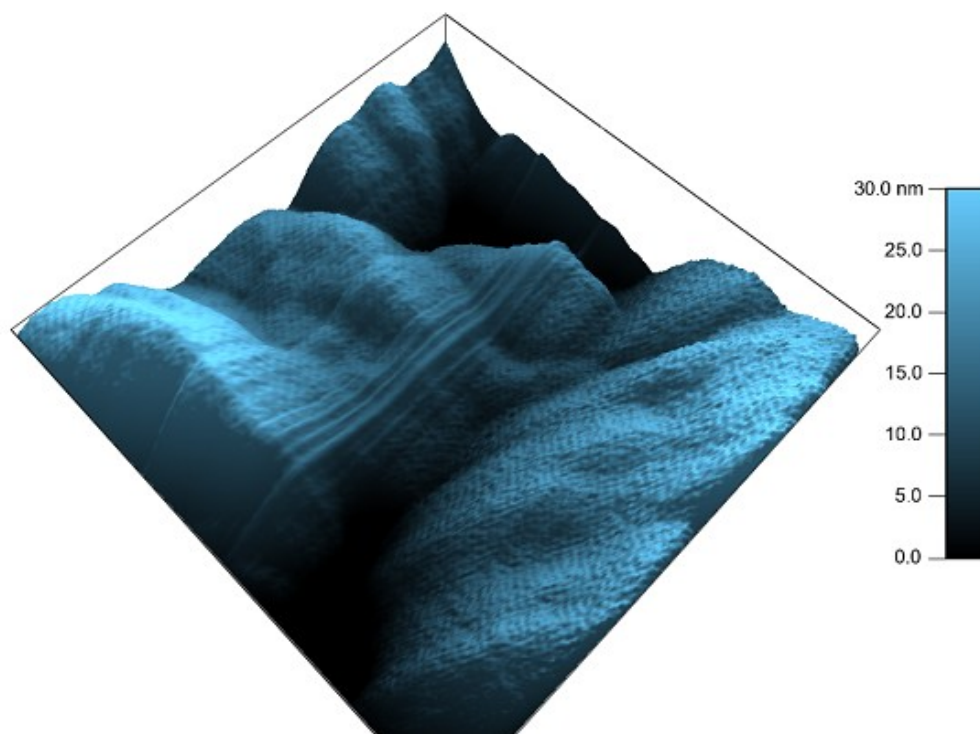
Recycled TMP, 25 μm^2



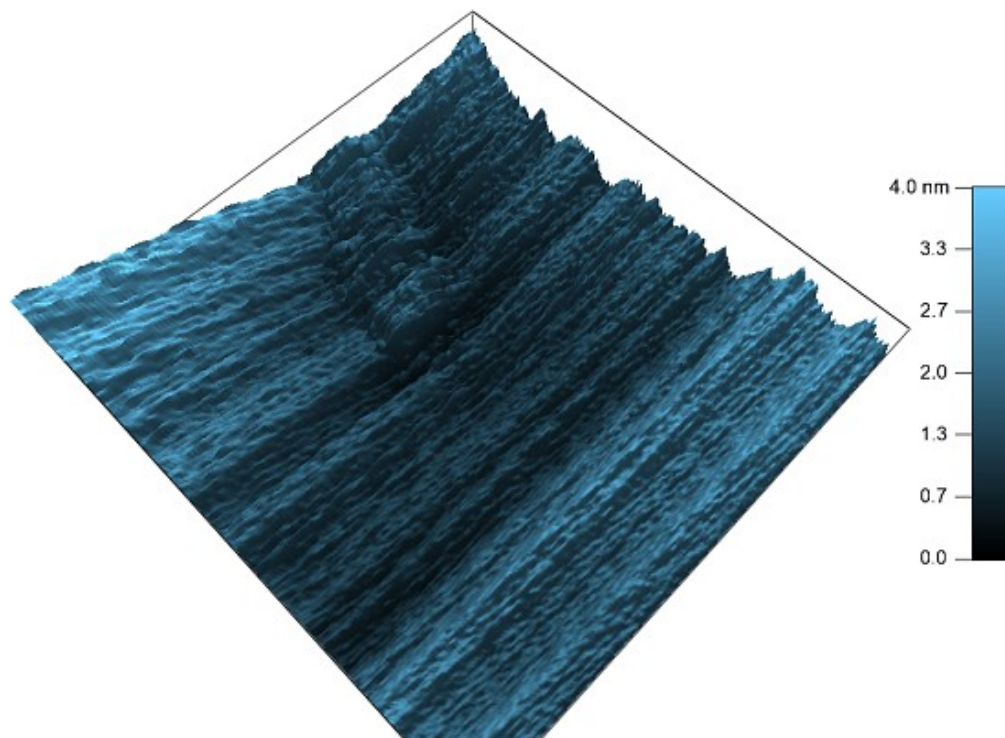
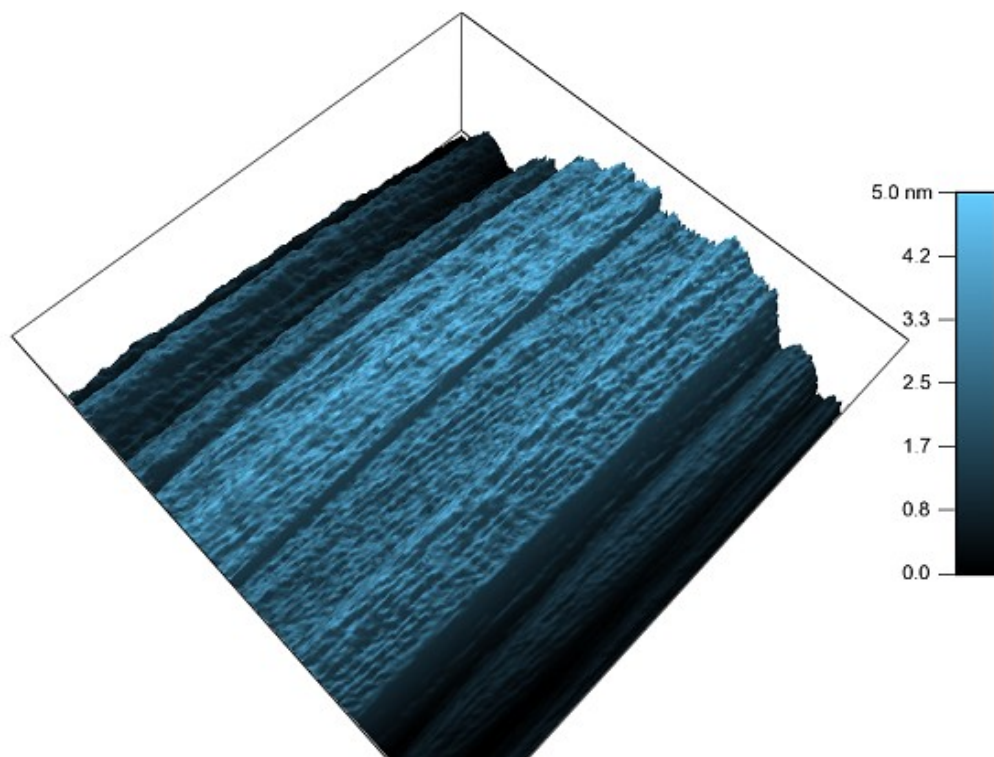
Unrecycled TMP, 0.25 μm^2



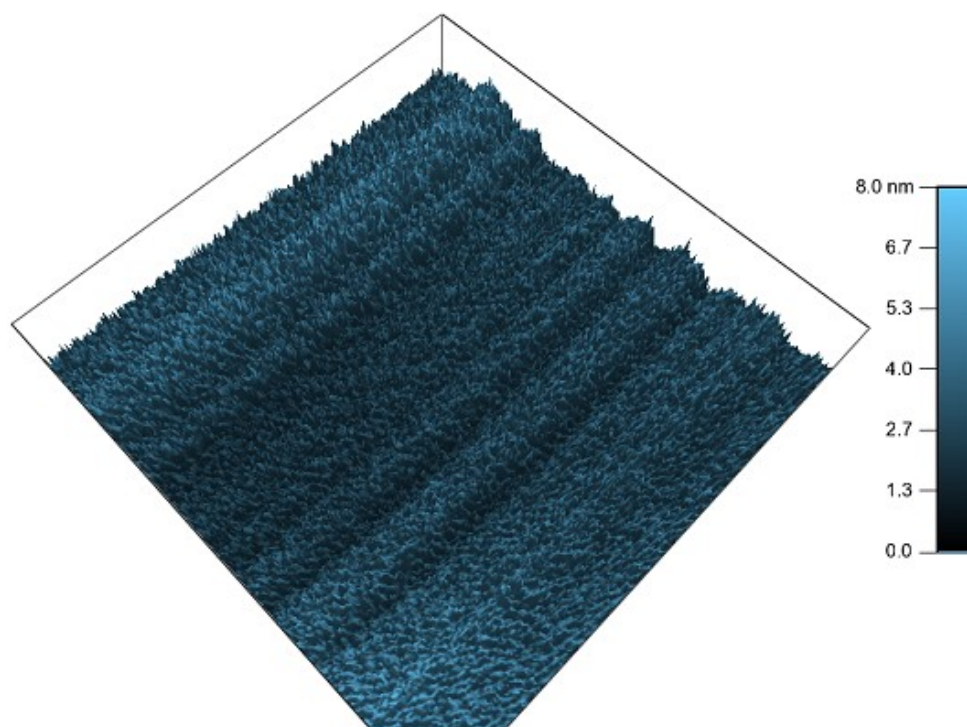
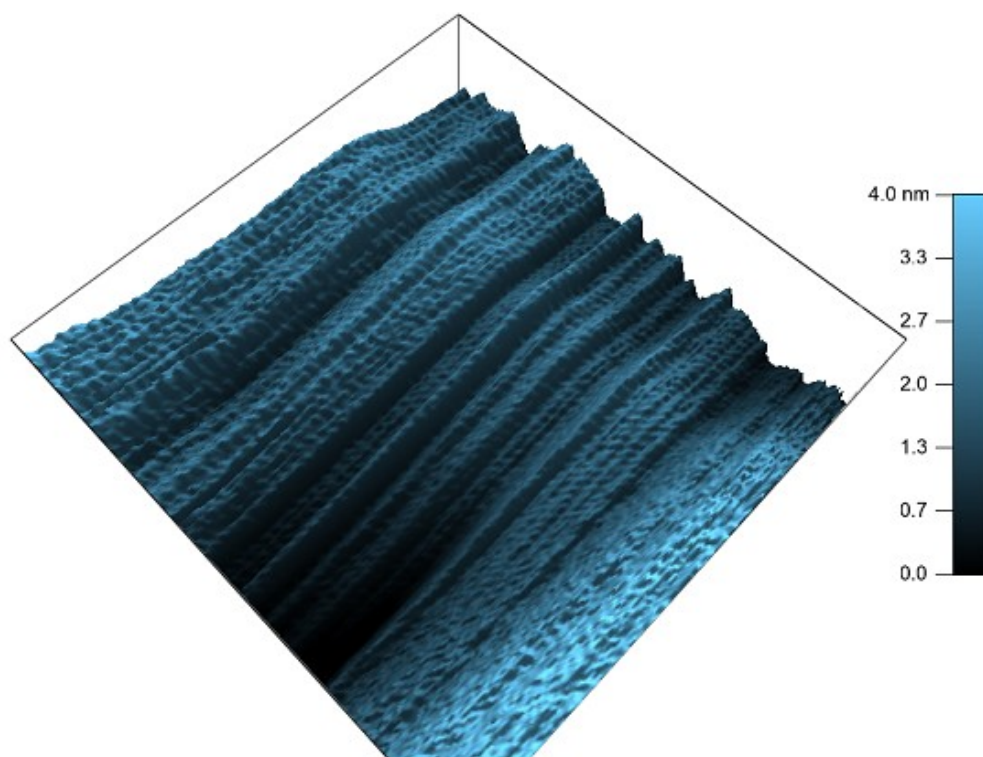
Recycled TMP, 0.25 μm^2



Unrecycled TMP, 2500 nm²



Recycled TMP, 2500 nm²



REFERENCES

1. Asylum Research, "BioHeater",
<http://www.asylumresearch.com/Products/BioHeater/EnvironmentalControls.pdf> (accessed on April 2, 2008)
2. Asylum Research, "MFP-3D Stand Alone AFM",
<http://www.asylumresearch.com/Products/Mfp3DSA/Mfp3DSA.shtml> (accessed on April 2, 2008)
3. Avijit, D., *The current state of paper recycling, a global review*. IPPTA. 1995. 7(4): p. 1-12
4. Back, E.L., *Thermal auto-crosslinking in cellulose material*. Pulp & Paper Magazine of Canada. 1967. 68(4): p. T165-T171
5. Back, E.L., H.M. Thoung, M. Jackson, and F. Johanson, *Effect of auto crosslinking reactions on the thermal softening of cellulose*. Textile Research Journal. 1967. 37(5): p. 432-433
6. Badar, T.A. *Environmental Impact of Recycling in the Paper Industry*. Recycled Paper Technology. 1992: p. 235-245
7. Batchelor, W., *Refining and the development of fibre properties*. Nordic Pulp and Paper Journal, 1999. 14(4): p. 285-291
8. Bawden, A.D. and R.P. Kibblewhite. *Effects of multiple drying treatments on kraft fibre walls*. 3rd Research Forum on Recycling CPPA, Vancouver. 1995: p. 171-177
9. Bendzalova, M., A. Pekarovicova, B.V. Kokta, and R.B. Chen, *Accessibility of swollen cellulosic fibers*. Cellulose Chemistry and Technology. 1996. 30(1-2): p. 19-32
10. Biermann, C.J., *Handbook of Pulping and Papermaking*. 1996, Academic Press: San Diego, California.
11. Bovin, A., N. Hartler, and A. Teder, *Changes in pulp quality due to repeated papermaking*. Paper Tech. 1973. 14(5): p. 261-264
12. Brown, et al, "Cellulose biosynthesis in higher plants",
<http://www.botany.utexas.edu/infores/cen/library/recpub> 2002 (accessed 2002)

13. Campbell, W.B., *The Mechanism of bonding*. TAPPI. 1959. **42**(12): p. 999-1001
14. Child, T.F. and D.W. Jones, *Broad-Line NMR measurement of water accessibility in cotton and woodpulp celluloses*. Cellulose Chemistry and Technology, 1973. **7**: p. 525-534
15. Christensen, P.K. and H.W. Giertz. *The cellulose/water relationship. In Consolidation of the Paper Web*, Trans. 3rd Fund. Res. Symp. 1965. Cambridge: FRC, p. 59-84
16. Clark, J.d.A., *Pulp technology and treatment for paper*. 2nd ed. 1985, San Francisco, California: Miller Freeman Publications, Inc.
17. Cole, B. and R. Fort. "Research in the Cole-Fort Group", <http://chemistry.umeche.maine.edu/Fort/Cole-Fort.html> (accessed on June 03, 2008)
18. Concalves, C., *The eucalyptus fiber for tissue papers*. 7th Brazilian symposium on the chemistry of lignin and other wood components. 2001: p. 317-323
19. Corte, V.H. and H.Schaschek, *Physikalische Natur de Papierfestigkeit*. Das Papier. 1959. **9**: p. 5119-5130
20. Dimmel, D.R., *A6130 Wood and Fiber Science, Lecture 7 Wood Components*. 2001, Institute of Paper Science and Technology.
21. Emerton, H.W., *Fundamentals of the beating process*. The British Paper and Board Industry Research Association. 1957: p. 431-435.
22. Environmental Protection Agency, "Basic Information - Recycle on the Go", <http://www.epa.gov/epaoswer/osw/conserves/ontheinfo/index.htm> (accessed on May 05, 2008)
23. Ehrnrooth E.M.L., *The swelling of dried and never-dried acid chlorite delignified fibers*. Svensk Papperstidning. 1984. **87**: p. R74–R77
24. Fahlen, J. and L. Salmen, *Cross-sectional structure of the secondary wall of wood fibers as affected by processing*. Journal of Materials Science, 2003. **38**: p. 119-126.
25. Fauler, C.C. and H.P.Makkonen, *Determination of mechanical fiber content in mixed office papers using image analysis*. Recycling Symposium, New Orleans, 1996: p. 279-287

26. Fernandes Diniz, J.M.B., M.H. Gil, and J.A.A.M Castro, *Hornification – its origin and interpretation in wood pulps*. Wood Sci. Technol. 2004. **37**: p. 489-494
27. Forsstrom, J., B. Andreasson, and L. Wagberg, *Influence of pore structure and water retaining ability of fibres on the strength of papers from unbleached kraft fibres*. Nordic Pulp and Paper Research Journal. 2005. **20**(2): p. 176-185
28. Garcia, Ricardo; Perez, Ruben. *Dynamic atomic force microscopy methods*. Surface Science Reports. 2002. **47**(6-8), p. 197-301
29. Giertz, H.W., *The effects of beating on individual fibres, in Fundamentals of Papermaking Fibres*. 1st Fund. Res. Symp. 1957. F. Bolam, Editor. Cambridge: FRC: p. 389-409
30. Gurnagul, N., Howard, R. C., Zou, X., Uesaka, T. and Page, D. H. (1993) *The mechanical permanence of paper: a literature review*. Journal of Pulp and Paper Science. 1994. **19**(4): p. J160-J166
31. Heinz, H., *Getting Physical with your chemistry*. Journal of Chemical Education. 2005.
32. Hietanen, S. and K. Ebeling, *Fundamental aspects of the refining process*. Paperi ja Puu, 1990. **72**(2): p. 158-170
33. Higgins H.G. and A.W. McKenzie, *The structure and properties of paper. XIV: Effects of drying on cellulose fibres and the problem of maintaining pulp strength*. Appita J. 1963. **16**: p. 145-161
34. Hillis, W. E.. *High temperature and chemical effects on wood stability. Part 1: general considerations*. Wood Science and Technology. 1984. **18**(4) 281-293
35. Howard, R.C. and W.J. Bichard, *The basic effect of recycling on pulp properties*. JPPS. 1993. **19**(2): p. J57
36. Institute of Paper Science and Technology, "Recycling in the paper industry", http://www.ipst.gatech.edu/amp/collection/museum_recycling.htm (accessed on May 05, 2008)
37. Iyer, P. B., S. Sreenivasan, P.K. Chidambareswaran, N.B. Patil, and V. Sundaram, *Induced crystallisation of cellulose in never-dried cotton fibres*. Journal of Applied Polymer Science. 1991. **42**(6): p. 1751-1757.

38. Jayme, G. *Properties of wood celluloses. II: Determination and significance of water - retention value*. TAPPI. 1958. **41**(11): p. 180A-183A.
39. Jones, R., H.M. Pollock, J.A.S. Cleaver, and C.S. Hodges, *Adhesion forces between glass and silicon surfaces in air studied by AFM: effects of relative humidity, particle size, roughness, and surface treatment*. Langmuir. 2002. **18**(21): p. 8045-8055
40. Jung, Y.C., B. Bhushan. *Contact angle, adhesion and friction properties of micro and nanopatterned polymers for superhydrophobicity*. Nanotechnology. 2006. **17**(19): p. 4970-4980.
41. Kerekes, R.J., R.M.Soszynski, P.A. Tam Doo, *Papermaking raw materials*. Punton V. ed. Trans 8th Fund. Res. Symp. Oxford, UK. 1996: p. 265
42. Klemm, D., B. Heublein, H.Fink, and A. Bohn, *Cellulose: fascinating biopolymer and sustainable raw material*. ChemInform, 2005: p. 36
43. Kleppe, P.J., *Kraft Pulping*. TAPPI. 1970. **53**(1): p. 35-47
44. Klunness, J.H. and D.F. Caulfield. *Mechanisms affecting fiber bonding during drying and aging of pulps*. TAPPI. 1982. **65**(12): p. 94-97
45. Koffas, T.S., A. Opdahl, C. Marmo, and G.A. Somorjai, *Effect of equilibrium bulk water content on the humidity-dependent surface mechanical properties of hydrophilic contact lenses studied by atomic force microscopy*. Langmuir. 2003. **19**(8): p. 3453-3460
46. Krkoska, P. and J. Hanus, *Description of paper aging by zero-span tensile strength*. Cellulose Chemistry and Technology. 1988. **22**(6): p. 633-645
47. Kuys, K. and Q. Zhu, *Surface chemistry of recycled paper furnishes*. Progress in Paper Recycling. 1997. **6**(2): p. 59-64
48. Laivins, G. V. and A.M. Scallan, *The mechanism of hornification of wood pulps*. In Products of Papermaking, Tenth Fundamental Research Symposium, (C. F. Baker, ed.) Vol. 2, Oxford. 1993: p. 1235-1260.
49. Lazzaroni, R., "Principles of Atomic Force Microscopy", www.ifm.liu.se/surfphys/laminate/common/Documents/AFMroberto.pdf (accessed May 12, 2008)
50. Lignin Institute, "Lignin and its properties: glossary of lignin nomenclature. Dialogue/Newsletters Volume 9, Number 1", <http://www.lignin.org/01augdialogue.html> (accessed on June 03, 2008)

51. Liitia, T., S.L. Maunu, and B. Hortling, *Solid state NMR studies on cellulose crystallinity in fines and bulk fibres separated from refined kraft pulp*. *Holzforschung*, 2000. **54**(6): p. 618-624
52. Luner, P., *Evaluation of paper permanence*. *Wood Science and Technology*. 1988. **22**(1): p. 81-97
53. Luner, P., *Paper permanence*. TAPPI. 1969. **52**(5): p. 796-805.
54. Mark, R.E., *Cell wall mechanics of tracheids*. 1967, New Haven and London: Yale University Press.
55. Martinez D.M., *Characterizing the mobility of papermaking fibers during sedimentation*. In "The science of papermaking" C.F. ed. Trans. 12th Fund. Res. Symp. Oxford, UK. 2000: p. 211
56. Matsuda, Y., A. Isogai, and F. Onabe, *Effects of thermal and hydrothermal treatments on the reswelling capabilities of pulps and papersheets*. *Journal of Pulp and Paper Science*. 1994. **20**(11): p. J323-J327
57. Meller, Alexander. *Cold alkaline purification of wood cellulose. II. The influence of surface properties on resistant pentosans*. *Paper Trade Journal*. 1947. **125**(11): p. 57-60
58. Mikromasch, "Hi'Res-W", <http://www.spmtips.com/probes/hiresw> (accessed on April 2, 2008)
59. Milichovsky, M., *A new concept of chemistry in refining processes*. TAPPI. 1990. **73**(10): p. 221-232
60. Nalaskowski, J, J. Drelich, and J.D. Miller, *Forces between polyethylene surfaces in oxyethylene dodecyl ether solutions as influenced by the number of oxyethylene groups*. *Langmuir*. 2008. **24**(4): p. 1476-1483
61. Nazhad, M. M. and L. Pazner, *Fundamentals of strength loss in recycled paper*. TAPPI. 1994. **77**(9): p. 171-179
62. Needles, H.L. and K.C.J. Nowak, *Heat-induced aging of linen*. in *Historic Textile and Paper Materials II: Conservation and Characterization*, ACS Symposium Series 1989. **410**: p. 167-169
63. Newman, R.H., *Carbon-13 NMR evidence for cocrystallization of cellulose as a mechanism for hornification of bleached kraft pulp*. *Cellulose*. 2004. **11**(1): p. 45-52.

64. Olympus Corporation, "Micro cantilever", <http://probe.olympus-global.com/en/en/explnafmE.html> (accessed on April 12, 2008)
65. Olympus Corporation, "Technical data of silicon cantilevers", <http://probe.olympus-global.com/en/en/specsisoftE.html> (accessed on April 12, 2008)
66. OpTest, *Fiber Quality Analyzer*. 1998.
67. Page, D.H., *The beating of chemical pulps - the action and the effects*. in Fundamentals of Papermaking. 9th Fund. Res. Symp. 1989. Cambridge: FRC.
68. Piantanida, G., M. Bicchierib, F. Pinzarib, and C. Coluzzaa, *Atomic Force Microscopy imaging "directly on paper": a study of library materials degradation*. Proceedings of SPIE 2005. **5857**: p. 57570R1-5750R11
69. Poggi, M.A., D.G. Mancosky, L.A. Bottomley, and L.A. Lucia, *Atomic force microscopic analysis of hydrogen peroxide bleached kraft northern black spruce fibres*. Journal of Microscopy. 2005. **220**: p. 77-83
70. Ramezani, O. and M.M. Nazhad, "The effect of refining on paper formation", http://www.tappsa.co.za/archive2/APPW_2004/Title2004/The_effect_of_refining/the_effect_of_refining.html (accessed on May 08, 2008)
71. Rao, R. and K. Kuys, *Surface chemistry of fibers in recycling of newsprint and magazines*. 8th International Symposium on Wood and Pulping Chemistry, Helsinki, 1995: p. 261-266
72. Roberson, D.D. *The evaluation of paper permanence and durability*. TAPPI. 1976. **59**(12): p. 63-69
73. Robertson, A. A., *The physical properties of wet webs. Part 2. Fiber. properties and wet web behavior*. Svensk Papperstidning. 1963. **66**(12): p. 477-497
74. Sader, J., Chon, J., and Mulvaney, P., *Calibration of rectangular atomic force microscope cantilevers*. Review of Scientific Instruments. 1999. **70**: p. 3967-3969
75. Scallan, A.M., *The accomodation of water within pulp fibres - fibre-water interactions in paper-making*. Transactions BPBIF Symp. 1997. 1: p. 9-27
76. Scallan, A.M. and J.E. Carles, *Correlation of the Water Retention Value with the Fiber Saturation Point*. Svensk Papperstidning. 1972. **75**(17): p. 699-703

77. Scallan, A.M. and A.C. Tigerstrom. *Elasticity of the wet fibre wall: effect of pulping and recycling*. 1st Research Forum on Recycling. 1991.
78. Sedin, D.L., K.L. Rowlen, *Adhesion forces measured by atomic force microscopy in humid air*. Book of Abstracts, 219th ACS National Meeting. 2000.
79. Seth, R. S. *Fiber quality factors in papermaking - II. The importance of fiber coarseness*. MRS Symposium Proceedings. 1990. **197**: p. 143
80. Sjöstrom, E., *Wood Chemistry Fundamentals and Applications 2nd ed.* 1993, New York, New York: Academic Press
81. Smook, G.A., *Handbook for Pulp and Paper Technologists*, ed. M.J. Kocurek. 1982, Montreal, Quebec Canada: TAPPI and CPPA.
82. Spandanberg, R.J., ed., *Secondary Fiber Recycling*. 1993, Atlanta, Georgia: TAPPI.
83. Stamm, A.J., *Wood and Cellulose Science*. 1964, New York, New York: Ronal Press
84. Stockman, L. and A. Teder, *The effect of drying on the properties of papermaking pulps. II. The effect of heat treatment on the mechanical properties*. Svensk Papperstidning. 1963. **66**(20): p. 822-832
85. Stone, J.E. and A.M. Scallan, *Influence of drying on the pores structures of the cell wall*. in Consolidation of the Paper Web, (F. Bolam, ed.). Trans. BPBMA Symp. 1965. **1**: p. 145-166.
86. Stone, J.E. and A. M. Scallan, *Structural model for the cell wall of water-swollen wood pulp fibers based on their accessibility to macromolecules*. Cellulose Chemistry and Technology. 1968. **2**(3): p. 343-58
87. Stone, J. E., A.M. Scallan, and B. Abrahamson, *Influence of beating on cell wall swelling and internal fibrillation*. Svenk Papperstidning. 1968. **19**(10): p. 687-694
88. Sudbury, J.B., *50 Simple things you Can do to Save the Earth*. 1989, Berkeley CA: Earthworks Press.
89. Sugawara, Y., M. Ohta, T. Konishi, S. Morita, M. Suzuki, Y. Enomoto, *Effects of humidity and tip radius on the adhesive force measured with atomic force microscopy*. Wear. 1993. **168**(1-2): p. 13-16

90. Swann, C.E., *Pulping, bleaching, recovery: How far can we go?* PIMA's Papermaker. 2000. **82**(10): p. 45-47
91. Swanson, J.W. and S. Cordingly, *Surface chemical studies of pitch 2. The mechanism of self-sizing in papers made from wood pulps*. TAPPI. 1959. **41**(10): p. 812-819
92. TAPPI T 227 om-04, "Freeness of pulp (Canadian standard method)," published by the TAPPI Press, Atlanta, Georgia.
93. TAPPI T 271 om-07, "Fiber length of pulp and paper by automated optical analyzer using polarized light," published by the TAPPI Press, Atlanta, Georgia.
94. TAPPI T 402 sp-03, "Standard conditioning and testing atmospheres for paper, board, pulp handsheets and related products," published by the TAPPI Press, Atlanta, Georgia.
95. TAPPI T 205 sp-06, "Forming handsheets for physical tests of pulp," published by the TAPPI Press, Atlanta, Georgia.
96. TAPPI T 200 sp-06, "Laboratory beating of pulp (Valley beater method)," published by the TAPPI Press, Atlanta, Georgia.
97. TAPPI T 220 sp-06, "Physical testing of pulp handsheets," published by the TAPPI Press, Atlanta, Georgia.
98. TAPPI Useful Method UM 256, "Water retention value (WRV)," published by the TAPPI Press, Atlanta, Georgia.
99. Thode, E.F., A.J. Chase, and Y. Hu. *Dye adsorption on wood pulp III*. TAPPI. 1953. **36**(11): p. 498-504
100. Thode, E.F., A.J. Chase, and Y. Hu. *Dye adsorption on wood pulp IV*. TAPPI. 1955. **38**(2): p. 88-89
101. Trepannier, R.J. *Automatic fiber length and shape measurement by image analysis*. TAPPI. 1998. **81**(66): p. 152-154
102. Tze, W.T. and D.J. Gardner, *Swelling of recycled wood pulp fibers: Effect on hydroxyl availability and surface chemistry*. Wood and Fiber Science, 2001. **33**(3): p. 364-376

103. Vietor, R. K. Mazeau, M. Lakin, and S. Perez, *A priori crystal structure prediction of native celluloses*. Biopolymers. 2000. **54**: p. 342-354
104. Walsh, F.L., *An Isotopic Study of Fiber-Water Interactions*. 2006, Georgia Institute of Technology: Atlanta, Georgia.
105. Walsh, F. L. and S. Banerjee, *Characterization of thin water layers in pulp by tritium exchange. Part 2: Effect of refining on water absorption*. Holzforschung. 2007. **61**(2): p. 120-123
106. Weise, U., T.C. Maloney, and H. Paulapuro, *Quantification of water in different states of interaction with wood pulp fibers*. Cellulose, 1996. **3**: p. 189-202
107. Wikipedia, "Gel", <http://en.wikipedia.org/wiki/Gel> (accessed on April 18, 2008)
108. Wikipedia, "Inkjet printer", http://en.wikipedia.org/wiki/Inkjet_printer (accessed on June 03, 2008)
109. Wikipedia, "Lignin", <http://en.wikipedia.org/wiki/Lignin> (accessed on June 03, 2008)
110. Wikipedia, "Laser printer", http://en.wikipedia.org/wiki/Laser_printer (accessed on June 03, 2008)
111. Wistara, N. and R.A. Young, *Properties and treatments of pulps from recycled paper. Part I. Physical and chemical properties of pulps*. Cellulose, 1999. **6**(1): p. 291-324
112. Xiao, X. and L. Qian, *Investigation of humidity-dependent capillary force*. Langmuir. 2000. **16**(21): p. 8153-8158
113. Xu, L., A.Lio, J. Hu, D.F. Ogletree, and M. Salmeron, *Wetting and capillary phenomena of water on mica*. Journal of Physical Chemistry B. 1998. **102**(3): p. 540-548
114. Yan, L., J.Y. Wan Li, and Q. Zhu, *Direct vizualization of straw cell walls by AFM*. Macromolecular Bioscience. 2004. **4**: p. 112-118
115. Yan, Y.D., T. Sun, and S. Dong, *Study on effects of tip geometry on AFM nanoscratching tests*. Wear. 2007. **262**(3-4): p. 477-483
116. Young, R. A. and R.M. Roswell, ed., *Cellulose: Structure, Modification and Hydrolysis*. 1986, New York: Wiley.

117. Yu, Y., H. Kettunen, E. Hiltunen, and K. Niskanen, *Comparison of abaca and spruce as reinforcement*. TAPPI International Paper Physics Conference, San Diego, U.S.A, 1999: p. 161-169
118. Zou, X., N. Gurnagul, T. Uesaka, and J. Bouchard, *Accelerated aging of papers of pure cellulose: mechanism of cellulose degradation and paper embrittlement*. Polymer degradation and stability. 1994. **43**(3): p. 393-402